Interference Measurements and Throughput Analysis for 2.4 GHz Wireless Devices in Hospital Environments

by

Seshagiri Krishnamoorthy

Thesis submitted to the faculty of the
Virginia Polytechnic Institute and State University
in partial fulfillment of the requirements for the degree of

MASTER OF SCIENCE
in
Electrical Engineering

Dr. Jeffrey H. Reed, Chair

Dr. Dennis G. Sweeney

Dr. Srikathyayani Srikanteswara

April 21, 2003

Blacksburg, Virginia

Keywords: 2.4 GHz ISM, Electromagnetic Interference (EMI), hospital environments, Bluetooth throughput, WLAN, Microwave Ovens

Interference Measurements and Throughput Analysis for 2.4 GHz Wireless Devices in Hospital Environments

Seshagiri Krishnamoorthy

(Abstract)

In recent years, advancements in the field of wireless communication have led to more innovative consumer products at reduced cost. Over the next 2 to 5 years, short-range wireless devices such as Bluetooth and Wireless Local Area Networks (WLANs) are expected to become widespread throughout hospital environments for various applications. Consequently the medical community views wireless applications as ineludible and necessary. However, currently there exist regulations on the use of wireless devices in hospitals, and with the ever increasing wireless personal applications, there will be more unconscious wireless devices entering and operating in hospitals. It is feared that these wireless devices may cause electromagnetic interference that could alter the operation of medical equipment and negatively impact patient care. Additionally, unintentional electromagnetic radiation from medical equipment may have a detrimental effect on the quality of service (QoS) of these short-range wireless devices.

Unfortunately, little is known about the impact of these short-range wireless devices on medical equipment and in turn the interference caused to these wireless devices by the hospital environment. The objective of this research was to design and develop an automated software reconfigurable measurement system (PRISM) to characterize the electromagnetic environment (EME) in hospitals. The portable measurement system has the flexibility to characterize a wide range of non-contiguous frequency bands and can be monitored from a remote location via the internet. In this work electromagnetic interference (EMI) measurements in the 2.4 GHz ISM band were performed in two hospitals. These measurements are considered to be very first effort to analyze the 2.4 GHz ISM band in hospitals.

Though the recorded EMI levels were well within the immunity level recommended by the FDA, it can be expected that Bluetooth devices will undergo a throughput reduction in the presence of major interferers such as WLANs and microwave ovens. A Bluetooth throughput simulator using semi-analytic results was developed as part of this work. PRISM and the Bluetooth simulator were used to predict the throughput for six Bluetooth Asynchronous Connectionless (ACL) transmissions as a function of piconet size and interferer distance.

This work was supported by the Carilion Biomedical Institute, the Medical Automation Research Centre at the University of Virginia and the MPRG affiliates program.

Acknowledgements

My sincere appreciation goes to my advisor, Dr. Jeffrey H. Reed for his professional guidance, support and encouragement throughout my course of study at Virginia Tech. He has allowed me a free hand in exploring many opportunities and I have gained immensely from them. I am grateful to Dr. Dennis Sweeney for his ideas, help and suggestions especially with the microwave oven measurements. I would also like to thank Dr. Srikathyayani Srikanteswara for being ever-willing to listen to my suggestions and offering her expertise in my project.

I would like to express my gratitude to Max Robert for his persistent help and inspiration. His research experience and knowledge on Bluetooth and WLANs has helped me immensely. I am greatly indebted to Chris Anderson for sharing his wealth of knowledge on wireless propagation and measurement campaigns. I would also like to thank him for helping me with my measurement campaign at the veterinary hospital and tirelessly proofreading the entire thesis. Special thanks go to Bill Newhall for his suggestions and ideas on RF channel measurements.

My association with MPRG for the past two and a half years has been an exciting experience. I am grateful towards all my fellow researchers and the staff of MPRG. Additionally, I would like to thank Ramesh Chembil Palat for being a great companion and source of encouragement during my stay at MPRG.

I would like to acknowledge Brian Brindle of Carilion Health Information Systems for his time and patience in helping me with the measurements at Carilion Roanoke Memorial Hospital. His knowledge on in building wireless network deployment and the fruitful discussions I have had with him has helped me a lot.

I would like to take this opportunity to thank the Center for Wireless Telecommunication (CWT) for providing access to their Bluetooth lab and software tools.

It is my pleasure to acknowledge the contributions of valuable time and expertise from numerous individuals. Their support has helped my research immensely.

Randall Nealy of the Virginia Tech Antenna Group (VTAG) for his help in designing and building the 2.45 GHz coaxial sleeve dipole antenna for the measurement system. Dr. Seong Youp Suh was kind enough to measure the antenna parameters and patterns.

Tom Rondeau of CWT and Sapna Ananthnarayanan for helping me in developing the Bluetooth protocol stack.

Dr. John Robertson of the Virginia Maryland College of Veterinary Medicine for providing access to the veterinary hospital.

Greg Walton and Benny Banton of Carilion Health Information Systems for providing access and support for the EMI measurements at the Carilion Roanoke Memorial Hospital.

Finally, I would like to thank my brothers Ram and Swami and my sister Akila for their love and continuous support during my academic studies.

Contents

List of Figures

List of Tables

Chapter 1

1 Introduction

1.1 Motivation

Over the past decade, there has been unprecedented growth in wireless standards and services. The advancements in the field of wireless communications have led to more innovative consumer applications. These wireless applications have evolved to cater to the needs of the commercial industry, defense, private home users and educational institutions.

In recent years, the health care industry has been anticipating the proliferation of medical wireless applications and other personal wireless devices in hospitals and clinics. Currently in the United States, nurses represent the single largest labor expense for hospitals, and workforce shortages are threatening the financial viability of many hospitals [App]. The domino effect of having fewer workers, more delays in delivering patient care, dissatisfaction among patients and hospital staff, decreasing quality of care and loss of market share is alarming. The medical community recognizes the use of wireless technology as an excellent solution to improve manpower productivity, ease patient data storage, strengthen inventory control, and improve patient monitoring and patient care. Consequently medical applications have been targeted as an attractive and potential market by wireless device manufacturers.

Short-range wireless devices such as Bluetooth and wireless local area networks (WLANs), which operate in the unlicensed 2.4 GHz Industrial, Scientific and Medical (ISM) band, are potential wireless standards for medical applications. Bluetooth in particular is very promising due to its low cost, low power consumption and wide acceptance among manufacturers. Bluetooth chipsets can be readily integrated with the existing medical equipment to render them wireless.

1.2 Problem Definition

Presently, the use of wireless devices such as cell phones, PDA's and walkie-talkies are restricted in hospitals due to fear of detrimental Electromagnetic Interference (EMI). There have been few sporadic reported cases of EMI causing malfunctioning of medical equipment such as pace-makers, apnea monitors, hearing aids, powered wheel chairs and anesthetic gas monitors [Sil93], [Sil95]. Healthcare providers therefore play it safe by restricting the use of any wireless devices. Unfortunately, there exist no quantified results to define the tolerable levels of emission in hospitals for various frequency bands. Currently no commercially off the shelf equipment exists that has both the versatility to characterize EMI, as well as the ability to monitor and diagnose interference from remote locations via the internet. Furthermore, knowledge of measured EMI caused by medical equipment and other sources in a hospital can help in determining the throughput of wireless devices operating in hospital/ clinical environments.

1.3 Approach

The purpose of this research was to:

1. Design and develop a versatile, user-friendly and portable wireless measurement instrument to characterize the RF spectrum over a wide range of frequencies with particular emphasis on the 2.4 GHz ISM band investigated in this work. The measurement instrument was designed with the following key features

    - Software reconfigurable
    - Ability to measure non-contiguous frequency bands
    - Ability to monitor spectrum from a remote location via the internet.
    - Completely automated
    - Small and easy to transport
    - Sensitive to very weak signals
    - Minimal data storage requirements
    - Easy to use and operate

A MATLAB post-processing software suite was also desired to allow the user to analyze and characterize measured interference data as a function of location, frequency and time of day.

2. Develop a Bluetooth throughput simulator in MATLAB, to use the post-processed EMI data from the measurement system to predict throughput of Bluetooth devices as a function of the environment.

1.4 Original Contributions and Overview of Research

The first phase of this project was to establish Bluetooth infrastructure (Figure 1.1), comprising of both hardware and software, in the Mobile and Portable Radio Research Group. To boost this initiative, we developed a software stack for Bluetooth which allowed two or more Bluetooth devices to establish communication and transmit data for range estimation and position location. The software stack shown in Figure 1.2 was developed in Visual C++ incorporating all the essential commands specified in the Bluetooth Host Controller Interface (HCI) standard [Kri02d].The developed Bluetooth software stack is vendor independent and was used to communicate between an Ericsson ROK 101 008 Bluetooth starter kit and a Cambridge Silicon Radio Bluetooth development kit. The goal of this phase was to establish a proof of concept hardware that would allow Bluetooth devices to transfer patient records as well as track and monitor patients. Range estimation techniques were developed using HCI inherent parameters and preliminary range estimation measurements were performed using two Bluetooth devices. The results were found to be very much dependent on the surrounding environment. Since these devices were intended for deployment in hospital environments, a literature study was undertaken to understand the RF environment in the ISM band where Bluetooth operates.

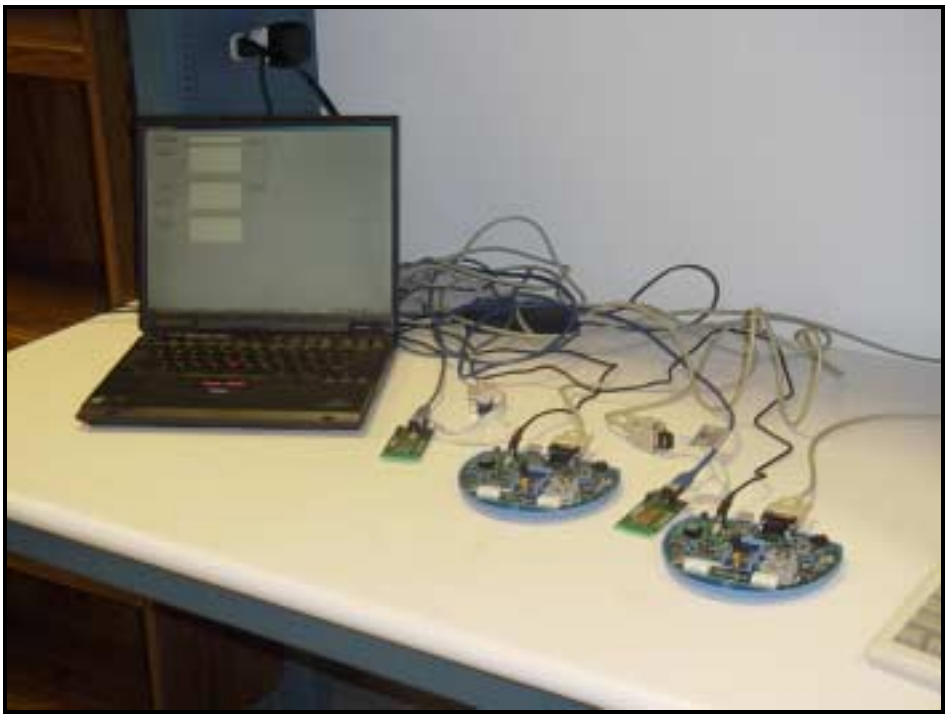

Figure 1.1 MPRG Bluetooth Hardware Facility

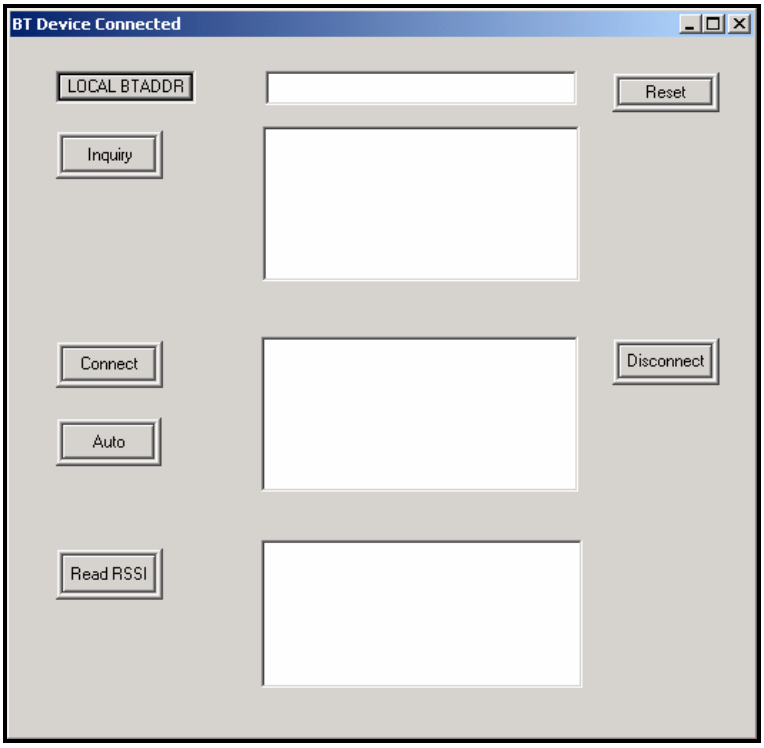

Figure 1.2 MPRG Bluetooth Software Stack

Unfortunately, there have been very few studies and published data on interference in the 2.4 GHz ISM band. Therefore, the second phase of this project was to design and develop a RF measurement system for investigating the RF environment in ISM band. PRISM[1] an acronym for PRobe ISM was developed as a software reconfigurable measurement system [Kri02c]. PRISM was designed using LabVIEW to not only provide a very friendly Graphical User Interface (GUI) but to make it a completely automated system. Beyond being a measuring system for the ISM band, PRISM can also be used to measure RF interference over non-contiguous frequency bands between 9 kHz and 2.9 GHz by using wideband antennas. Later, the software was updated for monitoring interference measurements via the web from remote locations.

The third phase of this project involved a brief measurement campaign at the Virginia-Maryland College of Veterinary Medicine at Virginia Tech. The measurement campaign involved weeks of measurement at different locations of the Veterinary hospital. It was observed that microwave ovens were a major source of interference in this environment [Kri02a]. In order to investigate the impact of microwave ovens on Bluetooth devices, PRISM was used to record emissions from microwave ovens in an office environment. The results were used in a semi-analytic simulation to estimate the Frame Error Rate (FER) for six ACL Bluetooth packets [Kri02b].

The fourth phase of this project involved an extensive measurement campaign to characterize the RF environment at various blocks of the Carilion Memorial Hospital (CRMH) in Roanoke, Virginia. It is believed that this has been the very first effort to measure EMI levels for the 2.4 GHz ISM band in hospitals. At CRMH, 802.11b WLANs and microwave ovens were found to create most of the RF activity in the ISM band.

Finally, we developed a Bluetooth throughput simulator using 802.15 channel models [Wpaa] and the Bluetooth throughput analysis provided in [Val02]. Measurement results from PRISM were then applied to the Bluetooth simulator to obtain expected throughput for six Bluetooth ACL transmissions in the presence of WLAN and microwave oven interference. This study can be very useful for analyzing adaptive

[1] Disclaimer- 'PRISM' is an acronym for PRobe ISM and was coined for educational purposes alone, any resemblance to an existing product or equipment name is purely coincidental.

frequency hopping techniques and adaptive packet selection and scheduling schemes under study by the IEEE P802.15 Working Group for Wireless Personal Area Networks™.

1.5 Thesis Overview

This thesis presents the design and development of a software reconfigurable measurement system along with interference measurements in hospital environments and a throughput simulator for Bluetooth. Chapter 2 will review wireless propagation concepts and provide background information on the propagation environment in hospitals. Next in Chapter 3 we provide a detailed discussion on the design and implementation of the measurement system – PRISM. The software and hardware of PRISM along with its capabilities and limitations are discussed. This chapter also explains the post-processing software suite built using MATLAB.

The results of the extensive measurement campaign at the Virginia-Maryland College of Veterinary Medicine at Virginia Tech and the Carilion Memorial Hospital in Roanoke, Virginia along with their analysis are presented in Chapter 4. These results will be crucial to clinical and network engineers who wish to deploy wireless infrastructure in a hospital environment.

Chapter 5 discusses the throughput analysis for Bluetooth and provides results on Bluetooth throughput in the presence of microwave ovens and an 802.11b WLAN based on experimental testing. Chapter 5 also provides some background on short-range wireless devices such as Bluetooth and 802.11 which is necessary for having a better appreciation and understanding of the throughput analysis.

Chapter 6 summarizes the contributions of this work, and suggests further avenues of research.

Chapter 2

2 Background and Literature Survey

2.1 Introduction

Several aspects of radio wave propagation, large-scale path loss and terminology related to electromagnetic interference need to be addressed to provide the proper background for understanding the available literature. Once the appropriate groundwork is laid, the interference measurements and their impact on short-range wireless devices can be explained.

The chapter is organized as follows: Section 2.1 discusses the mechanics of radiowave propagation. Section 2.2 introduces the reader to terminology and measurement parameters used in the field of EMC. Section 2.3 gives a detailed literature review on the research and results conducted to date on background EMI in hospitals and EMI measured from RF devices and medical devices. This section also discusses the role of EMC standards and regulatory bodies. Finally we draw a short chapter summary in Section 2.4.

2.2 Radiowave Propagation

Propagation is the underlying mechanics which affect how a radio signal travels. All radio transmitters have a particular coverage area. The coverage area of a radio transmitter or a signal source will depend on several factors like how much power is being transmitted from the antenna (source), the surrounding environment and the distance of separation between the receiver and the transmitter. The surrounding environment plays a very important role in the propagation mechanics, such as reflection, diffraction and scattering [Rap99]. These in turn affect signal strength and give rise to signal fading.

Propagation models take into consideration the characteristics of the transmitter such as power, frequency, antenna design and factors that affect signal propagation to predict the signal strength at a given distance from the transmitter. Propagation models are classified into two categories

1. Large-scale propagation or path loss models
2. Small-scale propagation or fading models

Large-scale propagation models are concerned with estimating signal strength at given distance of separation from the transmitter where the distance is on order of 100's of λ's. Small-scale propagation models place emphasis on signal variations over a small duration of time or small area in space. In our work we are more concerned about large-scale propagation models and hence place less emphasis on small-scale signal variations.

2.2.1 Free Space Propagation Model

The received signal strength $P_r(d)$ at d particular distance from a transmitter decreases as function of distance and is given by

$$P_r(d) \propto 1/\left(d^n\right) \tag{2.1}$$

where, n is the path loss exponent which is a function of the environment and indicates the rate at which received signal strength drops with distance.

Free space propagation refers to the scenario where there is an unobstructed line of sight between the transmitter and receiver. For the free space propagation model the path loss exponent $n = 2$, and received signal strength $P_r(d)$ in watts is given by

$$P_r(d) = \frac{P_t G_t G_r \lambda^2}{(4\pi)^2 d^2} \tag{2.2}$$

where, P_t is the power of the transmitter in watts, G_t and G_r are the antenna gains of the transmitter and receiver respectively, λ is the wavelength in meters and d is the path length in meters.

The power received can be related to an electric field E in volts/metre using the power flux density P_d and effective antenna aperture A_e [Rap99],

$$P_r(d) = P_d A_e \tag{2.3}$$

The power flux density in watts/m^2 is given by

$$P_d = \frac{E^2}{\eta} \tag{2.4}$$

where, $\eta = 120\pi$ is the intrinsic impedance of free space.

The effective antenna aperture (m^2) is dependent on the physical antenna characteristics and is given by

$$A_e = \frac{G_r \lambda^2}{4\pi} \tag{2.5}$$

Using Equations 2.2 to 2.5 we obtain

$$E(V/m) = \frac{5.5\sqrt{P_t G_t}}{d} \tag{2.6}$$

Path Loss Models

In order to predict the large scale signal variations for both indoor and outdoor environment an empirical method is used. The empirical formula is based on actual measured data and analysis of propagation factors. It has been observed that the received signal power decreases logarithmically with distance and can be expressed as [Rap99]:

$$PL(dB) = 10n\log(d) + 20\log\left(\frac{4\pi}{\lambda}\right) + FAF + X_\sigma \tag{2.7}$$

where n is the path loss exponent that describes the rate of decrease of signal strength in a particular environment with distance d for signal propagating at a given frequency and X_σ (dB) is a Gaussian distributed random variable with zero mean and standard deviation σ (dB). X_σ describes the random shadowing effects and accounts for the varying levels

of clutter along different propagation paths and *FAF* (dB) is the floor attenuation factor that accounts for path loss between floors.

Site General and Site Specific Propagation Models

For indoor channels, signal propagation can be modeled using site-general or site-specific models. Site-general models consider fewer details pertaining to the environment and the path loss is characterized by an average path loss and in some cases includes the associated shadow fading statistics and attenuation due to multiple floors. The International Telecommunications Union (ITU) has considered three site categories residential, office and commercial over the 900 MHz, 2 GHz, 4 GHz, 5.2 GHz and 60 GHz frequency range. Path loss exponents, floor attenuation factors and shadowing statistics for these sites and frequency ranges are provided in [ITU01]. Since our work is confined to the 2.4 GHz ISM band, let us take a look at the ITU specification for the 2 GHz range summarized in Table 2.1.

Table 2.1

Site General Characteristics for Indoor Channels at 1.8 – 2 GHz

Site	Residential	Office	Commercial
n (n≥1)	2.8	3	2.2
FAF (dB)	4n	15 + 4(n-1)	6 + 3(n-1)
σ (dB)	8	10	10

For site-general models the loss due to walls, windows and obstructions within a single floor are considered in a very general sense and is accounted for in the path loss exponent. On the other hand, Site-specific models explicitly account for the attenuation from walls, partitions and other obstructions. Typical values of n, FAF and σ for various propagation environments along with attenuation experienced through various building materials are provided in [Rap99].

Indoor channel measurements at 2.4 GHz in an office environment by Jannsen, yielded a path loss exponent of 1.86 (LOS) and 3.33 (OBS) [Jan96].

Recently, radio wave propagation measurements of the attenuation caused by walls and doors in various hospital rooms at 2.45 GHz and 5.2 GHz were performed by Schafer *et al*. Their study was particularly interesting because certain rooms (MRT, X-ray and operating rooms) in hospitals are constructed with walls containing metallic layers in their structure for limiting radiation to safe levels. At 2.45 GHz, they observed that the walls of MRT room, X-ray room and operating room provided very high attenuation of 91.5 dB, 51.3 dB and 61.6 dB respectively in comparison to the unshielded walls of sick-rooms which provided a relatively low attenuation of 6.4 dB. However, in the case of rooms with shielded walls the doors were relatively a weak spot due to slots in the shielding between the door and wall [Sch02]. Table 2.2 provides details on the building materials used in constructing the walls in these rooms and their respective signal attenuation levels. This kind of information can be very useful for planning the deployment of 2.45 GHz wireless devices such as WLANs by network engineers.

Table 2.2

Attenuation Posed by Walls in various Hospital Rooms at 2.45 GHz [Sch02]

Type of Room	Wall/ Door Attenuation (dB)
MRT (copper EMC shielding)	91.5/ 73.2
X-ray (lead shielding)	51.3/ 41.5
Operating Room (CrNi-steel facing/ Trespa™ facing and lead shielding)	61.6/ NA
Sick Room and Treating Room (plaster Board)	6.4/ NA
Sick Room (concrete 27 cm)	35.5/ NA

The IEEE P802.15 Working Group for Wireless Personal Area Networks™ specifies an indoor propagation model at 2.4 GHz given by Table 2.3 [Kam99].

Table 2.3
802.15 WPAN In-building Path loss Model
$f = 2.45\,GHz, \lambda = 0.1124\,m$

Distance	n	Path Loss (dB)
d ≤ 8 m	2	$40.2 + 20\log(d)$
d > 8 m	3.3	$58.5 + 33\log(d/8)$

The IEEE P802.15 WPAN path loss model does not consider the effect of multiple floors but the path loss exponent makes an implicit allowance for the shadowing effect. In fact this model provides a deterministic limit on the range of path loss at a particular distance. Figure 2.1 shows a plot of in-building path loss based on the 802.15 WPAN model as a function of distance.

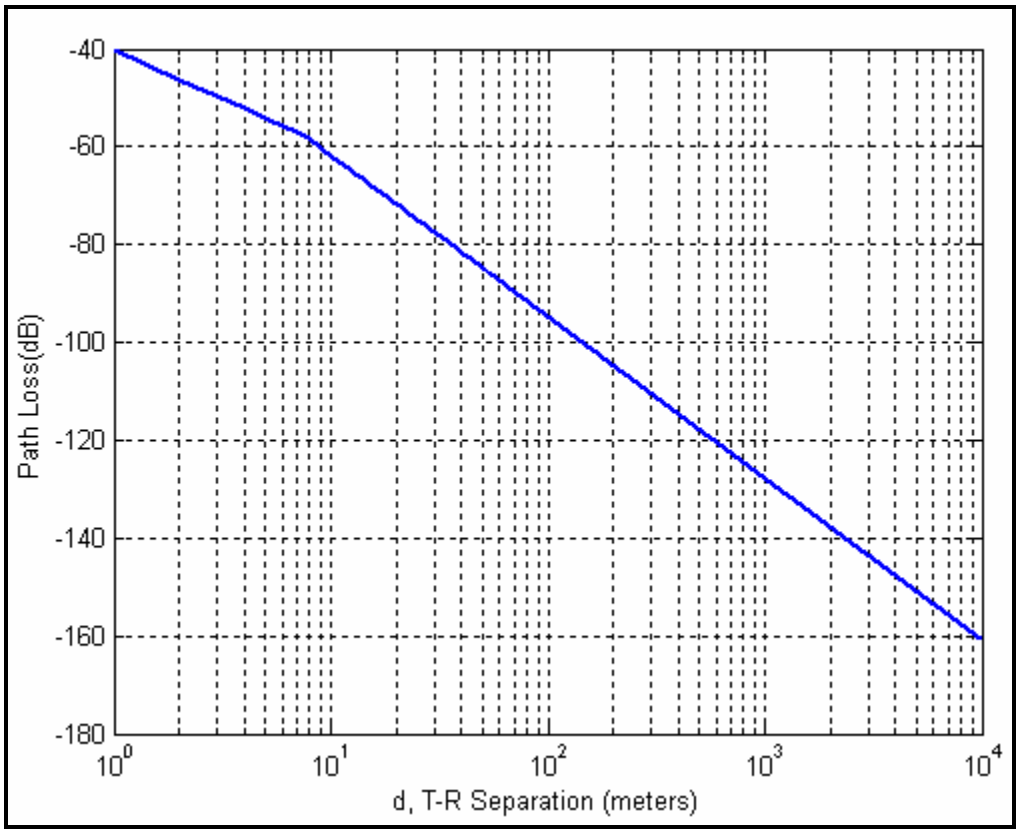

Figure 2.1 Path Loss as a Function of Distance for 802.15 Channel Model

For the analysis and simulation to be presented in Chapter 5, we have adhered to the 802.15 WPAN channel model. This model is widely used for developing and simulating

802.11 and Bluetooth networks in order to study their coexistence. Hence, the use of the WPAN indoor channel model will allow the throughput results to be used and compared on a common platform.

2.2.2 The Antenna Factor – Relating Received Voltage to Measured E-Field

Antenna factor (AF) is one of the most widely used device descriptors in the Electromagnetic Compatibility (EMC) area. However, it is not a part of antenna terminology and is often confused with effective antenna aperture A_e. Antenna factor is the factor by which one would multiply the output voltage of a receiving antenna to obtain the incident electric or magnetic field [Rap99], [Jam], [Smi82], [Sko85]. For example, an antenna factor of 1 implies 1 volt output from an antenna for an incident field strength of 1V/m. The antenna factor is given by

$$AF = \frac{E}{V} \tag{2.8}$$

where, E is the incident electric field in volts/meter, V is the received voltage in volts and AF is in m^{-1}. Using Equations 2.2 and 2.3 we obtain

$$E = \sqrt{\frac{480\pi^2 P_r(d)}{G_r \lambda^2}} \tag{2.9}$$

The input rms voltage V at the antenna is related to the received power $P_r(d)$ by [Rapp99]:

$$P_r(d) = \frac{V^2}{R_{ant}} \tag{2.10}$$

Substituting for $P_r(d)$ in Equation 2.9, we obtain

$$E(V/m) = V\sqrt{\frac{480\pi^2}{G_r \lambda^2 R_{ant}}} \tag{2.11}$$

Hence we arrive at an expression for the antenna factor (*AF*),

$$AF(m^{-1}) = \frac{E}{V} = \frac{2.293\times10^{-7} f}{\sqrt{GR_{ant}}} \tag{2.12}$$

Considering a 50 Ω system and f in MHz,

$$AF(dB/m) = 20\log_{10}(f_{MHz}) - 10\log_{10}(G) - 29.8 \tag{2.13}$$

2.3 Terminology and Units used in EMC

In this section we shall introduce the technical jargons and measurement parameters used by biomedical engineers, doctors and regulatory bodies in the field of EMC. A conversion table is also provided to translate between commonly used units in EMC.

2.3.1 Terminology

EME – Electromagnetic Environment pertains to the environment that contains both electrical and magnetic energy.

EMI – Electromagnetic Interference refers to radiation of electrical and mechanical energy into the environment by a device that may cause malfunction of other devices in the vicinity. An interesting fact is that though EMI refers to interference caused by electric fields and magnetic fields, in most literature it has been used when referring to interference caused by E-fields alone.

EMC – Electromagnetic Compatibility means that a device is compatible with its EME and it does not emit levels of EM energy that cause electromagnetic interference (EMI) in other devices in the vicinity.

RFI – In the early days, when biomedical engineers became aware of electromagnetic interference due to radios, they usually referred it to Radio Frequency Interference.

EM immunity – Electromagnetic immunity of a particular medical device refers to the maximum level of EMI it can withstand for reliable operation. It means that the device has been designed and tested for this level of EMI and if subjected to greater EM fields it may cause malfunctioning of the device.

2.3.2 Units and Conversion Tables for EMI

Measured radiated power and fields can be expressed in a number of units. In fact it has been observed from various literatures on EMI that no standard units are used. However, most regulatory bodies tend to use V/m and dBμV/m when relating to E-field radiations. In our discussion we have resorted to the use of V/m and dBμV/m to characterize all radiate E-fields. Table 2.4 provides methods for conversion between units.

Table 2.4
EMI Conversion Tables

Convert From	To	Function
dBm	dBμV	Add 107 dB
dBm/m^2	dBmμV/m	Add 115.7 dB
dBμV	dBμV/m	dBμV + Antenna Factor (dB/m)
V/m	W/m^2	$(V/m)^2 \div 377$
dBμV/m	V/m	$10^{-6} \times 10^{(dB\mu V/m \div 20)}$

2.4 Electromagnetic Environment in Hospital – A Literature Review

The past three decades have witnessed the rapid increase of radio communication standards and devices. This has led to an intensifying use of the existing RF spectrum and additional allocation of frequency bands. Apart from fixed radio transmitters such as paging antennas, AM and FM transmitters which are primarily outdoors, there has been a proliferation in the use of wireless communication equipment such as handheld radios, cellular phones, paging systems and personal communication systems. The use of

communication equipment therefore has led to an increase in RF energy in the surrounding electromagnetic environment. Meanwhile, advancements in the field of medicine and engineering have created sophisticated and more sensitive medical devices which are even capable of monitoring and controlling life critical functions. The operations of some medical devices heavily rely on their ability to measure very weak biological signals and hence necessitate a 'clean' electromagnetic environment. There have been reported cases of malfunctioning of pace makers, apnea monitors, powered wheel chairs, anesthetic gas monitors and hearing aids due to the use of cellular phones, walkie-talkies and other RF broadcast equipment. Some of these reports were real life incidents which affected patient care and resulted in loss of human life [Sil93],[Sil95], while other reports were based on experimental testing [Don94], [Tan 94], [Tan97], [Tan95a], [Sko98], [Seg95], [Sch96], [Rob97], [Rav96], [Kur98], [Kim95],[Gra98], [Car95]. Silberberg has an excellent compilation of reported incidents on malfunction of medical devices due to EMI. [Sil93] reported an instance wherein a patient monitoring system affected by radiated RF interference failed to detect arrhythmia (disorders of the regular rhythmic beating of the heart) resulting in the death of two patients. In another incident a blood warmer malfunctioned when an electrosurgical unit a few feet away was activated in the cut or coagulate mode.

The importance of human life and patient care has led the medical community to restrict (and in some cases even ban) the use of communication equipment in order to maintain a 'clean' electromagnetic environment [Sil93], [Sil95]. However, with the increasing ubiquitous nature of wireless personal systems, there are a larger number of wireless device users entering and operating in hospitals without the knowledge that they are radiating energy. Moreover the medical community is not completely aware of the impact of external radiators such as AM, FM, cellular base station and TV transmitters and EMI caused by electrostatic discharges (ESDs), power supply lines and microwave ovens [Bas94], [Kri02a] , [Sil95], [All98]. Furthermore, studies have shown medical equipment such as Electro Surgical Units (ESU) and diathermy units produce higher electric fields compared to communication equipment [Ban95], [Boi97], [Nel99].

These factors have led to an increasing concern regarding the safety and reliability of the EME in hospitals and have prompted many researchers from the engineering as well as

the medical community to study the EMC of medical devices, communication equipment and other sources of interference. These studies have helped regulatory bodies such as the Food and Drug Administration (FDA), International Electrotechnical commission (IEC), Association for the Advancement of Medical Instrumentation (AAMI), International Special Committee on Radio Interference (CISPR), The American National Standards Institute (ANSI), the C63 committee (accredited by ANSI) and the Emergency Care Research Institute (ECRI) to define immunity levels for medical equipment and place restrictions on the usage of personal wireless equipment to maintain patient health care and avoid human fatalities. Currently the immunity level for non-life-supporting medical electrical equipment and/or medical electrical systems from radiated RF field is 3 V/m (130 dBμV/m) over the frequency range of 80 MHz to 2.5 GHz and 10 V/m (140 dBμV/m) for life-supporting medical electrical equipment and/or medical electrical systems over the frequency range of 80 MHz to 2.5 GHz [IEC01]. Though the FDA recommends equipment manufacturers to comply by the IEC standard they are not mandatory. Moreover, these regulations pertain to newer equipment and older equipment may not meet these guidelines. Most hospitals continue to use equipment as old as 10-15 years due to the cost associated with replacing them. However, medical devices must withstand incident electric fields of 3 V/m and 10 V/m for non-life-supporting and life-supporting medical equipment in order to operate error free in the presence of unintentional radiators.

Another interesting issue is the location of wireless base stations and communication equipment on rooftops of hospitals. Since hospitals tend to be tall buildings, many wireless service providers especially in cities find their rooftops to be ideal locations for their transmitters. These high RF radiators output extremely high level of radiation which could pose serious EMI for medical equipment inside the hospital building.

In the following sections we shall discuss the research that has been conducted so far on characterizing -

1. RF interference from communication equipment
2. EMI from medical devices

3. EMI from other sources

Finally, we shall discuss about the role of regulatory bodies and the standards that exist for EMC in Europe and the United States.

2.4.1 Radio Frequency E-Fields in Hospitals due to Communication Equipment

The most common sources of RF interference that affect the EME at hospitals can be classified into two categories [Seg96]:

1. **Portable Communication Sources**

Portable sources include walkie-talkies, cellular phones, pagers, PDA's and other hand-held communication equipment.

2. **Fixed Communication Sources**

Fixed sources consist of AM/FM transmitters, TV stations, paging antennas and cellular base stations.

Portable sources have significantly lower transmitted power compared to fixed sources. Walkie-Talkies have power ranging from 2 to 5 watts; cellular phones have power levels ranging from 5 to 600 mW, whereas a commercial FM transmitter broadcasts at up to 100 kilowatts. In order to compare the risk of EMI due to these two classes of sources, we need to consider their distance of separation from the device under test (receiver or medical device) and the propagation characteristics. Considering line of sight (LOS) free space propagation we can predict the electric field E at a distance d from a transmitter with power P_t using Equation 2.6,

$$E(V/m) = \frac{5.5\sqrt{P_t G_t}}{d} \tag{2.14}$$

Assuming the transmitting antenna to be a dipole (G_t = 1.76), Figure 2.2 shows the resultant E-field in V/m as a function of distance due to a 600mW cellular phone, 5 watt

walkie-talkie, a 100 kilowatt FM transmitter and 200 kilowatt TV transmitter. It can been observed that the cell phone, walkie-talkie, FM transmitter and TV transmitter each at distance of 2 meters, 5.8 meters, 824 meters and 1166 meters from a medical device would subject the medical device to the same level (3 V/m) of EMI.

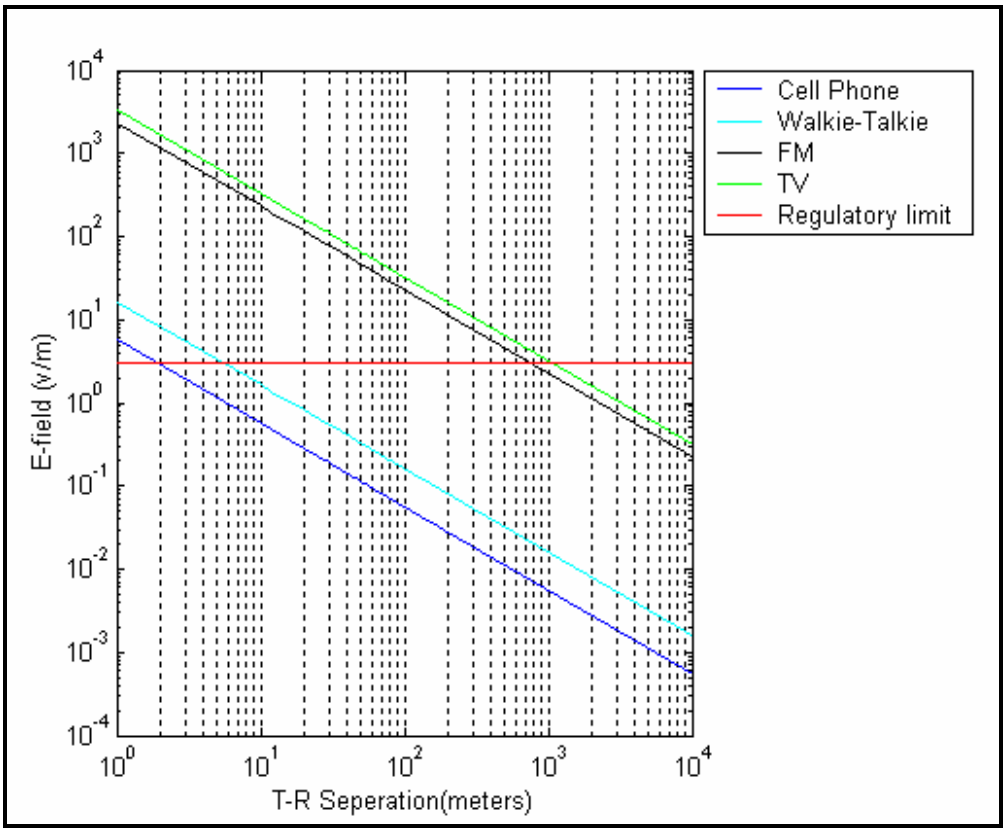

Figure 2.2 E-Field Strength from Fixed & Portable Radio Sources as a Function of Distance

Maximum field strengths at various separation distances under LOS free space propagation for various portable and fixed communication devices were measured by the Center for Devices and Radiological Health (CDRH) and are provided in Table 2.5 [Bas94].

Table 2.5

Maximum Measured Field Strengths for Commonly Encountered RFI sources in Non-Clinical Environment [Bas94]

Source	Category	Power (Watts)	Frequency (MHz)	Field Strength		Distance (meters)	Duty Factor
				V/m	dBμV/m		
Cellular Phone	User Handheld	0.6	824-849	5.3 - 2.6	134.4855 - 128.2995	1 – 2	Medium
Cellular Phone held by person	User Handheld	0.6	824-849	3.1	129.8272	1	Medium
VHF Transceiver held by person	User Handheld	5	154	3	129.5424	2.6	Low
VHF Transceiver held by person	User Handheld	4.3	464	3	129.5424	3	Low
Ambulance Van w/ Roof Antenna	Local	100	155	9	139.0849	4.5	Low
Emergency Jeep	Local	40	155	4	132.0412	4.5	Low
Broadcast TV-VHF	Distant	200,000	48 – 223	3	129.5424	1000	High
Broadcast AM	Distant	50, 000	0.5 – 1.6	3	129.5424	1500	High
Broadcast FM	Distant	100, 000	88 – 108	3	129.5424	830	High

However these measurements were performed in non-clinical environments. It is expected that hospital environments may not have the same LOS free space propagation characteristics. Measurements by Davis *et al.* for a 836 MHz, 600 mW cellular phone show that for a corridor above ground level the E-field as a function of distance was below the free space propagation estimate, whereas for the corridor below ground level the E-field estimate exceeded the free space propagation estimate [Dav99].

EME in Hospital Environments

Initial efforts on characterizing EME in hospitals began in early 1970 [Fra71], [Hof75], [Rug75], [Tol75]. The surrounding EME in hospitals has considerably changed since then due to advancement in medicine and engineering. More recent studies have characterized the RF spectrum in hospitals from 20 MHz to 2 GHz [Arn95], [Ban95], [Boi91], [Boi97a], [Dav97], [Dav98], [Dav99], [Nel99] ,[Pha00], [Vla95a], [Vla95b], [You97]. The sub bands and communication equipment that were of particular interest were fixed FM (87.5 – 108.0 MHz) and TV (Low VHF: 54 - 88 MHz), TV and UHF mobile radio (175 – 806 MHz), hand held mobile radios, (408 – 470 MHz), cellular telephones (824 - 894 MHz), paging systems (925 – 940 MHz), wireless PBX systems (944 – 948.5 MHz) and PCS cellular telephones (1895 – 1990 MHz).

Vlach *et al.* [Vla95a] measured the EME inside and outside five urban hospitals in Montreal, Canada. Table 2.6 summarizes the maximum recorded levels outside for all five hospitals.

Table 2.6

Maximum measured E-fields outside 5 hospitals in Montreal [Vla95a]

Frequency (MHz)	Maximum E-Field	
	V/m	dBμV/m
0 - 50	0.1	100.00
54 - 88	1.7783	125.00
88 - 108	5.31	134.50
138 - 174	0.056	94.96
400 - 470	0.3162	109.99
806 - 890	0.056	94.96
925 - 950	0.1	100.00

It can be seen from Table 2.6 that the highest fields were recorded in the FM and TV bands. The maximum field inside the hospitals was reported as 0.7586 V/m or 117.6

dBμV/m. The measured fields were generally below 3 V/m (130 dBμV/m) which is the regulatory immunity standard for non-critical medical equipment.

Phaiboon *et al.* [Pha00] measured RF interference outside and inside two hospitals in Bangkok. Their frequency range included all the bands as in the Montreal case and extended up to 1918 MHz. Table 2.7 gives a summary of the maximum recorded levels outside and inside for both hospitals.

Table 2.7

Maximum measured E-fields outside and inside 2 hospitals in Bangkok [Pha00]

Frequency (MHz)	Maximum E-Field (Outside)		Maximum E-Field (Inside)	
	V/m	dBμV/m	V/m	dBμV/m
55-88	10×10^{-3}	80	1.26×10^{-4}	42
88-108	100×10^{-3}	100	7.94×10^{-5}	38
138-174	12.6×10^{-3}	82	3.16×10^{-3}	70
400-470	3.16×10^{-3}	70	3.16×10^{-5}	70
806-890	3.16×10^{-3}	70	7.94×10^{-5}	38
925-950	0.8×10^{-3}	58.06	3.16×10^{-5}	30
1895-1990	71×10^{-3}	97.02	3.16×10^{-3}	70

It can be observed from the Table 2.7 that the EMI levels recorded at the Bangkok hospitals were far lower than those recorded in the Montreal hospitals. But the relative maximum levels in both hospitals were recorded in the FM and TV bands.

We shall now look at the EMI levels that have been recorded inside hospitals with emphasis on patient care locations such as Emergency Rooms (ER) and Intensive Care units (ICU). EMI levels at an ICU, Intermediate Care and an ER were recorded in a hospital in Newfoundland and studied by Young *et al.* [You97]. They recorded a maximum EMI of 0.17 V/m (104.6 dBμV/m) over a frequency range of 23-181 MHz in the ICU, 0.115 V/m (101.21 dBμV/m) over a frequency range of 19-186 MHz in the

intermediate care and 0.569 V/m (115.1 dBμV/m) over a frequency range of 0-200 MHz in the ER.

The first study that accounted for EMI level variation as a function of time of day was performed by Davis *et al.* [Dav97], [Dav98]. They performed E-field measurement in an ER over the 0.1-1 GHz range over 4.4-day period. Table 2.8 summarizes the recorded fields inside the ER.

Table 2.8

Maximum measured E-fields inside an ER [Dav97], [Dav98]

Frequency (MHz)	Maximum E-Field	
	V/m	dBμV/m
0-30	0.2	106.02
30-50	0.25	107.96
54-88	0.12	101.58
88-108	2.5	127.96
138-174	5.6×10^{-3}	4.96
400-470	0.56	114.9638
806-890	0.32	110.1030
925-950	5.6×10^{-2}	94.96

Similar to previous results, the maximum EMI level was recorded in the FM band. The most important and interesting aspect of this work was the recorded variation of EMI levels as a function of time of day. Davis et al. were able to conclude that most of the activity tended to take place during the day and early evening. The 0.8-0.9 GHz band exhibited high activity during the day and early evening, increased activity over weekends and reduced activity during midnight. This phenomenon was attributed to the usage of cellular phones. In contrast the 0.4-0.5 GHz band exhibited uniform activity during weekdays and an increased activity during weekends. This was attributed to the use of walkie-talkies by paramedical personnel. However, all EMI levels recorded were far below the 3 v/m (130 dBμV/m) immunity level.

Recently the 2.4 GHz ISM band has evoked great deal of interest in the health care sector. This is primarily because short-range wireless devices such as Bluetooth and WLANs are potential technologies for medical applications. So far there are no reported measurements or results on EMI for the complete 2.4 GHz ISM band in hospitals. [Tan01] has performed EMI measurements on a WLAN system operating at 2.42 GHz. The WLAN system generated an E-field of 0.1 V/m (100 dBμV/m) at separation distance of 1 meter from the antenna. The background EMI in the hospital test sites at 2.42 GHz was measured to be below 0.1 V/m.

2.4.2 Radio Frequency E-Fields in Hospitals due to Medical Equipment

Although several studies have shown the impact RF interference on hospital EME from fixed and portable communication sources, there exist very few materials on the E-fields caused by medical equipment. Electrosurgical units (0.5 – 5 MHz) and diathermy units (27.12 MHz) have been found to produce E-fields greater than those produced by communication equipment. Electrosurgical units (ESU) and diathermy units involve the passage of high frequency alternating current through body tissue for cutting body tissue or for coagulation. Fields exceeding 30 V/m (150 dBμV/m) were measured 30 cm away from an ESU in an urban hospital [Boi97], however the frequency of operation was not recorded. In another measurement effort, [Nel99] found that fields as strong as 44.6 v/m (153 dBμV/m) were experienced at a distance of 1 meter from the ESU operating at 0.75 MHz. The ESU in both these cases was operating during surgical procedures in the Operating Room (OR).

2.4.3 Interference in Medical Environment due to other Sources

Apart from RF sources and medical equipment which cause EMI, there exist other sources of interference such as microwave ovens, power supply lines and electrostatic discharges (ESD).

Microwave ovens have caused malfunction of cardiac pacemakers in the past. The FDA and the Association for the Advancement of Medical Instrumentation (AAMI) through a combine effort found solutions for the manufacturers of both pacemakers and microwave ovens [Hoo97]. However, since microwave ovens operate at 2.4 GHz they might affect the performance of wireless devices operating in the ISM band [Kri02b].

Power supply lines are associated with conducted susceptibility which poses a serious problem with digital logic families [Ban95]. EMI from power supply have caused malfunction of apnea monitors [Sil95]. Also, ESD can cause catastrophic damage by causing a voltage failure in a device [All98]. Malfunctioning of infant radiator warmers, infusion pumps and apnea monitors due to ESD induced EMI have been reported [Sil95].

2.4.4 Regulatory Bodies and Standards for EMC

United States of America

In the United States, the Food and Drug Administration (FDA) has federal responsibility for the safety and effectiveness of medical devices. The Center for Devices and Radiological Health (CDRH) is a part of the FDA and was formed in 1982 by integrating the Bureau of Radiological Health and the Bureau of Medical Devices [Hoo97]. The CDRH has regulatory authority over several kinds of medical devices from various manufacturers and addresses concern for the public health and safety. It has been in the forefront of testing EMC of medical devices, RF equipment as well as other devices which may pose a threat to health care. The first standard on Electromagnetic Compatibility for Medical devices was published in 1979 [And96], although standard was not mandatory and the test methods used were not harmonized with the international

standards. The American National Standards Institute (ANSI) C63 committee (accredited by ANSI) and the Emergency Care Research Institute (ECRI) have worked together with the FDA to develop standards, guides and recommended practices [Hoo97], [Hoo98], [Kni95]. However, the FDA has no concrete EMC standard of its own and primarily depends on the recommendations of the International Special Committee on Radio Interference (CISPR). The CISPR is operated under the auspices of the International Electrotechnical commission (IEC) and is responsible for the IEC 60601-1-2 standard that specifies general requirements for safety, electromagnetic compatibility and electromagnetic immunity levels [IEC01, IEC02]. Though the FDA recommends medical equipment manufacturers to comply by the IEC 60601-1-2 standard, it is not mandatory. Canada, Australia and Japan also follow the IEC 60601-1-2 standard.

In order to facilitate characterization of EMI using standard test methods, the IEEE has developed a standard, IEEE-Std 473-1985. This is again a voluntary standard and provides recommended practices for electromagnetic surveys in the 10 kHz to 10 GHz range.

Europe

The market for medical devices in Europe is second only to that of the United States. Initially there existed two standards in Europe, the Medical Device Directive (MDD) and the EMC Directive. All medical devices sold in Europe were required to comply by one of the directives. The EMC directive has been mandatory since January 1996 and the MDD become mandatory in June 1998. Currently both these standards have been harmonized to the IEC 60601-1-2 standard and are known as the EN 60601-1-2 European standard [And96].

2.5 Summary

In this chapter, a brief overview of radiowave propagation theory and application was presented. These basic concepts laid the necessary foundation for understanding the variation of radiated power and incident E-fields from RF sources and medical devices as a function of T-R separation. The main objective of this chapter was to review published literature that examined hospital environments, communication devices and medical

devices and provide an insight into the electromagnetic environment existing in hospitals. Key results for frequency ranges up to 2 GHz have been presented and analyzed. Observing and studying the EMI levels recorded inside and outside hospitals we can conclude that RF interference in each hospital environment is dynamic and time varying [Boi91], [Arn95], [Vla95b], [Boi97a], [Tan95b], [Tan01]. The RF interference levels recorded in a hospital are dependent on location, time, frequency, density of medical devices and proximity to fixed and portable communication sources.

The evolution and role of standards and regulatory bodies in this field have also been discussed. Current regulations for EMC of medical devices in Europe and USA have been presented.

Research conducted in hospitals so far have considered frequency ranges only up to 2 GHz. However, there are short-range wireless devices such as Bluetooth and WLANs which operate in the 2.4 GHz ISM band and fall under the category of portable communication sources. These devices are expected to lead the industry in creating wireless medical applications and could proliferate in hospital environments. Currently many modern hospitals possess WLAN infrastructure for transferring patient records. The RF interference due to WLANs and the background EMI cause by medical equipment in the 2.4 GHz ISM band in hospitals has not been characterized. The EMI data and analysis for the 2.4 GHz ISM band has a two fold importance:

1. The medical community can be informed about the EMI risk to life-support devices due to wireless devices operating in the ISM band.

2. The engineering sector which seeks to develop medical applications can predict performance and improve the Quality of service (QoS) of their wireless products based on prior knowledge of interference levels.

Chapter 3 will discuss the design and implementation of a software reconfigurable measurement system 'PRISM' for the 2.4 GHz ISM band. Chapter 4 will present results for EMI in a hospital environment at 2.4 GHz measured using PRISM.

Chapter 3

3 PRISM – A Software Reconfigurable Interference Measurement Device

3.1 Introduction

The 2400-2483.5 MHz frequency band, also known as the ISM (Industrial, Scientific, and Medical) band, is a license free band allocated for a variety of consumer applications. While no license needs to be purchased to operate devices in this band, regulations exist. Part 15 of FCC code, limits not only output power, but also channel bandwidth and air interface on wireless devices. Furthermore, devices such as microwave ovens also operate around this band, and they have different restrictions than communications systems.

Devices in this band are expected to operate with no central coordination, therefore Part 15 directs that they employ either frequency-hopping or direct-sequence spread spectrum. Because devices can be deployed in this environment without an exclusive license for their use, it is viewed as an interference-prone band inappropriate for critical applications, since there are no guarantees on interference levels.

In spite of these drawbacks, use of the ISM band by Part 15 devices has attracted a number of applications, such as IEEE 802.11b, HomeRF, Bluetooth, and cordless phones. Other more exotic applications such as sulfur plasma lighting have also been suggested [Aeg00].

The plethora of devices using the ISM band can however create a chaotic signal environment. It is therefore desirable to measure the interference in this environment to analyze its impact on the functioning of devices operating in the ISM band. PRISM (PRobe ISM), a software reconfigurable passive measurement device was designed and developed for studying the frequency spectrum of the ISM band. In addition to the 2.4

GHz ISM band, PRISM can be configured to perform spectrum measurements between 9 kHz and 2.9 GHz.

The chapter is organized as follows: Section 3.2 discusses the need for a software reconfigurable interference measurement system. In Section 3.3 the system architecture of PRISM is presented. The hardware for the system is also described in detail. Section 3.3 also describes the software, instrument control and data logging features of PRISM. In Section 3.4 the post processing of measured data is discussed. Finally we draw a short chapter summary in Section 3.5.

3.2 Need for a Software Reconfigurable Measurement System

Currently no commercially off the shelf equipment exists that has both the versatility to characterize EMI, as well as well as the ability to monitor and diagnose interference from a remote location via the internet. A typical frequency domain measurement device consists of an RF front end and a spectrum analyzer operating in the frequency band of interest. The RF front end is made up of an antenna capable of receiving signals in the desired frequency bands. The frequency range of interest, amplitude scale and sweep settings are manually entered into the spectrum analyzer and the spectrum pertaining to those frequencies are viewed on the display of the spectrum analyzer. Details pertaining to strength and frequency of signals observed are recorded manually by freezing snap shots on the display. However, this manual method is tedious, cumbersome and error prone. Furthermore, when non-contiguous frequency bands needs to be observed and critical data recorded over a period of days it becomes impossible to use the manual approach.

The need for a software reconfigurable measurement device that could be programmed and controlled in software was the motivation behind the design of PRISM. Moreover, at this early point in the development of the medical-wireless market, spectrum surveillance and diagnosing system which could be monitored offsite via the internet can be a very valuable tool and could find a place as standard equipment for a

typical health care provider. Figure 3.1 shows a typical application for a miniaturized version of PRISM in a modern hospital. The measurement system can be placed at locations of interest and the measured EMI can be continuously transmitted via the existing LAN or WLAN infrastructure. A central control unit (CCU) can continuously monitor and diagnose the data. Additionally, pre-defined safe levels can be set for various locations depending on the nature of environment. When the levels are exceeded, an alarm will trigger at the CCU allowing corrective measures to be enacted.

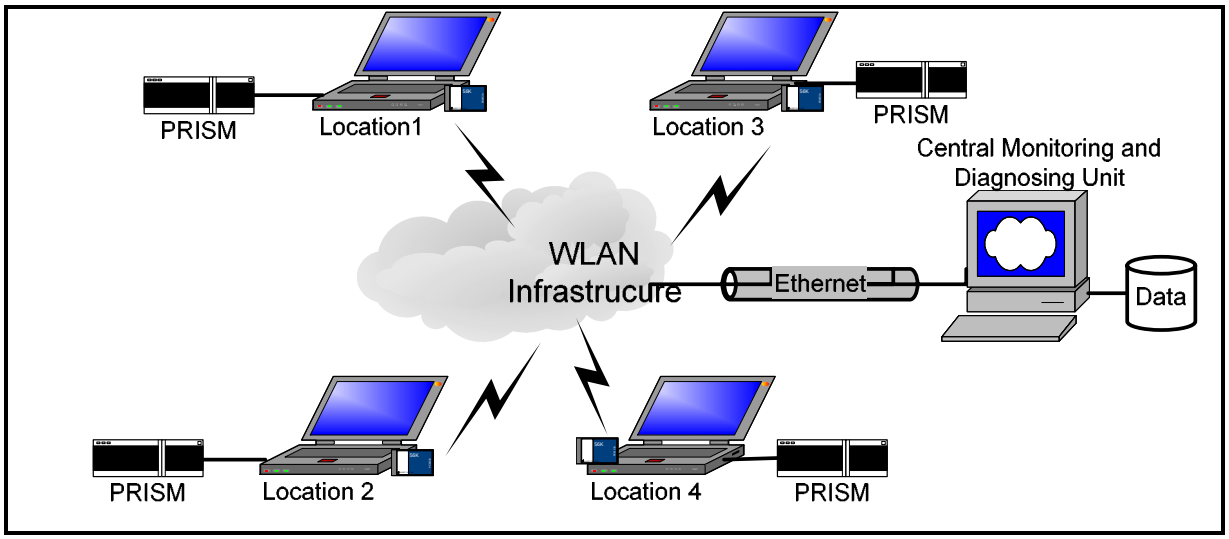

Figure 3.1 Typical Application of PRISM in a Modern Hospital

3.3 System Architecture

PRISM's basic building block consists of an RF front end, an HP 8594E spectrum analyzer with a General Purpose Interface Bus (GPIB) interface card, and a PC with a GPIB interface card. PRISM's software written in LabVIEW allows communication between the hardware and PC via a GPIB cable. Figure 3.2 shows the system model of PRISM.

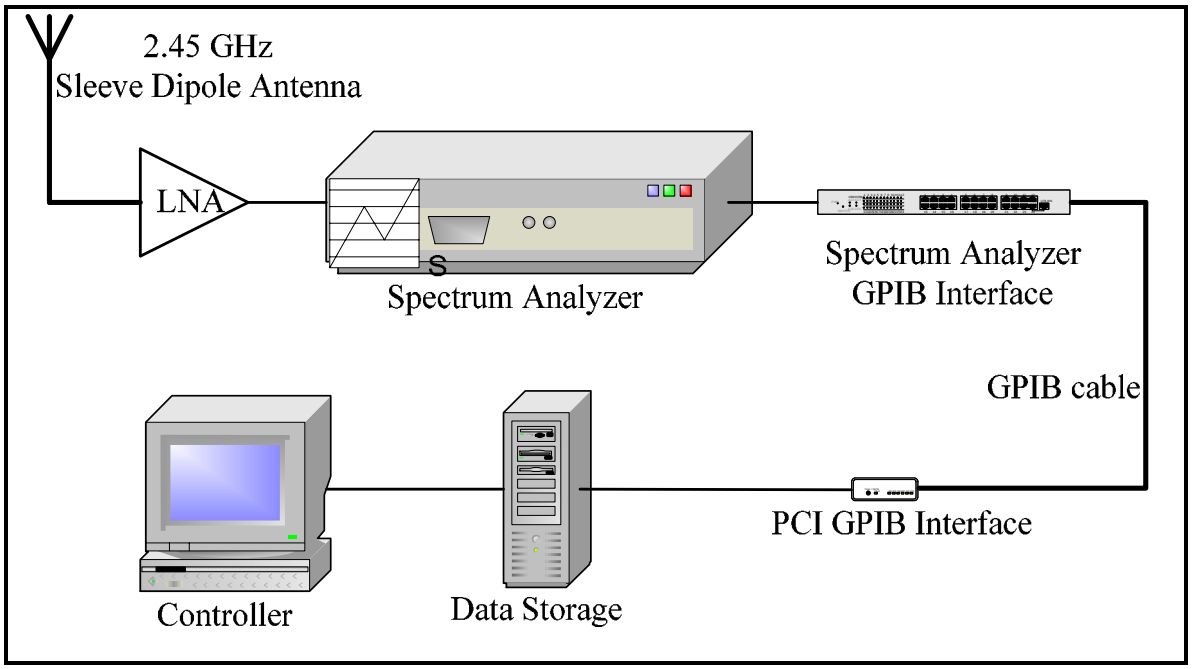

Figure 3.2 System Model of PRISM

Using PRISM's software, control signals are sent to the spectrum analyzer via the GPIB cable. The software has full control and graphical representation of all the settings found on the front panel of the spectrum analyzer and can be simultaneously viewed on PRISM's Graphical User Interface (GUI). Moreover, recorded data is polled by the computer at specific intervals and stored in user-desired format. PRISM's post processing MATLAB software suite channelizes the recorded interference into user defined channels (e.g. Bluetooth, WLAN) and generates 3-D plots showing spectral occupation, signal strength and time of occurrence.

3.3.1 RF Front End Design Considerations and GPIB Hardware

PRISM's hardware consists of a RF front end and a Hewlett-Packard 8594E spectrum analyzer. The RF front end consists of a 2.45 GHz sleeve dipole antenna and a Low Noise Amplifier (LNA).

3.3.1.1 Spectrum Analyzer – Hewlett Packard 8594E

PRISM uses a HP 8594E spectrum analyzer for performing frequency domain spectrum measurements. The HP 8594E is an easy-to-use RF spectrum analyzer that offers a wide range of performance. Table 3.1 provides some of the basic specifications of HP-8594E. Detailed specifications are provided in [HPA95].

Table 3.1
Hewlett-Packard 8594E Frequency and Amplitude Specifications

Category	Range
Frequency Range	9 kHz to 2.9 GHz
Frequency Span	0 Hz (zero span), 10 kHz to 2.9 GHz
Frequency Sweep Time	20 ms to 100s
Resolution Bandwidth	1 kHz to 3 MHz
Amplitude Range	-112 dBm to 30 dBm
Noise Figure	30 dB

The HP-8594E is no longer manufactured and has been replaced by the Agilent 4402B ESA-E Series Spectrum Analyzer (30 Hz to 3.0 GHz).

3.3.1.2 RF Front End of PRISM

The front end of a receiver is one of the most critical elements in a wireless system. The purpose of the RF front end is to isolate the desired signal from out of band interference and noise [Ree02]. The choice of components in the receiver's RF front end ultimately decides the integrity of the received signal.

This section describes the design issues related to the RF front end of the measurement system, specifically the choice of antenna design and concerns on receiver sensitivity.

Antenna Design and Issues

An antenna is simply a transducer, which converts electromagnetic wave propagated in space to a radio frequency electrical energy fed to receiver. This process is reciprocal in nature. The length of the antenna is inversely proportional to the operating frequency.

Since PRISM was designed to be operated in the 2.4 GHz ISM, the antenna was expected to have a small mechanical size (at 2.45 GHz, $\lambda = 0.1224m$). Therefore, for our application we chose a coaxial sleeve dipole design [Stu81] as shown in Figure 3.3.

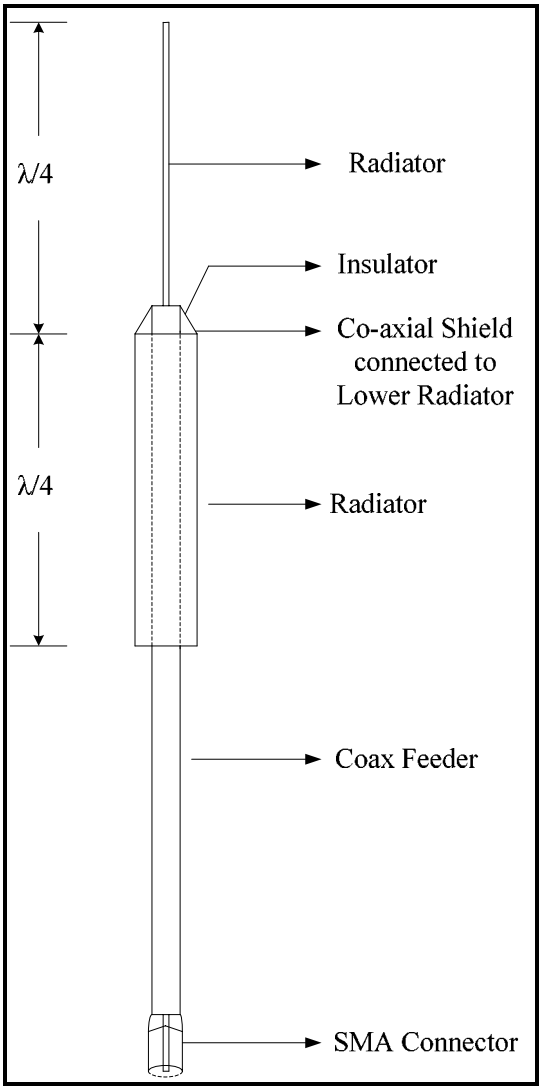

Figure 3.3 Coaxial Sleeve Dipole Antenna

The antenna was designed and built using a copper tube, coaxial cable and an SMA connector. The electrical characteristics of the antenna were measured using a network analyzer and the radiation patterns were measured in an anechoic chamber. Table 3.2 gives the antenna parameters and Figures 3.4(a) and 3.4(b) show the azimuth and elevation radiation patterns respectively of the 2.45 GHz sleeve dipole antenna.

Table 3.2

Antenna Parameters of Custom made Vertically Polarized Coaxial Sleeve Dipole Antenna

Parameter	Value
Characteristic Impedance	50Ω
VSWR	1.478:1
Gain	≈1.64
Center Frequency	2.45 GHz
VSWR Bandwidth (3 dB)	160 MHz

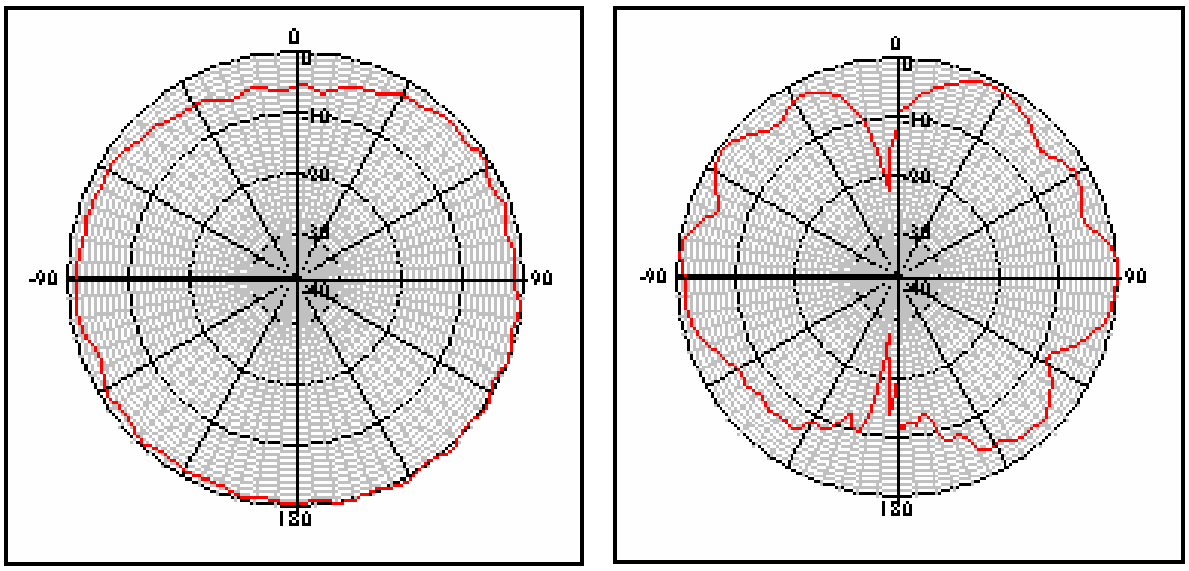

(a) **(b)**

Figure 3.4(a) Azimuth and (b) Elevation Patterns of 2.45 GHz Sleeve Dipole Antenna

Receiver Sensitivity

A receiver's sensitivity is defined by the smallest possible signal that can be received by the receiver. It is determined by the overall noise added by all of the sub-systems in the receiver chain to the thermal noise floor. In a communication system, receiver sensitivity plays an important role in the systems overall SNR which in turn determines link quality and probability of error. Noise Figure is a convenient metric that defines the receiver sensitivity.

In a receiver, the signal strength of the received signal is influenced by the propagation characteristics of the environment. These propagation characteristics can be modeled in a wide variety of ways. However, the overall receiver noise is determined by the gains and noise figures of the sub-systems in the receiver chain, as well as the ambient noise temperature at the antenna [Rap99]. Noise Figure of a receiver is a parameter that takes into consideration these details and allows the user to deal with a single metric. The principle behind the use noise figure is that the noise levels of the sub-systems in the receiver chain can be referred to an equivalent level at the receiver input [Cou97].

Like gain, noise figure can be expressed as a ratio given by F [Rap99],

$$F = \frac{\text{Measured noise power out of device at room temperature}}{\text{Power out of device if device were noiseless}} \tag{3.1}$$

For a cascaded communication system with sub systems in the receiver chain having gains G_1, G_2, G_3 …G_N and noise figures F_1, F_2, F_3….F_N respectively, the overall noise figure of the receiver F_{system} is given by

$$F_{system} = F_1 + \frac{F_2 - 1}{G_1} + \frac{F_3 - 1}{G_1 G_2} + ... + \frac{F_N - 1}{G_1 G_2 G_3 .... G_{N-1}} \tag{3.2}$$

From Equation 3.2 it can observed that the cascaded noise figure F_{system} is affected most profoundly by the noise figure of the components closest to the input of the system as long as some positive gain exists in the cascade.

Low Noise Amplifiers

The LNA is an indispensable element of a communication system and provides the first level of amplification of the signal received at the antenna. It therefore has the greatest impact on the noise performance of the system. The main function of the LNA is to amplify extremely weak signals without adding noise, thus preserving required signal to noise ratio of the system at extremely low power levels. Furthermore, for large signal levels, the LNA amplifies the received signal without introducing any distortions, preserving waveform quality.

PRISM uses a broadband linear low noise amplifier with a maximum noise figure of 1.5 dB and minimum gain of 25 dB. Using Equation 3.2 the Noise Figure of PRISM was calculated to be 6.5 dB.

Table 3.3 gives the specifications of Mini-Circuits ZQL-2700MLNW LNA [Min01] used in PRISM.

Table 3.3
Specifications of Mini-Circuits ZQL-2700MLNW LNA [Min01]

Frequency (MHz)	NF (dB)	Gain (dB)		Maximum Power (dBm)		IP3 (dBm)	VSWR		DC Power	
	Max	Flatness		Output (1 dB Comp.)	Input (no damage)		Max		Volt (V)	Current (mA)
		Min	Max	Typ		Typ	In	Out		
2200-2400	1.3	25	±1	25	+3	+38	1.25:1	1.15:1	15	325
2200-2700	1.5	25	±2.3	25	+3	+38	1.25:1	1.15:1	15	325

3.3.2 Communication Using GPIB

The General Purpose Interface Bus (GPIB) was originally developed by Hewlett-Packard in the late 1960s. It was developed to connect and control programmable instruments, and to provide a standard interface for communication between instruments from different sources [Nai02]. It was initially referred to as HP-IB, since this technology was developed primarily for instruments manufactured by Hewlett-Packard.

The HP-IB gained immense popularity in the industry and there was a requirement for a standard interface that would allow communication between instruments and controllers of various vendors. In 1975, the Institute of Electrical and Electronics Engineers published the ANSI/IEEE 488-1975, IEEE Standard Digital Interface for Programmable Instrumentation. This standard set the guidelines for mechanical, electrical and functional specifications of an interface [Nai02]. The primary standard underwent a revision in 1978 for editorial changes. In 1990 the IEEE 488.2

standard was released, the initial IEEE 488 was renamed as IEEE 488.1. The new standard was introduced to increase the functionality of the IEEE 488.1.

3.3.2.1 Instrument Control using IEEE 488

GPIB (IEEE 488-1975) is a digital, 8-bit parallel communications interface with data transfer rates of up to 8 Mbytes/s. The bus has two 24-pin connectors and allows one system controller (usually a computer) to be interfaced to a maximum of 15 instruments, called devices.

Devices are assigned a unique primary address, ranging from 0-30, by setting the address switches on the device. Secondary addresses are optional and can also be specified. The secondary addresses can be set to 0 or range from 96-126.

To achieve maximum data transfer rate, cabling between controller and a single device should be limited to less than 20 meters and between devices it should be limited to 2 meters. These restrictions can be relaxed by using a bus extender.

The IEEE 488 standard is very versatile in that it can be used in almost any instrument. This is because unlike other standards, IEEE 488 does not consider the operations and functions of the instrument or its data; it merely acts as a separate controller interface that can be added to the instrument on an as needed basis. Most RF lab equipment such as network analyzers, spectrum analyzers, logic analyzers have an on-board GPIB interface or provisions for a GPIB interface card to be installed.

Devices that are connected to the IEEE-488 bus fall under three categories:

1. **Listeners** – devices that can receive data when instructed by the controller e.g. oscilloscope, network analyzer, PC. Up to 14 listeners can receive data at a given time.
2. **Talkers** – devices that can transmits data onto the bus when instructed by the controller e.g. oscilloscope, network analyzer, PC. Only one talker can communicate at a given time.
3. **Controllers** – devices that can enable a talker to transmit and a group of listeners to receive data, thereby allowing communication between listeners, e.g. a GPIB PCI card installed in a PC or a GPIB PCMCIA card installed in a laptop. A GPIB

system may contain multiple controllers but only one Controller can be active at a given time. Among the many possible controllers in a GPIB system, there exists one Controller that is designated as the System Controller. When the Controller is not transmitting, the Talker can transmit thereby allowing the Controller to be a Listener [Mat02].

From the above discussion we can observe that it is possible for a device to don the role of one or more of these functions. However, a minimum GPIB system should include one Controller and one Talker or Listener device.

3.3.2.2 Instrument Control and Automation of HP 8594E

One of the key building blocks that constitute PRISM is the spectrum analyzer. Though PRISM is an acronym for 'PRobe ISM', PRISM is capable of performing frequency domain measurements for cellular, PCS and other hand-held mobile radio bands. The change in frequency bands is completely software reconfigurable within the limits of the spectrum analyzer. Moreover, PRISM can be set to monitor and simultaneously record data over non-contiguous frequency bands. Figure 3.5 shows the setup of the measurement system.

Instrument control and communication was achieved using a GPIB interface installed in the spectrum analyzer connected via a GPIB cable to a National Instruments plug-in GPIB PCMCIA interface card installed in a PC. PRISM's software resides in the PC and controls the frequency, amplitude, sweep, and bandwidth settings of the spectrum analyzer. The software also allows the user to specify the sampling rate, recording intervals and also the format and location of the file in which data recorded from spectrum analyzer is to be stored. Although PRISM's software was designed to operate a HP 8594E spectrum analyzer using a GPIB interface, it is generic enough that it can be used to operate any of the HP 8590E series analyzers using a parallel or serial interface by specifying the changes in PRISM's software.

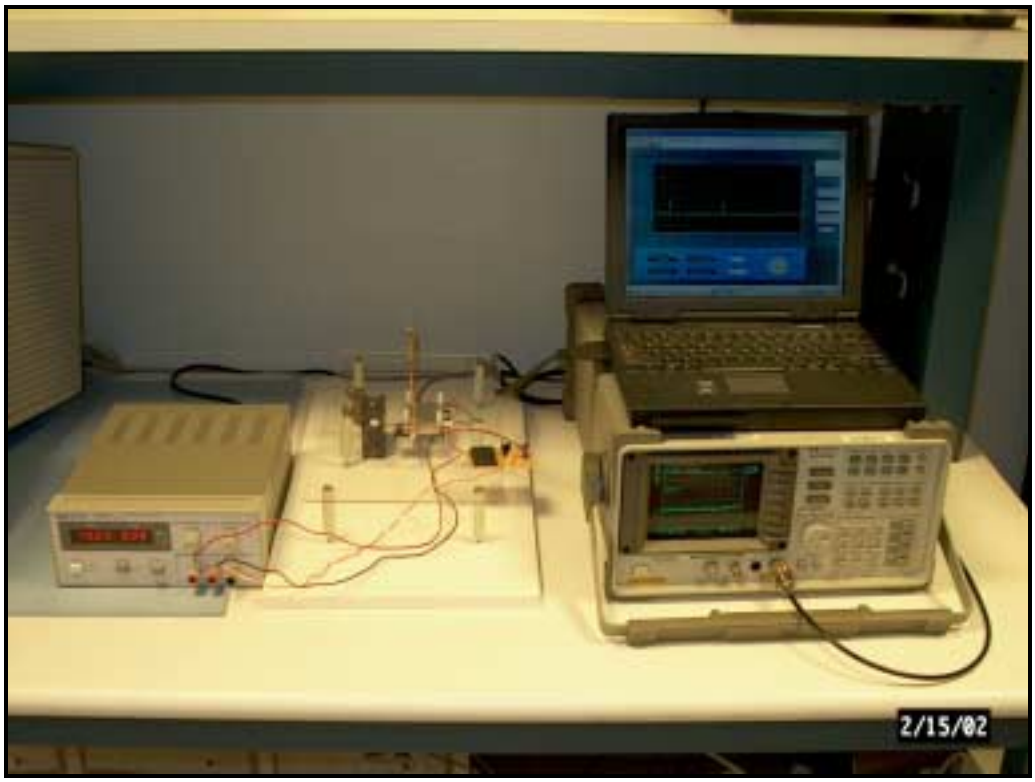

Figure 3.5 Hardware Setup of the Measurement System - PRISM

3.3.2.3 Configuring Hardware for Instrument Control

In order to use software to talk to the instrument and to control it, we need to have prior knowledge of the device address. Devices are assigned a unique primary address, ranging from 0-30, by setting the address switches on the device. The device address can be detected using National Instrument's Measurement and Automation Explorer tool. This tool is primarily used for installing, trouble shooting and configuring GPIB interfaces. Once the corresponding device address has been detected, the address can be used to send and receive commands and data to the instrument.

3.3.3 Software for Instrument Control, Data Acquisition and Post Processing

After having configured the spectrum analyzer to communicate with the PC and perform simple read/write commands through the GPIB interface, an instrument control and data acquisition driver was created for PRSIM. This software was developed in LabVIEW

using modular programming combined with text based instrument specific commands [Hpp95]. The text based instrument specific commands were used for optimizing the overall software architecture in order to reduce the hardware delay in configuring and fetching trace data.

3.3.3.1 LabVIEW

LabVIEW is a graphical programming environment that is used for instrument control, data acquisition, measurement analysis, process monitoring and data visualization. The versatile graphical development environment of LabVIEW gives tools to create and program applications without writing any text-based code and provides an intuitive environment for programmers. Moreover, instrument drivers for various signal generators, oscilloscopes, and spectrum analyzers compatible with LabVIEW are readily available. These instrument drivers reduce development time and the learning curve involved in creating the interface.

3.3.3.2 Instrument Drivers

An Instrument Driver is a set of software routines that allows a PC to control a programmable instrument [Nai02]. These operations include resetting, configuring, reading from, writing to, and activating the instrument and allow the end user to operate the instrument from the PC just as if he were sitting at the bench, entering data into the instrument front panel. An instrument driver simplifies programming and allows the user to develop the application for without any knowledge of the exact programming protocol for the instrument.

PRISM uses a National Instruments certified instrument driver written in LabVIEW and uses the Virtual Instrumentation Software Architecture (VISA). The VISA architecture provides a standard foundation for development and interoperability of instrument drivers for various I/O interfaces. This feature allows PRISM to be operated using either a serial interface or a parallel interface.

Figure 3.6 shows a high level block diagram of PRISM depicting the software and hardware dependencies.

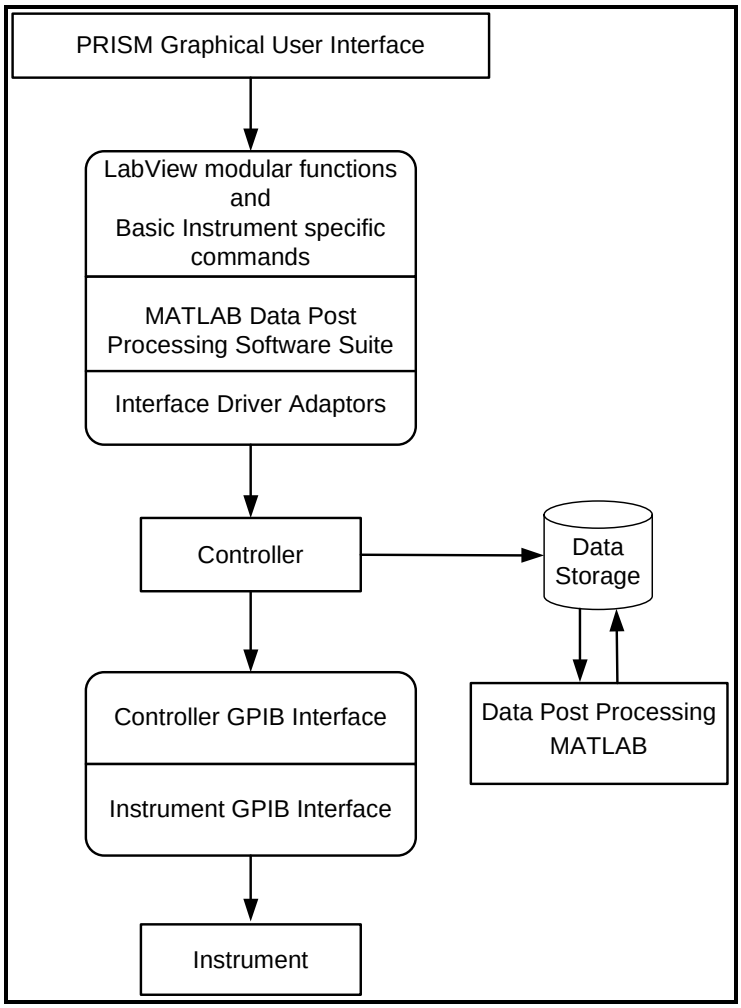

Figure 3.6 High Level Block Diagram of PRISM

3.3.3.3 PRISM's GUI and Web Interface

Figure 3.7 shows a flowchart for PRISM describing the sequence of commands passed by the software to the hardware before a measurement is recorded.

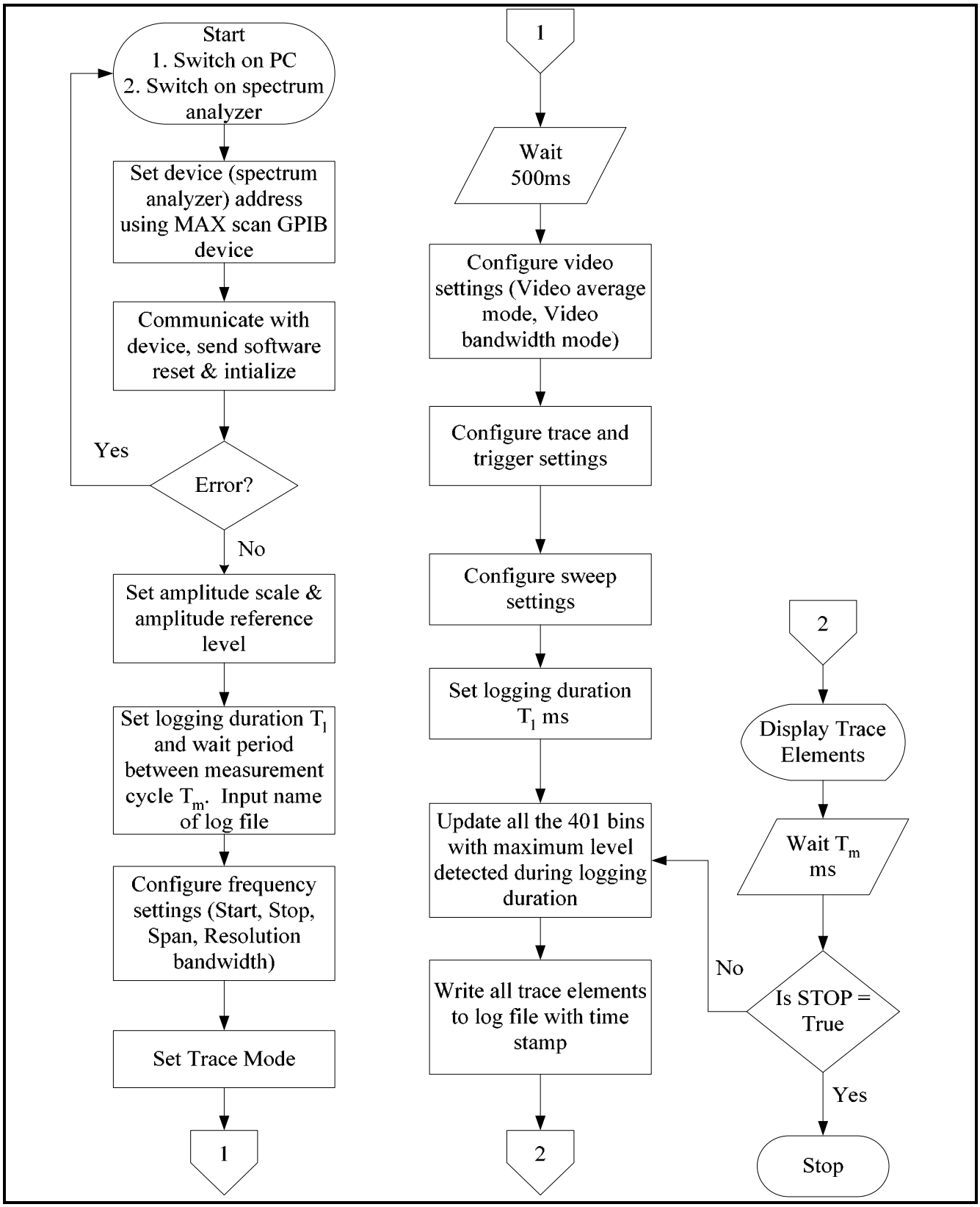

Figure 3.7 Flowchart for PRISM describing the sequence of commands between software and hardware

The software controls for configuring the amplitude, frequency, sweep time, video and trigger settings are provided on PRISM's GUI. Figure 3.8 shows a screen shot of the GUI. One of the key features of PRISM is its user friendly GUI. The user can set the parameters for the measurement and can simultaneously view and record the measured data.

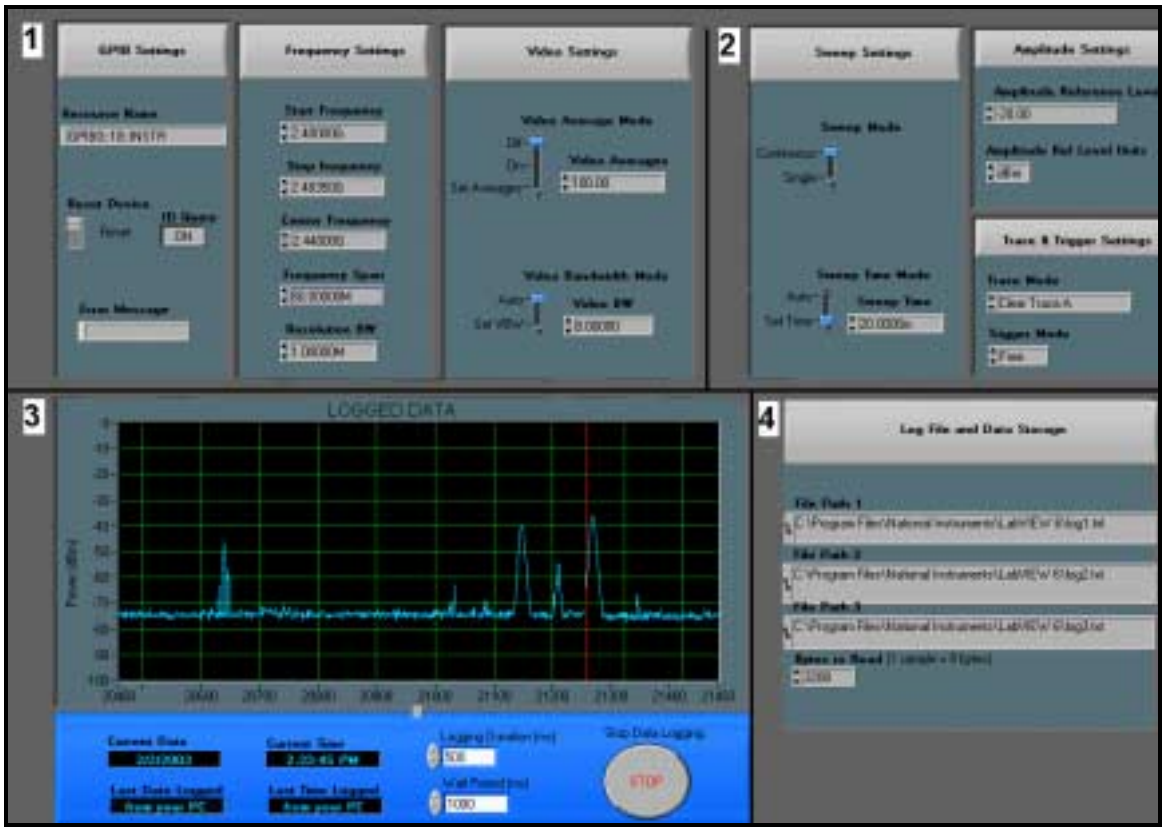

Figure 3.8 Graphical User Interface of PRISM

For the purpose of clarity, Figure 3.8 has been subdivided into 4 sections and is described with individual snapshots. Figure 3.9 shows the dialogs that allow the user to control the GPIB, frequency and video settings (segment 1). The GPIB settings dialog allows the user to specify the device address and displays any error messages. The user can then perform a software reset. The frequency settings dialog allows the user to specify the center frequency, frequency span and resolution bandwidth corresponding to the spectrum under investigation. The resolution bandwidth is the minimum bandwidth over which two signals have to be separated in order to be viewed as two separate signals on

the display. A higher resolution bandwidth will increase the noise floor power and prevent very weak signals from being observed and recorded. The video setting of the spectrum analyzer are controlled using the video setting dialog. The video bandwidth impacts how well spectrum analyzer's circuitry (post-detection low-pass filter) filters noise. A narrower bandwidth will result in filtering more noise, but the tradeoff is increasing the sweep time of the spectrum analyzer [Mar02].

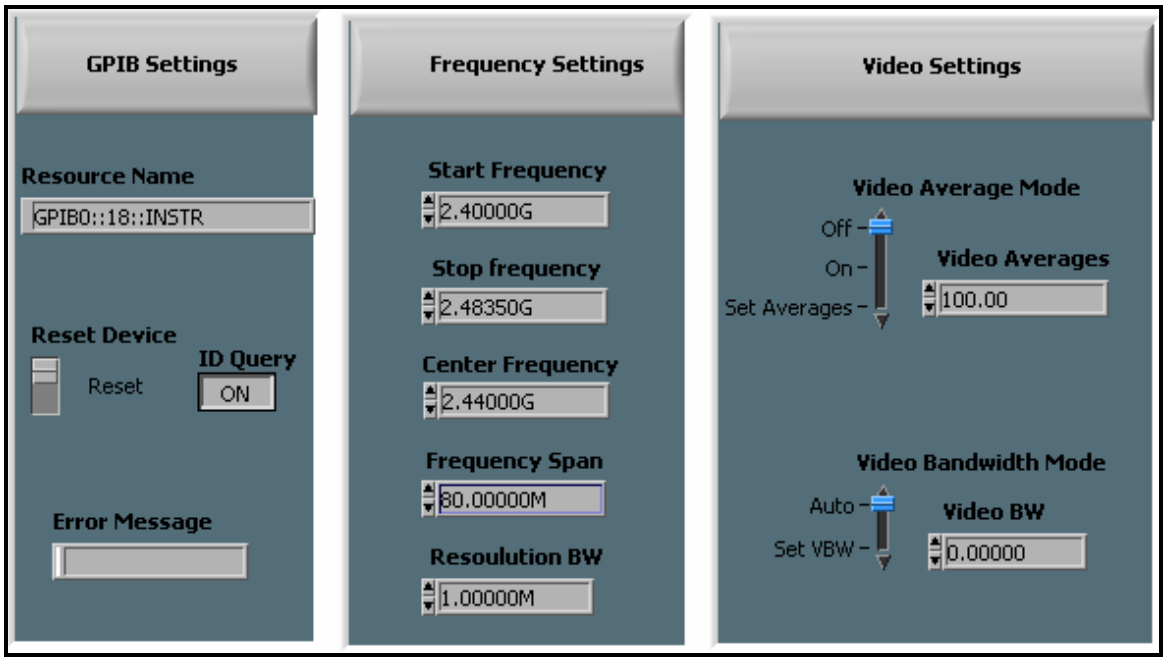

Figure 3.9 Dialog for Configuring GPIB, Frequency and Video Settings

The sweep, amplitude, trace and trigger settings are regulated by the dialog shown in Figure 3.10 (segment 2). The sweep setting allows the user to specify the sweep time, i.e., the time required to sweep the frequency range specified by the user. The HP 8594E is limited by a maximum sweep rate (fastest rate) of 20 ms. The trigger setting gives the user the option of sweeping the frequency band based on continuous mode (free trigger), or trigger based on an external voltage supply, or trigger with the AC line. The amplitude settings determine the maximum range of signals that can be measured and its unit (dB, dBmV, dBµV, V, W). The trace setting specifies the trace (Trace A or Trace B) to be used when operating the spectrum analyzer.

However, selections of the sweep time, resolution bandwidth, video bandwidth are all interrelated and they involve some tradeoffs.

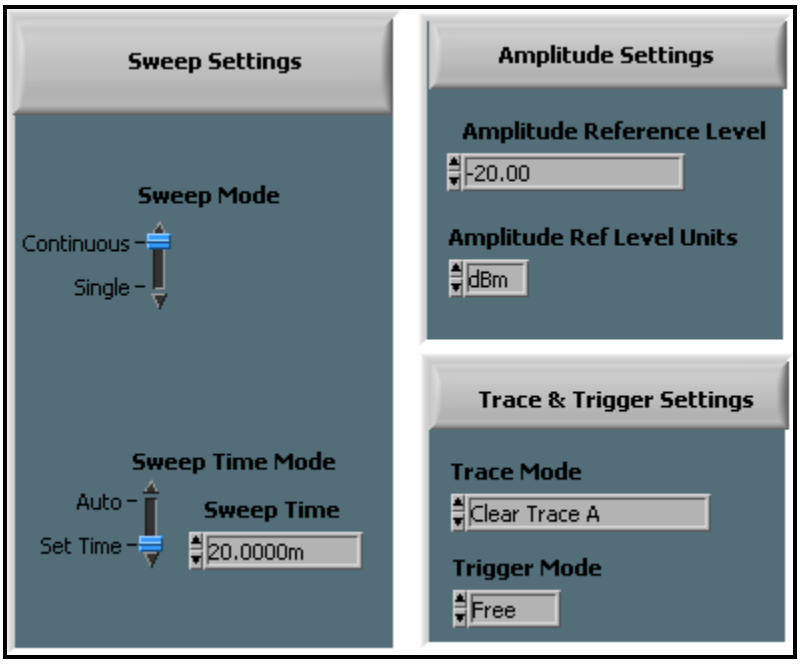

Figure 3.10 Dialog for Configuring Sweep, Amplitude and Trigger Settings

Figure 3.11 (segment 3) shows the display dialog which allows the user to view the measured data as it is being recorded. The display shows a plot with Y-axis indicating power and X-axis indicating sampling points in the frequency domain. These sampling points are equally spaced between the start and stop frequencies specified initially. The post processing software converts the sampling point number into the associated frequency. The dialog below the display provides controls for changing the sampling rate and recording intervals besides presenting the date and time stamp. Also, the STOP control allows the user to manually halt the program.

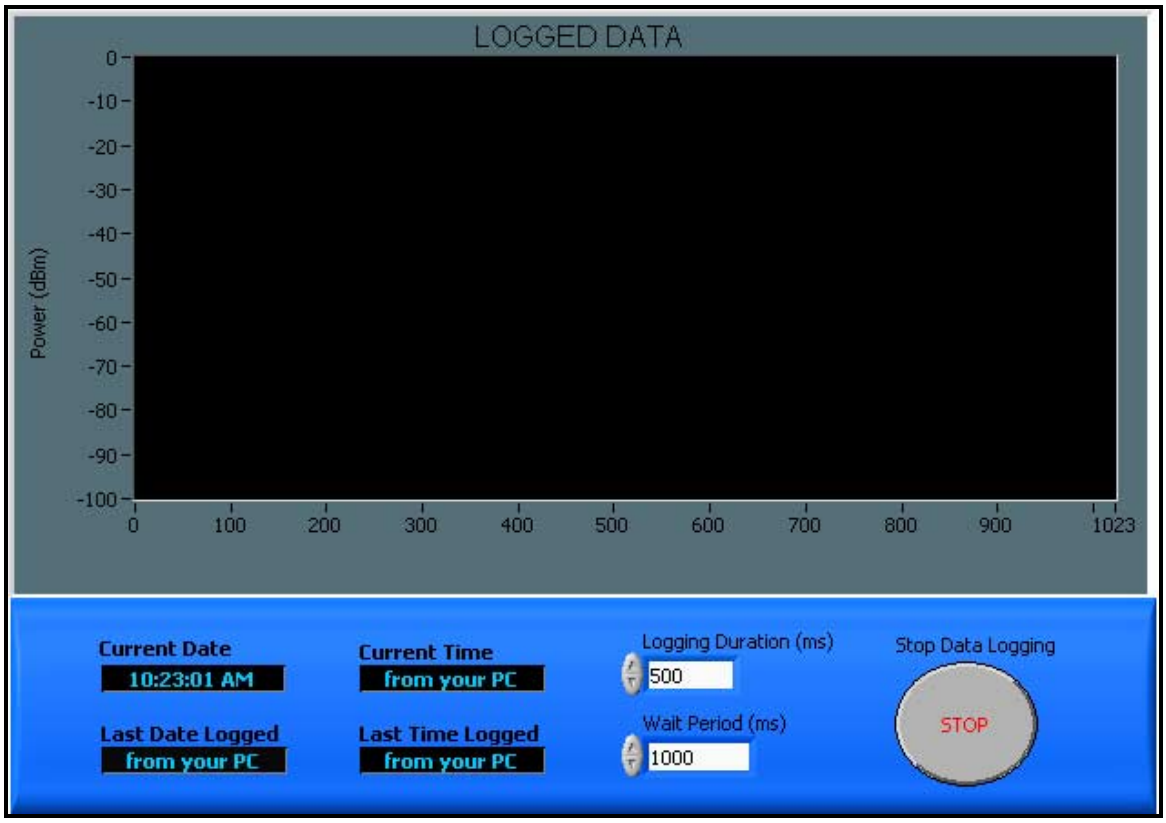

Figure 3.11 Dialog for Spectrum Display and Configuring Sampling Rate and Recording Intervals

Figure 3.12 (segment 4) shows the log file and data storage dialog wherein the user can specify the log file name and its location. There are three log files which record power, time and frequency separately for ease of data post processing. This dialog also contains a field that specifies the amount of data that is written to the files at one write cycle. 3208 bytes correspond to the 401 sample points on the spectrum analyzer display each accounting for 8 bytes of information per data point. The maximum number of sample points (401) was chosen to obtain maximum frequency resolution.

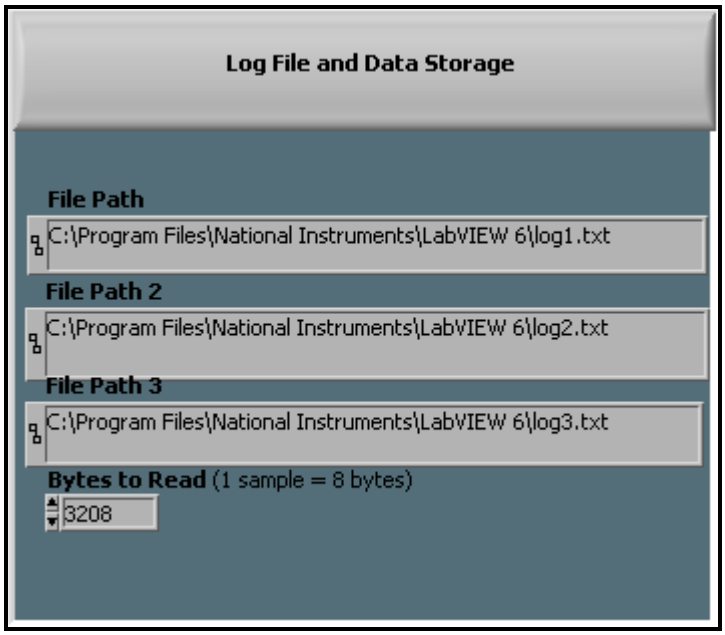

Figure 3.12 Dialog for Specifying Measured Data Log Files

The data stored in the log file is post-processed using PRISM's software suite developed using MATLAB.

As described before, PRISM is completely automated through software and can perform spectrum measurements over a number of days without any operator intervention. Additionally, the spectrum measurements can be monitored from an offsite location via the internet using PRISM's web interface. Figure 3.13 shows a screen shot of the web interface. The data streaming feature of PRISM via the internet was developed using LabVIEW's DataSocket, a data sharing protocol developed by National Instruments. DataSocket simplifies data exchange in measurement and automation applications. LabView's web publishing tool was programmed to control the web interface that enables and monitors the internet communication and security. The web interface can be configured to allow access only by specifically certified IP addresses. Also, the user at the offsite location can control PRISM, provided there is an independent LabVIEW license, at the offsite PC.

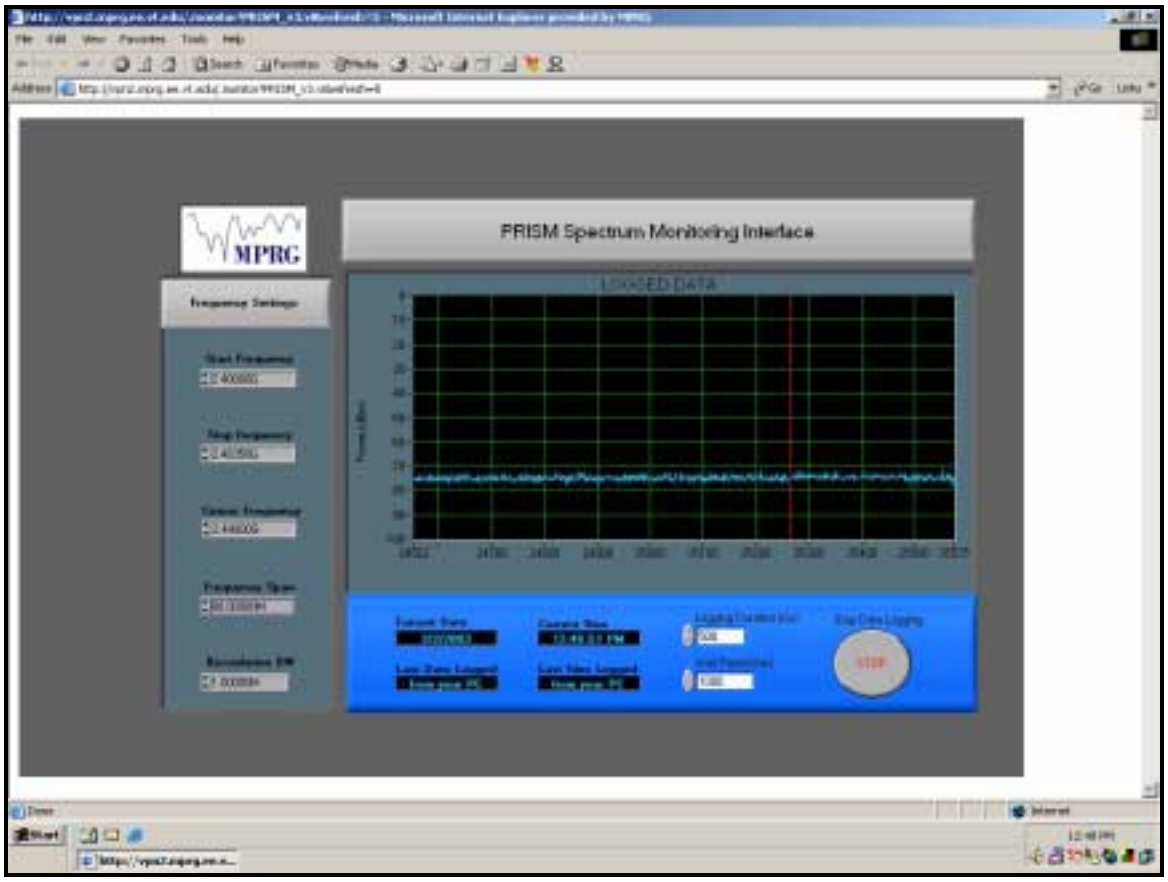

Figure 3.13 Web-Interface of PRISM as Viewed from a Remote Monitoring Site

3.4 Data Post Processing

In order to reduce the complexity of the measurement software, the data is recorded and then post processed at a later time. Post processing of data collected through PRISM is performed in MATLAB, which provides an extensive tool set for data analysis and visualization. PRISM's MATLAB software suite consists of routines that allows treatment of raw measured data and decomposes them into to a more concise format for further analysis.

- RawData_VectorData.m – This routine converts raw measured data into to meaningful data vectors (power, frequency and time). This routine also account for cable loss and amplifier gain in the measurement system.

- 'Antenna Factor.m' – This routine estimates the antenna factor for the system depending on the frequency and antenna characteristics and allows the measured power to be represented as an E-field (V/m or dBμV /m).

- 'statistics.m' - Each snap shot (a single sweep of the frequency band) consists of 401 bins. The 'statistics.m' routines allow 'n' snap shots (over time) to be collapsed into a single snap-shot representing the maximum, minimum and mean powers observed over the 'n' snap-shots.

- 'channelize.m' – This routine discretizes the maximum, minimum and mean powers obtained using 'statistics.m' according to user defined channels (e.g. Bluetooth, WLAN) and generates 3-D plots showing spectral occupation, signal strength and time of occurrence. For example, in the 2.4 GHz ISM band (2.4 to 2.4835 GHz) power is recorded over 401 equally spaced frequency bins over time. Using 'channelize.m' and 'statistics.m' the user can observe the maximum, minimum and mean powers measured in each of the 79 individual Bluetooth channels or the 11 individual 802.11.b WLAN channels over that time period.

Figure 3.14 shows RF interference measured 3 meters away from a microwave oven operating at 2.4 GHz. The RF interference experienced by the 79 individual Bluetooth channels and 11 partially overlapping 802.11b WLAN channels due to the microwave oven at a distance of three meters is shown in Figure 3.15. The analysis of the measured data using the post processing software gives an insight into the Bluetooth and WLAN channels affected by microwave oven interference.

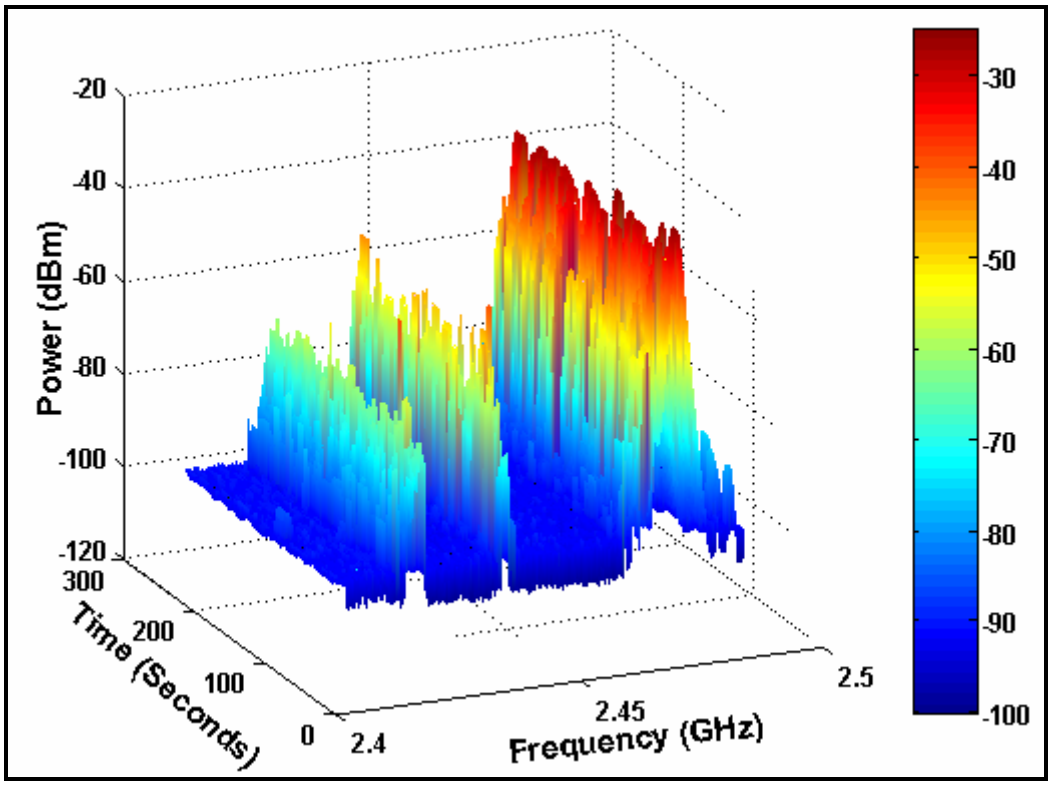

Figure 3.14 RF Interference Measured at a Distance of 3 meters from a Microwave Oven

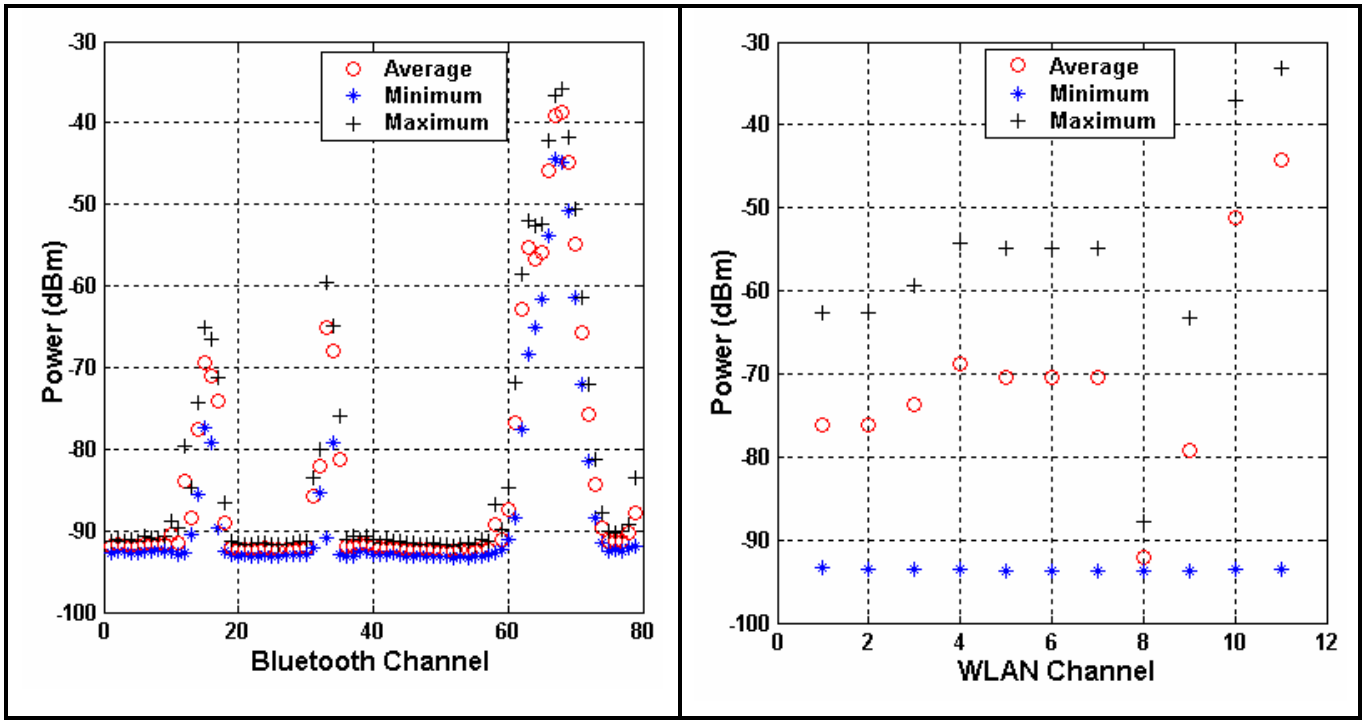

Figure 3.15 RF Interference Experienced by 79 Individual Bluetooth Channels and 11 partially overlapping 802.11b Channels

Similarly, PRISM can be used to quantify interference levels for Bluetooth due to various microwave ovens, WLANs, Bluetooth piconet and other devices in the ISM band. The measurement and analysis of the resulting interference can be very useful for analyzing the adaptive hopping schemes and adaptive packet selection and scheduling schemes under study by the IEEE P802.15 Working Group for Wireless Personal Area Networks™ (802.15 WPAN™ Task Group) [WPA01]. The 802.15 WPAN™ Task Group looks into collaborative and non-collaborative methods to ensure coexistence between 2.4 GHz WLANs and Bluetooth devices [Hpi02] [Cor02] [Wpaa].

The quantified channel interference in a particular environment could be used to estimate the throughput of Bluetooth and 802.11 devices, and hence define a QoS when operating in such environments. In Chapter 5, a Bluetooth throughput simulator using semi-analytical results and 802.15 channel models was developed and integrated into PRISM's MATLAB software suite. The simulator utilizes measured interference from an environment and predicts the throughput of six ACL Bluetooth packet transmissions.

3.5 Summary

In this chapter, a variety of hardware and software issues concerning the design and implementation of the interference measurement system were discussed. The objective was to create a completely automated web enabled software reconfigurable measurement system capable of characterizing RF interference and background EMI for frequency bands between 9 kHz and 2.9 GHz. A typical application of the designed system is spectrum surveillance and diagnosis for use in hospital environments, which could be monitored offsite via the internet.

The post-processing software suite developed in MATLAB was discussed. Post-processing results of measured data and quantifying interference for Bluetooth and 802.11 channels were also presented.

In Chapter 4 we will describe the EMI measurement campaign and data analysis performed using PRISM at the Virginia-Maryland College of Veterinary Medicine at Virginia Tech and the Carilion Memorial hospital in Roanoke, Virginia.

Chapter 4

4 EMI Measurements at 2.4 GHz in Hospital Environments

4.1 Measurement Scope

In today's world, the ubiquitous nature of wireless personal systems has lead to an increasing concern regarding the safety and reliability of the EME in hospitals. In addition, modern hospitals are becoming populated with wireless medical applications. Characterization of the electromagnetic environment in hospitals is now becoming more important than ever, especially when such measures can have a great effect on patient life and patient care.

Recently, there has been an increasing interest in designing and deploying in-building wireless networks in hospital in the unlicensed 2.4 GHz band. As part of this research, a measurement campaign was conducted at the Virginia-Maryland Regional College of Veterinary Medicine (VMRCVM) at Virginia Tech and the Carilion Roanoke Memorial Hospital (CRMH) in Roanoke, Virginia. These measurements look specifically at the EMI in the 2.4 GHz ISM band. Emphasis was given to locations such as Emergency Rooms, Intensive Care Units, Surgery blocks and Magnetic Resonance Imaging units including radiology. The medical devices and procedures used at the veterinary hospital and the regular hospital are similar in nature.

4.2 EMI Measurements at the Virginia Tech Veterinary Hospital

The VMRCVM is a fully equipped veterinary hospital located in the Virginia Tech central campus. The hospital facilities include a large animal clinic and a small animal

clinic. A number of procedures including computed tomography (CT), Ultrasound, digital fluoroscopy, nuclear medicine and surgery are performed on a regular basis.

4.2.1 Measurement System Setup and Procedure

PRISM was setup at three different locations - Radiology, Clinical Pathology and the ECG lab. PRISM was setup in a movable cart as shown in Figure 4.1; the antenna was placed 0.95 meters above the ground.

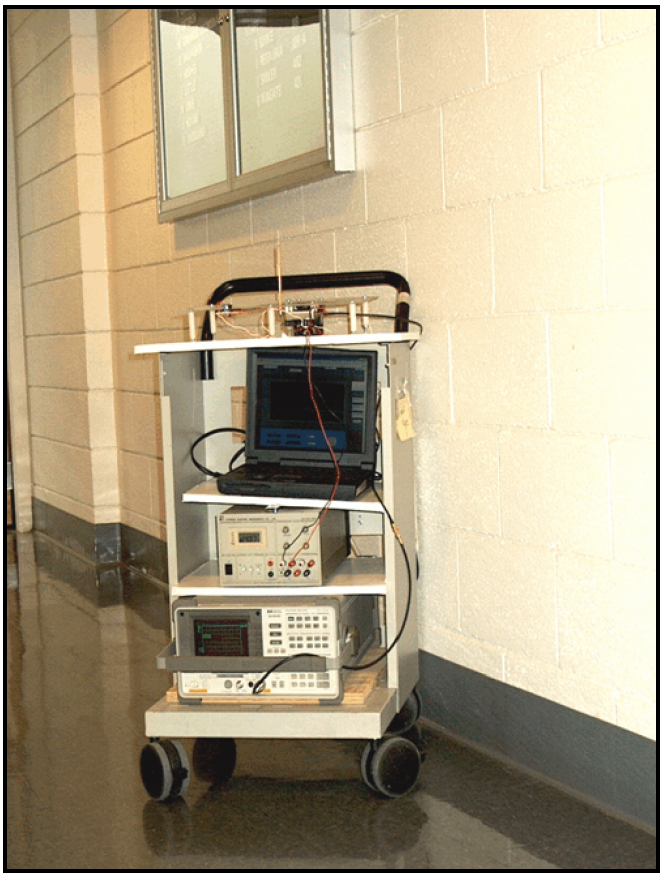

Figure 4.1 PRISM performing EMI Measurements along a hallway

In the VMRCVM measurement campaign, the ISM band was divided into 1 MHz bins and the maximum signal power observed in each bin during a two second time window was recorded. Table 4.1 shows the configuration of PRISM.

Table 4.1

PRISM Configuration for EMI Measurements at VMRCVM

Frequency	2.4 – 2.4835 GHz
Resolution Bandwidth	1 MHz
Video Bandwidth	100 kHz
Sweep Time	20 ms
Maximum Hold	2 seconds
Trigger	Free

4.2.2 Site Description and Maps

Two separate locations were chosen on the Phase I, first floor of the VMRCVM hospital (building #140, Figure 4.2). One half of this block consists of the radiology and X-ray facilities. The other half of the block consists of the small animal intensive care unit, the blood bank and the clinical pathology lab. The first measurement site (V1) was located by the side of the lead shielded wall outside the radiology lab (Figure 4.3(a)). The radiology office located adjacent to the measurement site had a turntable microwave oven. At this location, EMI was recorded every 2 minutes over a 24-hour duration. The second measurement site (V2) was located inside the clinical pathology lab (Figure 4.3(b)). This lab had a number of centrifuges using servo motors. EMI was recorded every 2 minutes for a period of two days.

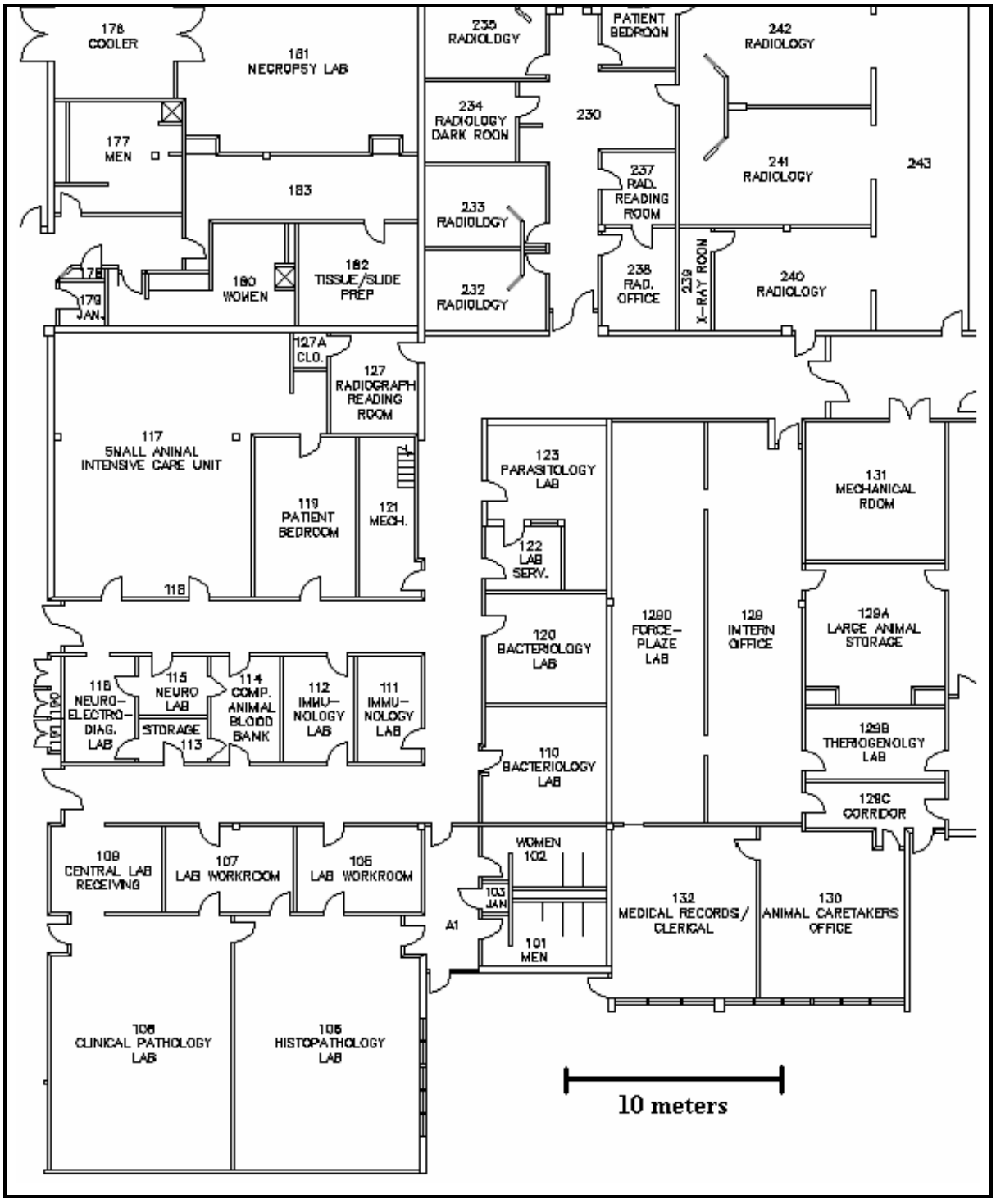

Figure 4.2 Map of Phase I, first floor of the VRMCV hospital (VT building #140)

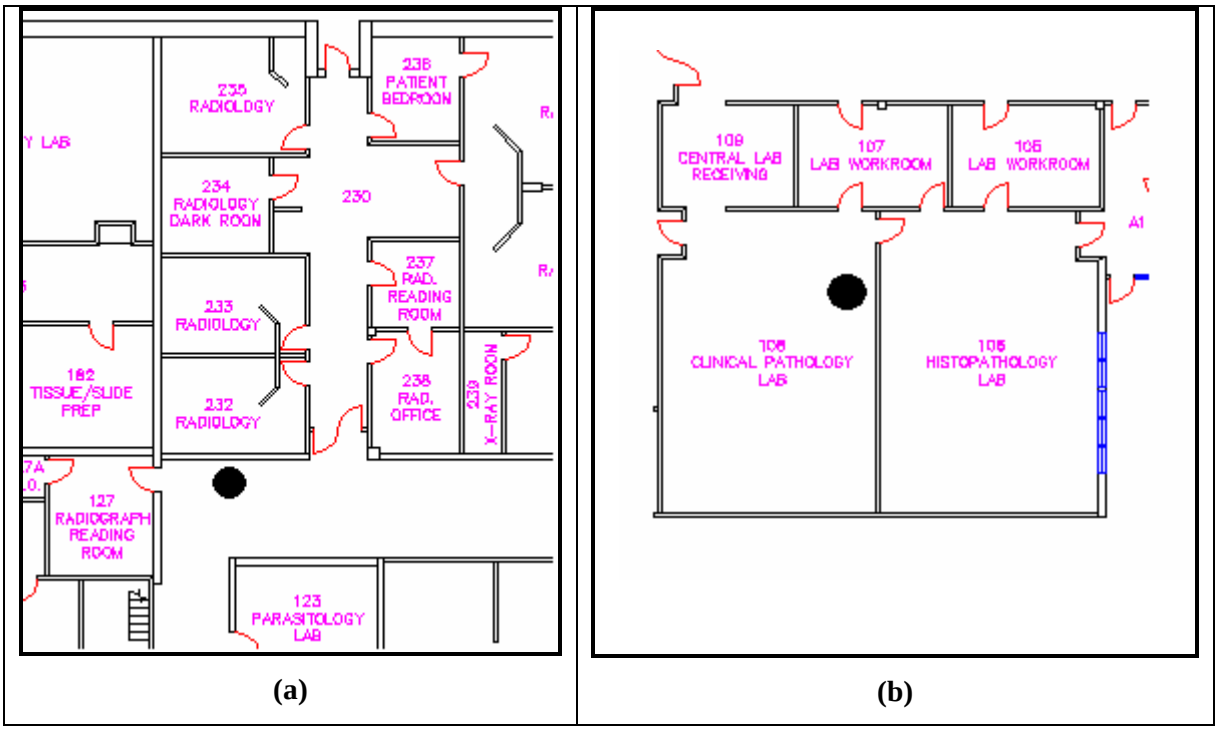

Figure 4.3 Measurement Locations V1 and V2, Phase I, First Floor, VMRCVM, Virginia Tech. PRISM was located outside Radiology (room 232) and inside the Clinical Pathology Lab (room 106). Actual position of PRISM indicated by dots

The third measurement site (V3) was located on the Phase III, first floor of the VMRCVM hospital (building #149, Figure 4.4). This part of the building accommodates the ECG, dentistry, special procedures, and anesthesiology facilities. The dental/ casting lab was equipped with an X-ray facility. EMI was recorded on the hallway in between the dental/ casting lab and the electro-diagnostics lab (Figure 4.5). The measurements were recorded every two minutes for a period of four days.

Figure 4.4 Map of Phase III, first floor of the VRMCV hospital (VT building #149)

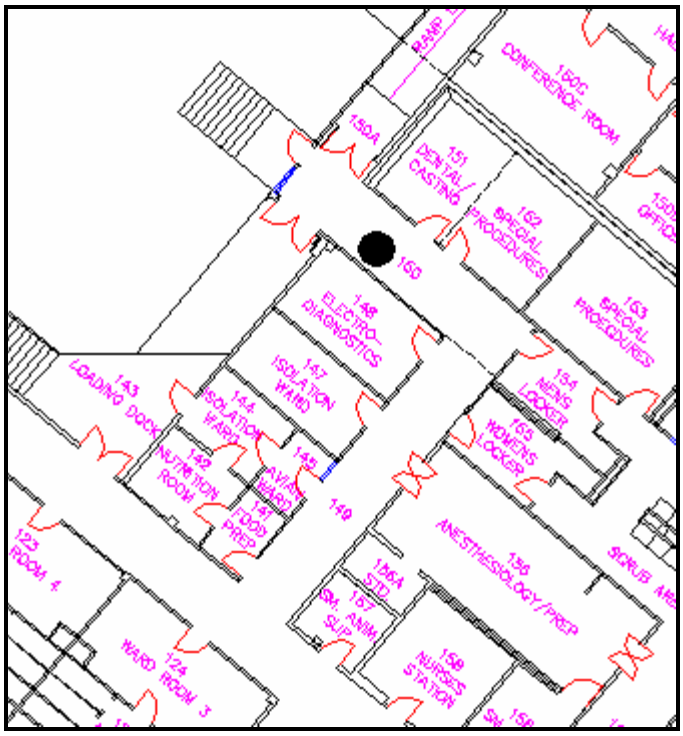

Figure 4.5 Measurement Location V3, Phase III, First Floor, VMRCVM, Virginia Tech. PRISM was located on the hallway in between the dental/ casting lab (room 151) and the electro-diagnostics lab (room 148). PRISM position indicated by dot

4.2.3 Measurement Results

Figures 4.6, 4.7 and 4.9 show the Electromagnetic Interference recorded at locations V1, V2 & V3. The 3-D plots show E-field as a function of frequency and time of day. Pronounced levels of interference (65 - 100 dBµV/m) were observed outside radiology between the hours of 11:00 am – 5:00 pm, and inside the clinical pathology lab between the hours of 11:00 am – 3:00 pm. At location V3, in the hallway between the dental/ casting lab and the electro-diagnostics lab significantly lower EMI levels and activity were observed. The maximum interference of 80 – 90 dBµV/m was recorded between 7:00 am – 9:00 am on the 1st and 3rd 24-hour cycle. At the very same location on the 4th 24-hour cycle there was continuous activity between 7:00 am – 9:00 am caused by transients with an E-field strength around 60 dBµV/m.

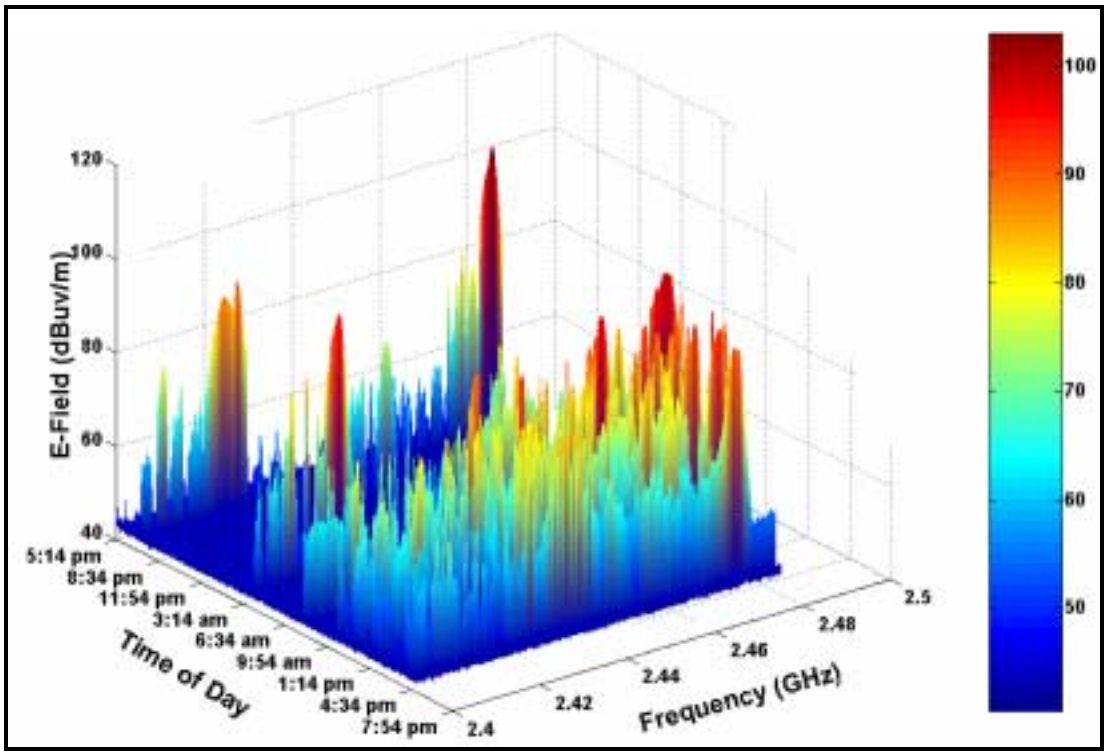

Figure 4.6 Background EMI noise in the 2.4 GHz ISM band recorded over a period of one day outside the radiology unit at the Virginia Tech veterinary hospital (Location V1)

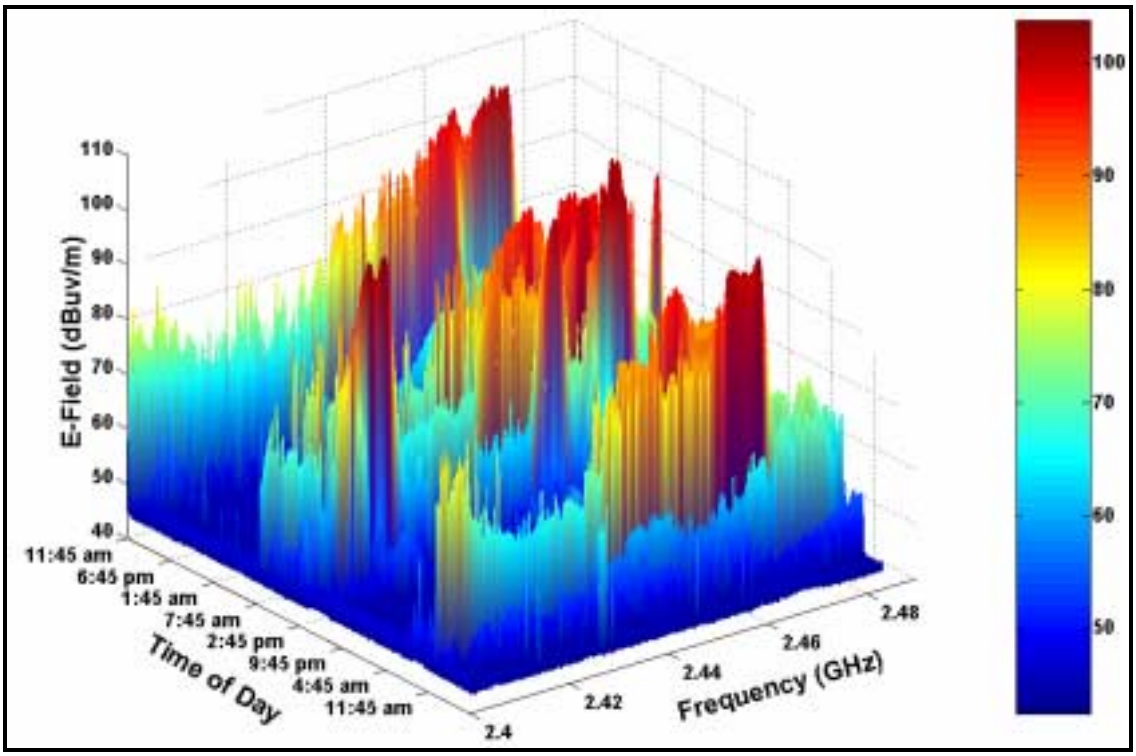

Figure 4.7 Background EMI noise in the 2.4 GHz ISM band recorded over a period of two days inside the Clinical Pathology unit at the Virginia Tech veterinary hospital (Location V2)

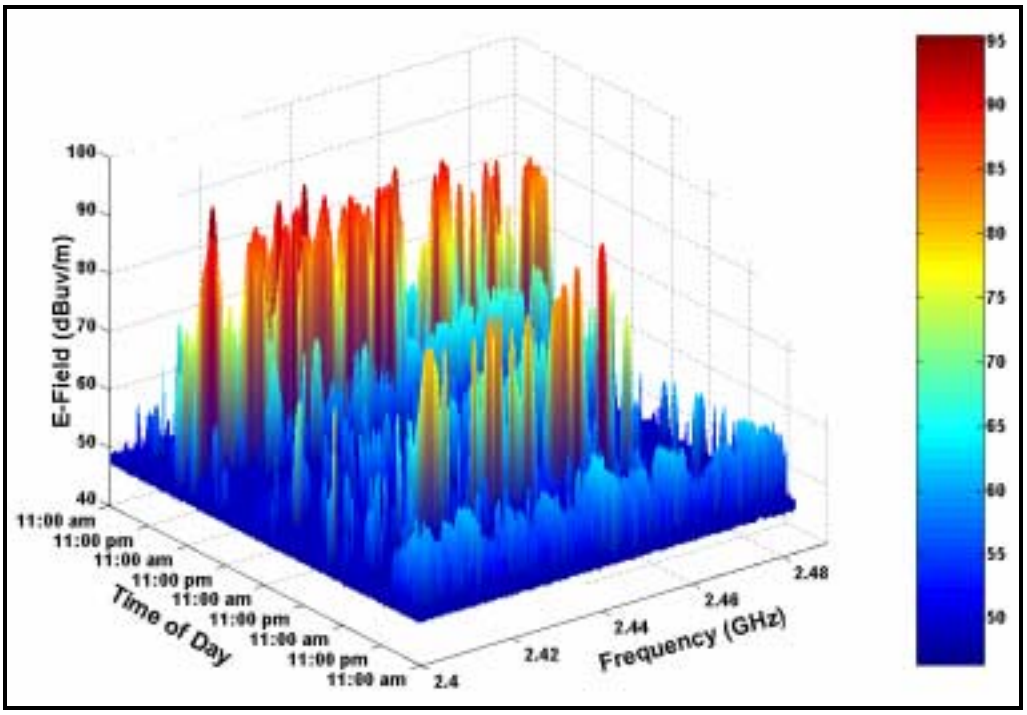

Figure 4.8 Background EMI noise in the 2.4 GHz ISM band recorded over a period of four days on the hallway between the dental/ casting lab and the electro-diagnostics lab (Location V3)

Table 4.2 summarizes the maximum EMI recorded at locations V1, V2 & V3.

Table 4.2

Maximum Recorded EMI at Locations V1, V2 and V3 at the Virginia Tech veterinary hospital

Location	Maximum Recorded EMI		Time of Day Observed
	dBμV/m	V/m	
Radiology	102.9	0.1396	6:30 pm
Clinical Pathology	103.71	0.1533	5:00 pm
ECG	95.4	0.0589	12:00 pm

4.2.4 Discussion of Results

The measured field levels from the measurement campaign at the Virginia Tech veterinary hospital were well below the FDA recommended immunity level of 130

dBµV/m (3 V/m). The highest field strength recorded was 103.71 dBµV/m (0.153 V/m). The majority of the EMI activity at all three locations were observed during normal business hours. Most of the strong interference can be attributed to the use of microwave ovens in the hospital, which can be identified by the signal strength, spectral characteristics and its frequency of operation [Kri02b].

4.3 EMI Measurements at Carilion Roanoke Memorial

The Carilion Roanoke Memorial Hospital is designated as a level 1 trauma center and contains 500 patient beds. The hospital ranks among the top 5% of modern hospitals in the United States. Apart from the medical facilities, the hospital has a sophisticated wireless infrastructure. Wireless medical telemetry systems are supported in the 560-614 MHz and 700 MHz band. Wireless phones are supported in the 900 MHz band and 802.11b WLANs are supported in the 2.4 GHz ISM band.

4.3.1 Measurement System Setup and Procedure

Due to the extensive area of the hospital and the density of medical equipment and personnel, measurements were performed on three floors (2, 4 and 7) which were expected to provide more intense and unique electromagnetic environments. Moreover, floors similar in nature were avoided (floor 2 is used for emergency care, floors 3 and 4 are used for surgery and floors 5, 6 and 7 are used for critical care). Five different measurement sites were selected on each of the three floors for recording EMI. The selection of the five measurement sites was based on surrounding areas where medical instruments were contained or procedures were performed, taking into account periodic activity and availability of space for performing the measurements without affecting patient care and the regular business of the hospital. PRISM was setup in the same movable cart used for the previous measurement campaign at the veterinary hospital.

In this measurement campaign, the ISM band was divided into 100 kHz bins and the maximum signal power observed in each bin during a two minute time window was recorded. On each of the fifteen sites, EMI was recorded for complete 24-hour duration

on regular weekdays. Table 4.3 shows the configuration of PRISM. The value for the resolution and video bandwidth were chosen in order to provide a better signal to noise ratio.

Table 4.3

PRISM Configuration for EMI Measurements at the Carilion Roanoke Memorial Hospital

Frequency	2.4 – 2.4835 GHz
Resolution Bandwidth	100 kHz
Video Bandwidth	100 kHz
Sweep Time	20 ms
Maximum Hold	2 minutes
Trigger	Free

4.3.2 Site Description and Maps

Floor 2:

The second floor of the Carilion Memorial Hospital accommodates the ER (Figure 4.9). This floor contains all the essential procedures and labs such as X-ray, Radiology (MRI), CT, ultrasound and nuclear medicine required for an emergency. The MRI rooms have walls embedded with copper and iron to provide RF shielding and magnetic shielding. The magnetic shielding is used to contain magnetic fields within the room to a safe level whereas the RF shielding is to minimize the level of RFI coming from outside the room and thereby providing a better signal to noise ratio for the MRI procedures. The X-ray rooms are protected by walls with lead shielding to keep radiation from equipment within the room to a safe level outside the room. Five measurement sites were chosen on the South section of the floor (Figure 4.10). These five sites (numbered 1-5) were chosen such that they could cover a variety of labs including MRI, CT, X-ray, ultrasound and the ER room itself. Also, this section of the floor supports WLAN connectivity through an 802.11 b Orinoco Access Point (AP) placed on the wall, in-between Exam Room 21 and Exam Room 22. The WLAN AP was operating on channel 6 (marked AP-6, Figure 4.10). At each site, EMI was recorded periodically every 5 minutes for a period of 24 hours.

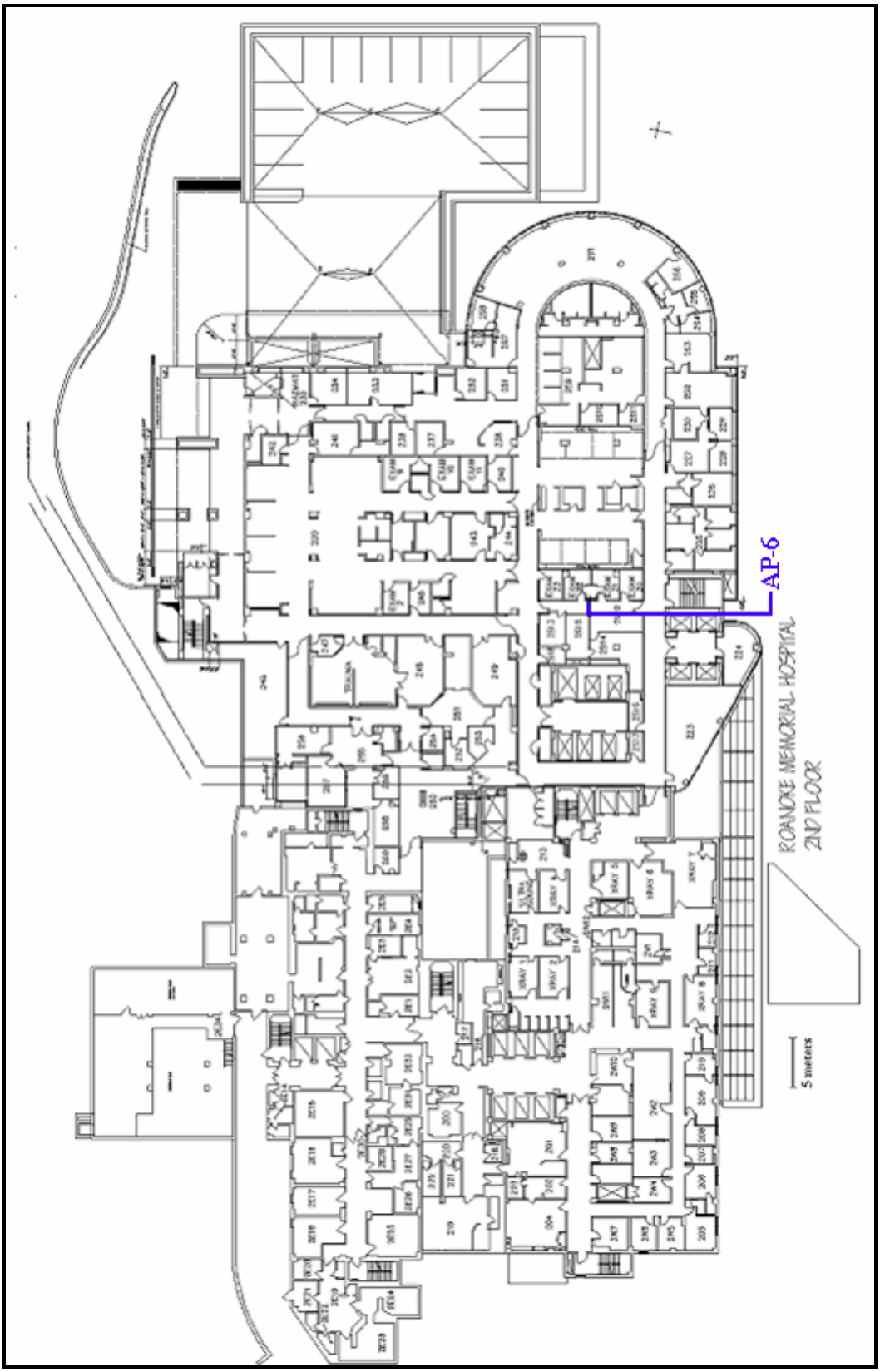

Figure 4.9 Map of the 2nd Floor of Carilion Memorial Hospital

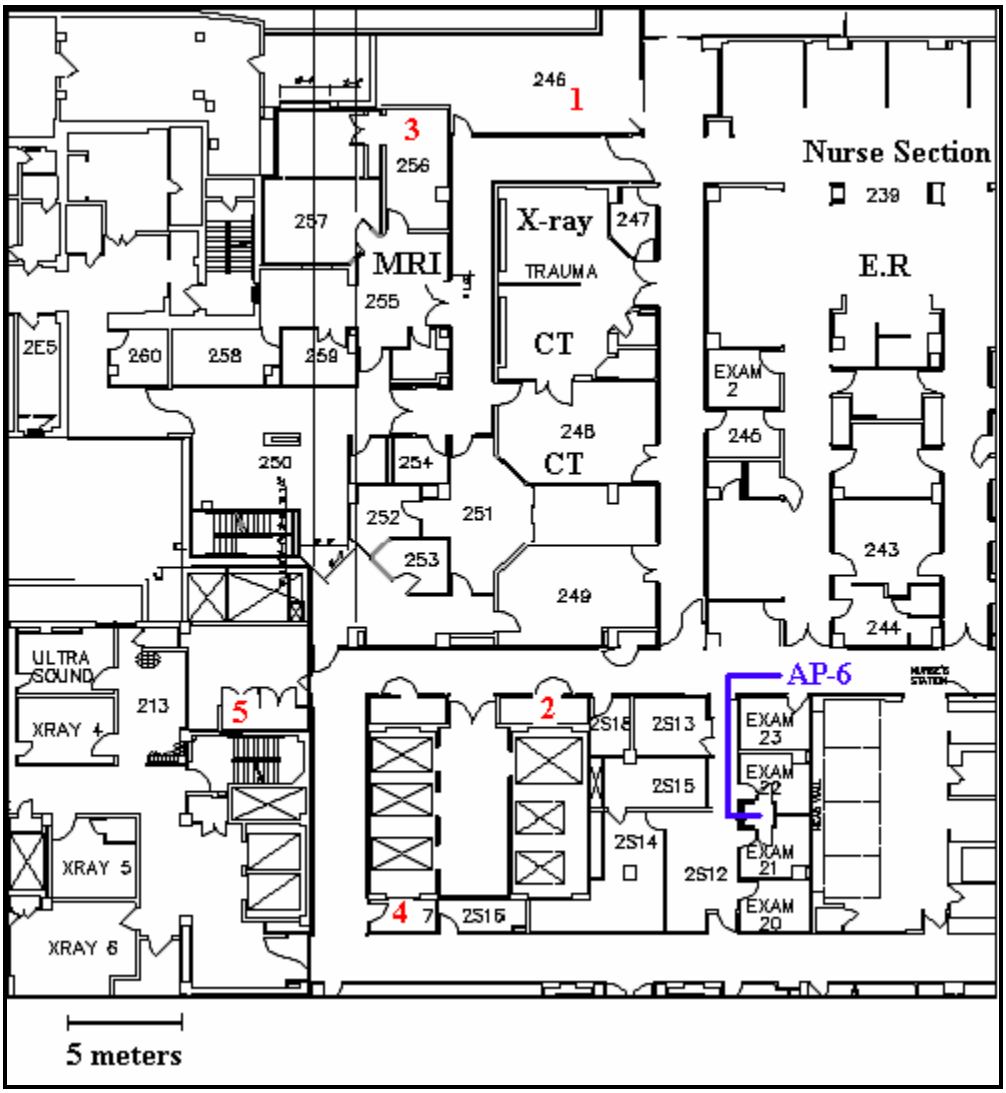

Figure 4.10 Measurement Sites 1-5, 2nd Floor, South Section, Carilion Memorial Hospital

Floor 4:

The fourth floor of the Carilion Memorial Hospital consists of a number of operating rooms and patient monitoring rooms (Figure 4.11). Surgeries are performed on this floor. A considerable portion of this floor is designated as a 'clean environment' and has restricted access. The 4th floor also has a considerable amount of WLAN deployment and is supported by four 802.11b Orinoco WLAN APs. The WLAN APs were operating on channel 11 (2 APs), 1 and 6 (1 AP).

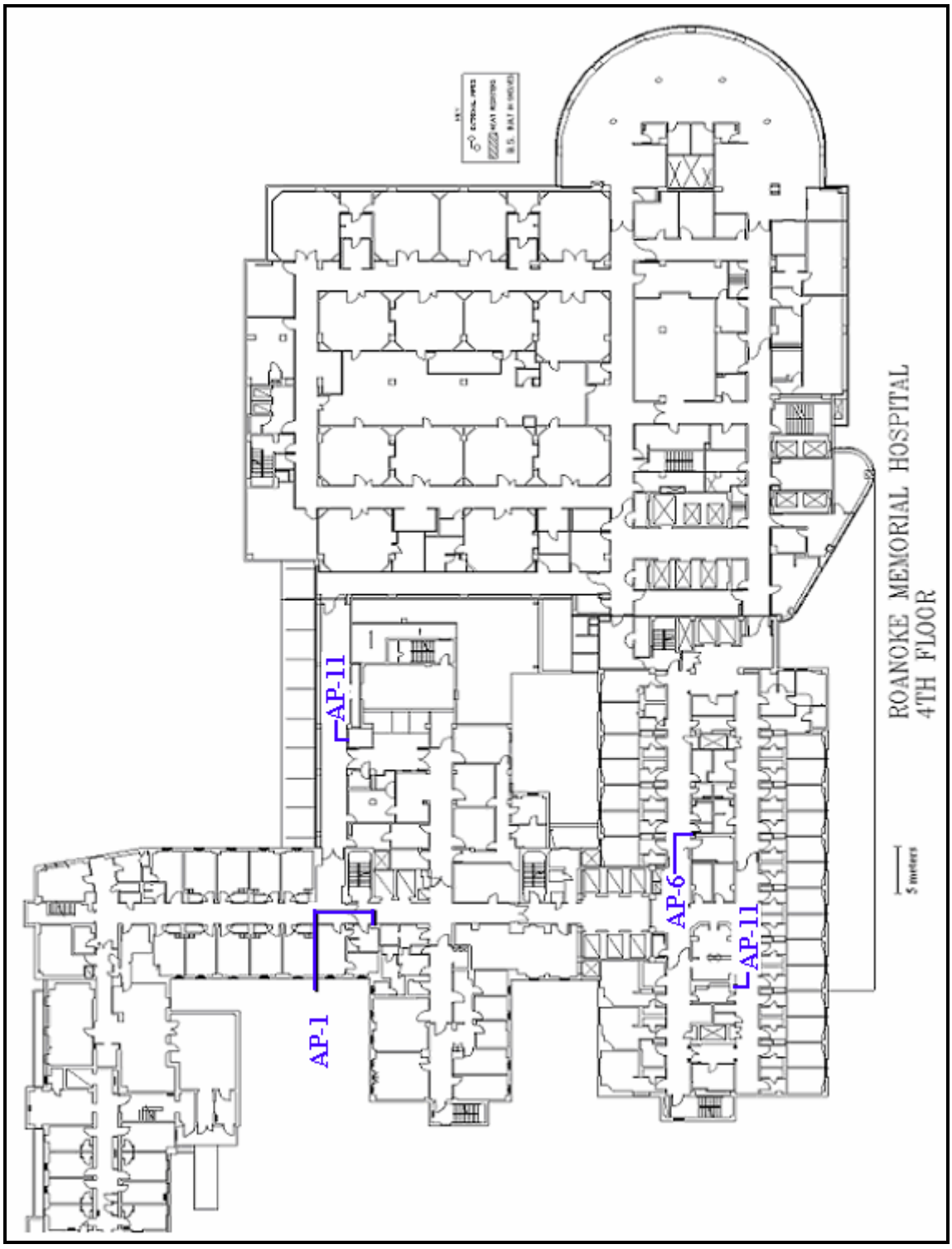

Figure 4.11 Map of the 4th Floor of Carilion Memorial Hospital

Five measurement sites were chosen on the South section of the floor (Figure 4.12). These five sites (numbered 1-5) were chosen to get as close as possible to the patient monitoring rooms and the operating rooms. The operating rooms consist of a number of

medical equipment including ESU, RF ablation unit, stereo tactic unit, surgical robots, anesthesia unit, ventilator, defibrillator, infusion pumps, CO_2 laser, YAG laser, wireless phones and portable X-ray. At each site, EMI was recorded periodically every 5 minutes for a period of 24 hours.

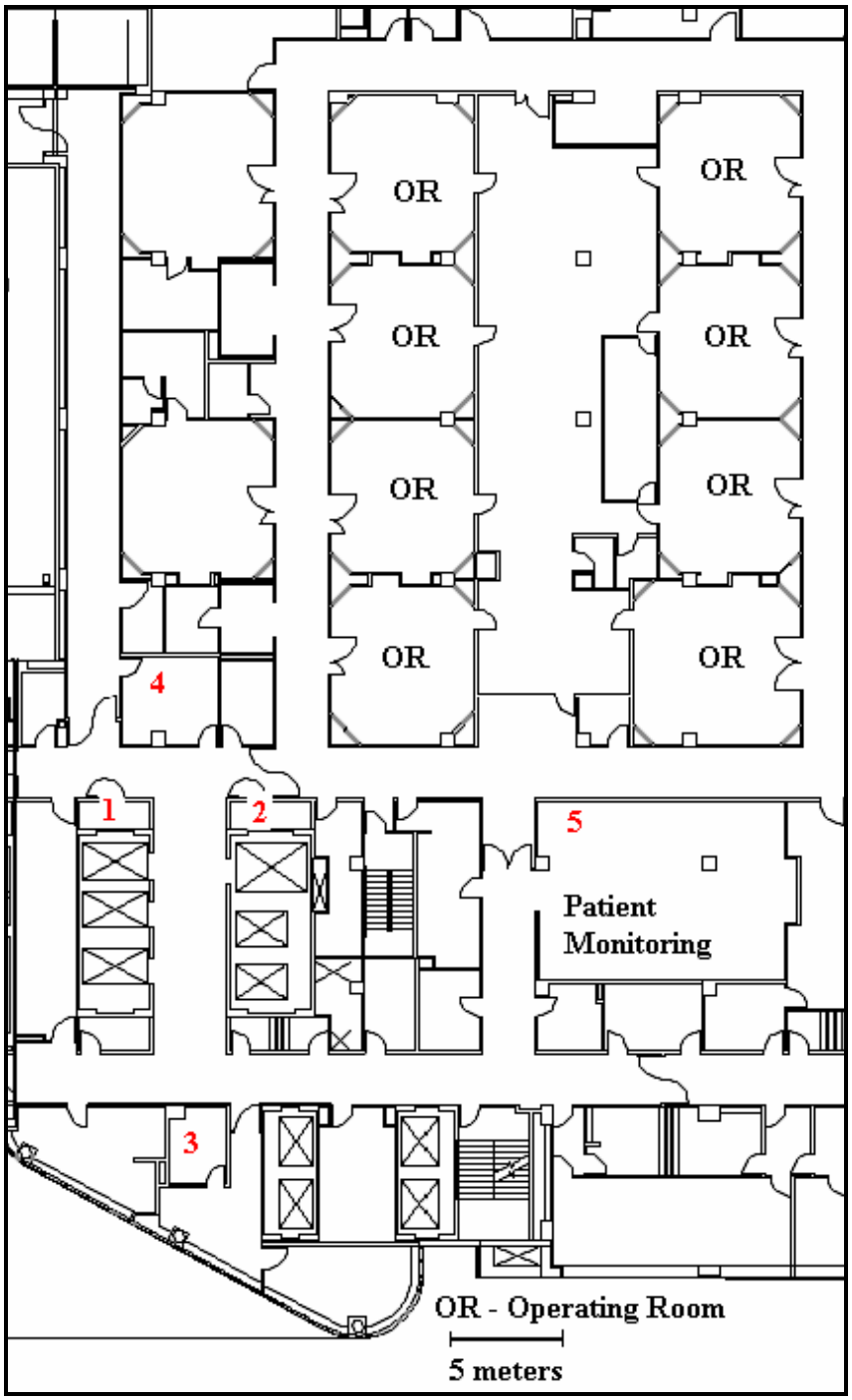

Figure 4.12 Measurement Sites 1-5, 4th Floor, South Section, Carilion Memorial Hospital

Floor 7:

The seventh floor of the Carilion Memorial Hospital consists of Critical Care Units (CCU), also known as Intensive Care Units (ICU) and regular patient rooms (Figure 4.13). Patients after surgery are brought to the CCUs and are monitored continuously. Equipment used on this floor include patient monitors, defibrillator, telm monitor, wireless phone, infusion pumps, televisions, ventilators, humidifiers, sequential compression device and bedside charting PC's. The 7^{th} floor has the maximum utilization of WLAN connectivity in the hospital. Apart from wireless enabled laptops, there are a number of wireless enabled carts used for providing medication for patients. There are five 802.11b Orinoco WLAN APs located along the hallways and networking closets on this floor. The WLAN APs were operating on channel 10 (1 AP), 1 and 11 (2 APs). Five measurement sites (numbered 1-5) were chosen on the East section of the floor (Figure 4.14). This section of the floor had a couple pantries consisting of a microwave oven. One pantry was located adjacent to measurement site 2. At each site, EMI was recorded periodically every 5 minutes for a period of 24 hours.

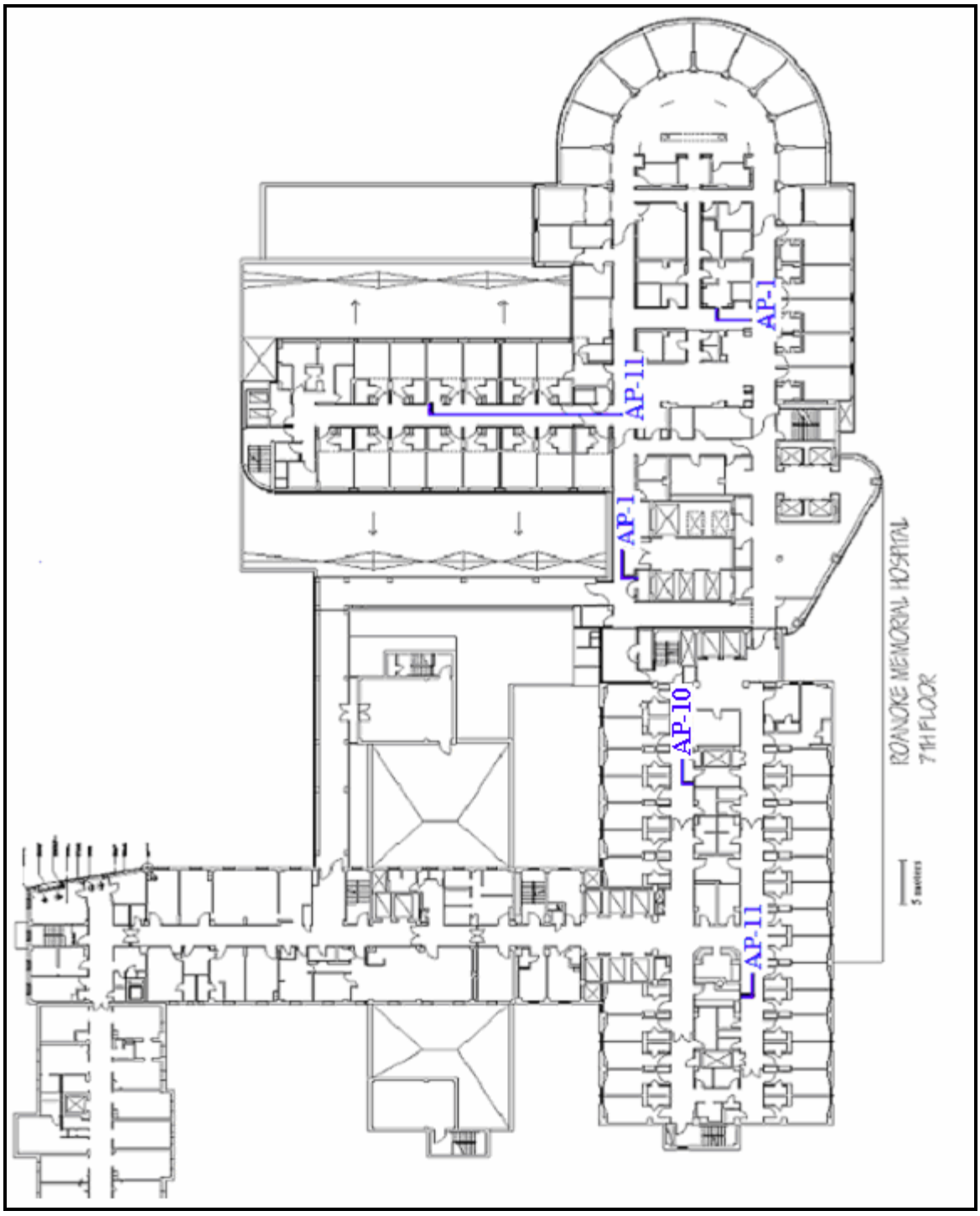

Figure 4.13 Map of the 7th Floor of Carilion Memorial Hospital

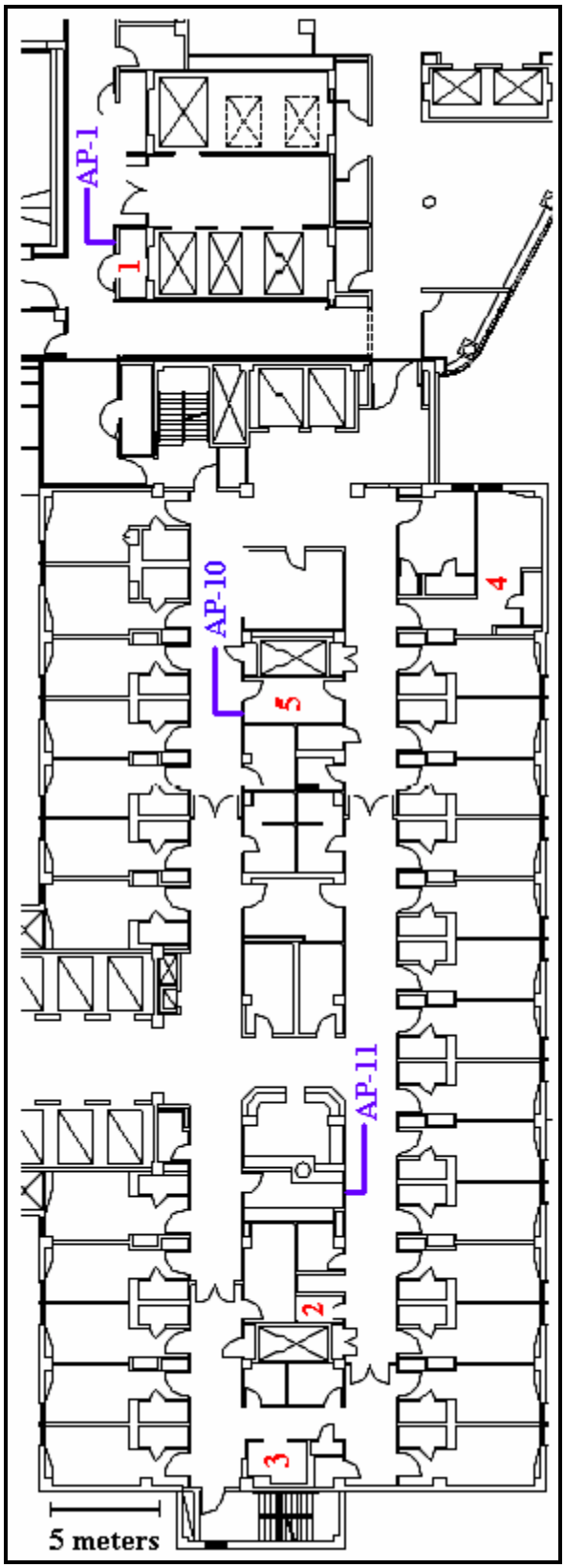

Figure 4.14 Measurement Sites 1-5, 7th Floor, South Section, Carilion Memorial Hospital

4.3.3 Measurement Results

In order to observe a worst case scenario, the recorded data from all five sites in a floor were time aligned and 3-D plots showing E-field as a function of frequency and time of day was plotted. The individual 3-D plots for each individual measurement site is provided in Appendix A, Section A1.

Floor 2:

Figure 4.15, shows the maximum Electromagnetic Interference recorded from all five sites on the 2nd floor. The 3-D plots show E-field as a function of frequency and time of day.

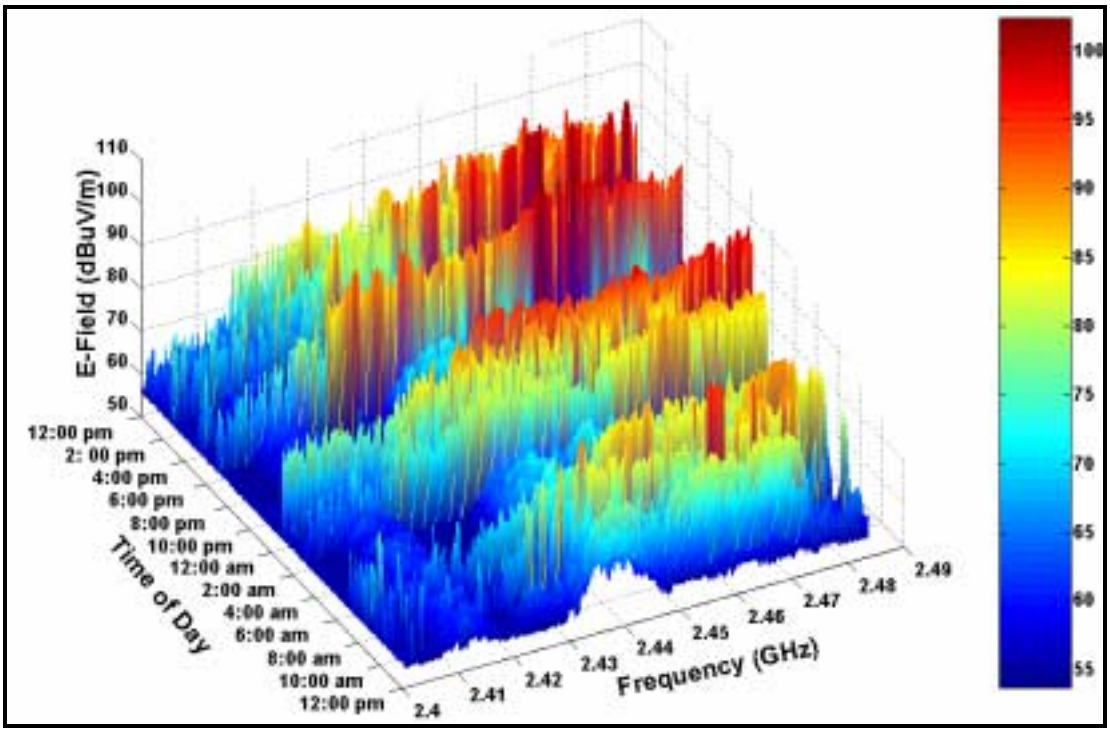

Figure 4.15 Maximum Observed Background EMI noise in the 2.4 GHz ISM band from all 5 sites on the South Section of the 2nd Floor of Carilion Memorial Hospital. EMI was recorded for a period of 24-hours on all 5 sites

Pronounced levels of interference (60 - 100 dBμV/m) were observed at the five measurement sites of floor 2 between the hours of 7:00 am – 3:00 pm. There were three occurrences of high interference between 1:00 am and 3:00 am which could be attributed

to the use of microwave ovens. Microwave oven activity was also observed between the hours of 12:00 pm and 1:00 pm and around 7:00 pm.

The maximum level recorded for all five sites was 102.32 dBμV/m (0.1306 V/m). Figure 4.16 shows a different view of the 3-D plot shown in Figure 4.15. Two wideband signals appearing like a tunnel, centered at 2.412GHz and 2.437GHz can be seen through out the day. The continuous wideband signal is due to the WLAN APs operating on channel 1 and channel 6. It can be observed that channel 6 is very strong (72.5 dBμV/m), which can be expected because the South Section of the 2nd floor has a WLAN AP operating on channel 6. The WLAN signal on channel 1 was caused by an AP operating in a neighboring floor, however, floor 1 and floor 3 have no WLAN deployment. Looking closer at the data, the channel 1 activity was only observed at measurement site 4 (Appendix, Figure A1.4). Because site 4 was located next to the elevators, it is possible that the elevator shafts acted like waveguides and provided a path for WLAN signals to propagate from a higher floor. Looking at the Blueprint, only floor 7 had an AP on channel 1 located in a closet beside this group of elevators.

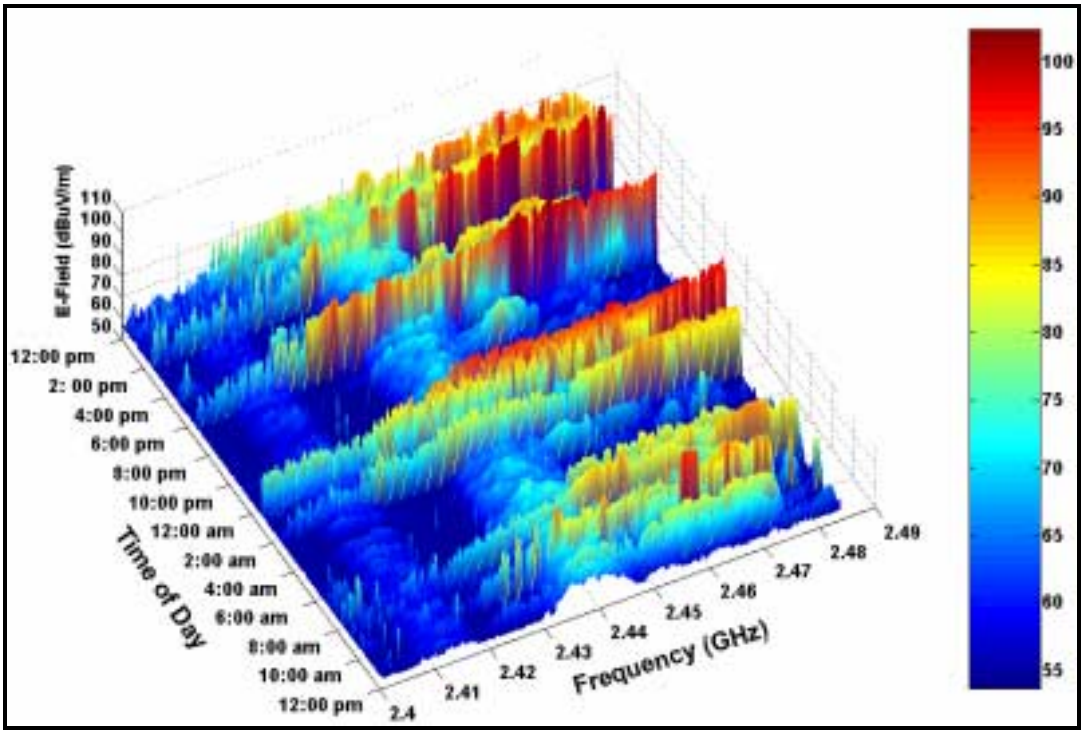

Figure 4.16 Different view of the Maximum Observed Background EMI noise in the 2.4 GHz ISM band from all 5 sites on the South Section of the 2nd Floor of Carilion Memorial Hospital

Floor 4:

Figure 4.17, shows the maximum Electromagnetic Interference recorded from all five sites on the 4th floor. The 3-D plots show E-field as a function of frequency and time of day.

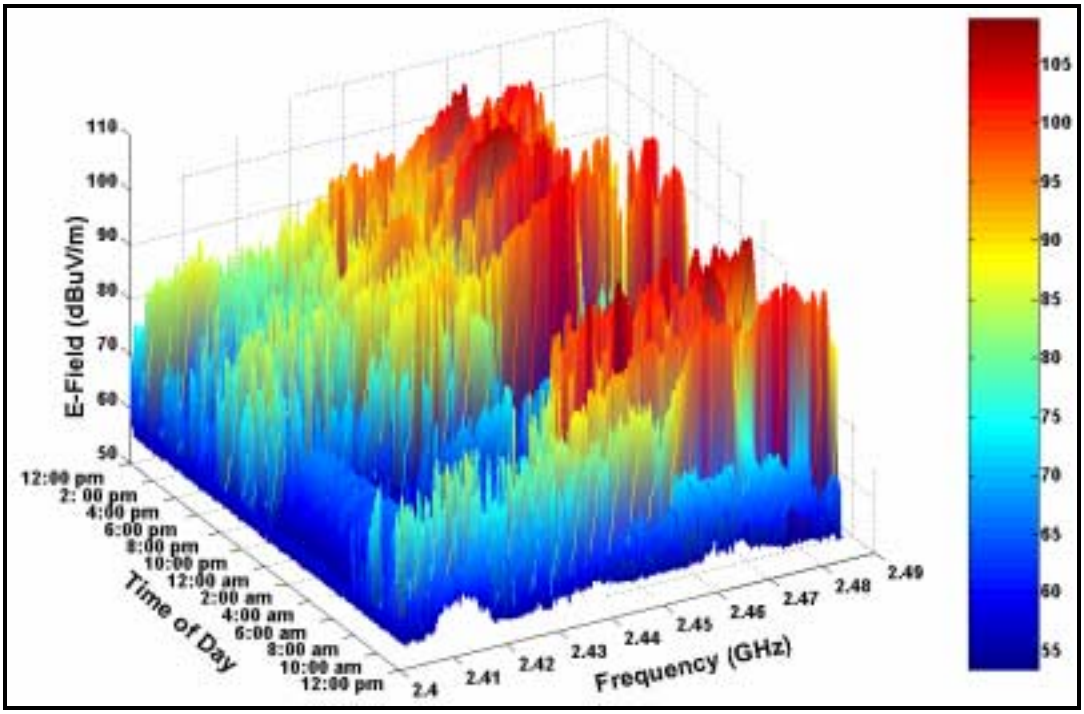

Figure 4.17 Maximum Observed Background EMI noise in the 2.4 GHz ISM band from all 5 sites on the South Section of the 4th Floor of Carilion Memorial Hospital. EMI was recorded for a period of 24-hours on all 5 sites

Moderate interference was observed between the hours of 7:30 am and 11:00 pm. Increased activity (75 - 105 dBμV/m) was observed during lunch time between 11:00am and 12:45 pm possibly due to use of microwave ovens, although the E-fields extend to the entire range of the ISM band. Radiation similar to microwave ovens was also measured around 6:00 pm, 8:00 pm, 10:00 pm and 9:00 am.

The maximum level recorded for all five sites was 108.84 dBμV/m (0.2767 V/m). Figure 4.18 shows a different view of the 3-D plot shown in Figure 4.17. Though the 4th floor did have three active WLAN channels (four APs) deployed, strong signals (65 dBμV/m) only on channel 1 were observed. In fact, WLAN channel 1 activity was observed from the data recorded from site 1, 2 and 4 (Appendix, Figures A1.6, A1.7 &

A1.9), located close to the elevators. As discussed above, these signals should have propagated from the WLAN AP on the 7th floor which was located close to the elevators.

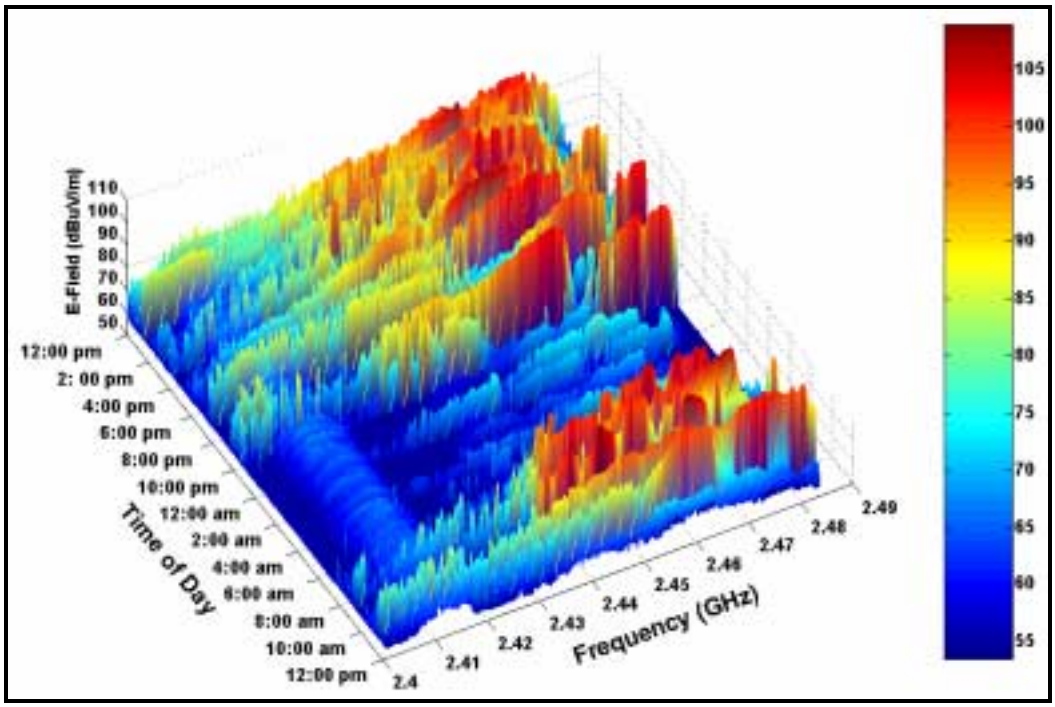

Figure 4.18 Different view of the Maximum Observed Background EMI noise in the 2.4 GHz ISM band from all 5 sites on the South Section of the 4th Floor of Carilion Memorial Hospital

Floor 7:

Figure 4.19, shows the maximum Electromagnetic Interference recorded from all five sites on the 7th floor. The 3-D plots show E-field as a function of frequency and time of day. Continuous activity throughout the day was observed on the 7th floor and pronounced levels of interference (90 - 110 dBμV/m) were observed at all five measurement sites. The maximum level recorded for all five sites was 114.83 dBμV/m (0.5516 V/m).

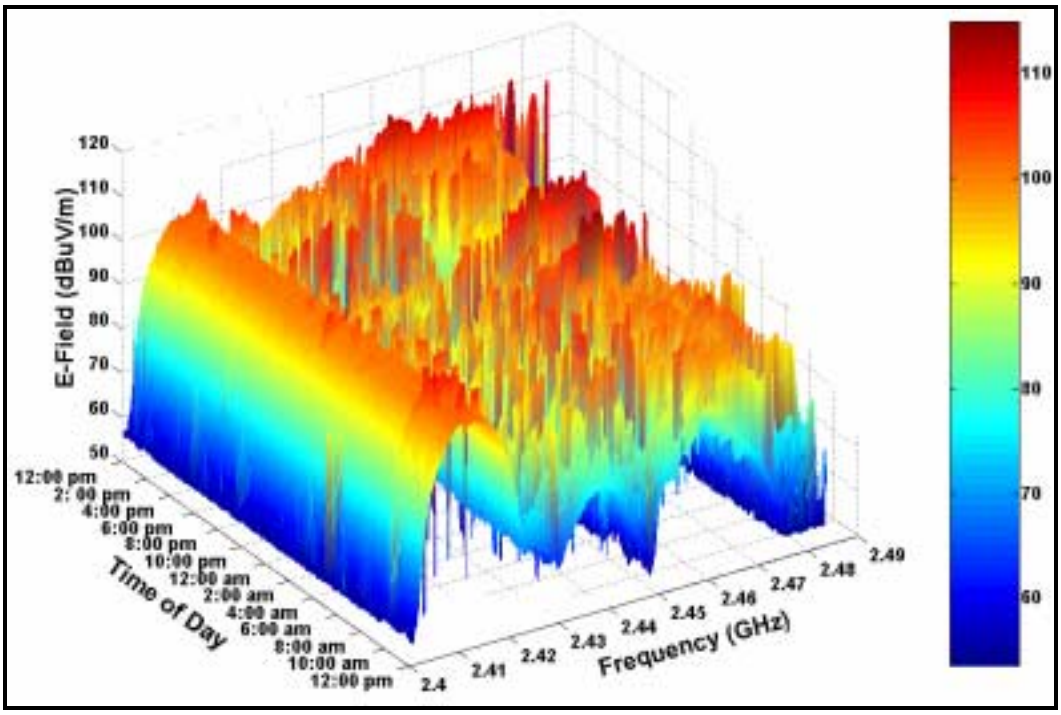

Figure 4.19 Maximum Observed Background EMI noise in the 2.4 GHz ISM band from all 5 sites on the South Section of the 7th Floor of Carilion Memorial Hospital. EMI was recorded for a period of 24-hours on all 5 sites

Figure 4.20 shows a different view of the 3-D plot shown in Figure 4.19. As mentioned earlier, the 7th floor has 6 WLAN APs deployed along hallways and inside networking closets. The presence of strong interference from WLAN APs operating on channel 1, 6, 10 and 11 can be observed. In particular, the interference from channel 1 is very prominent (100 dBμV/m), which is possibly because measurement site 1 was very close to the WLAN AP-1. The recorded data at site 5 (Appendix, Figure A1.15) showed the presence of strong signals on channel 10, which is expected because of its close proximity to the WLAN AP on channel 10. An interesting discovery during the measurement campaign was the WLAN signal on channel 10. The initial WLAN deployment on the 4th floor did not have a WLAN AP operating on channel 10; in fact the AP near site 5 was programmed to be on channel 1. A power failure in that section had caused the WLAN AP to reset to the AP's factory default setting – channel 10. Apart from WLANs, the other interferences were observed to be very bursty. Additionally, microwave oven interference was observed between the hours of 12:00 pm - 1:00 pm, 9:00 pm - 10:00 pm, 1:00 am - 2:00 am, and 5:00 – 5:30 am.

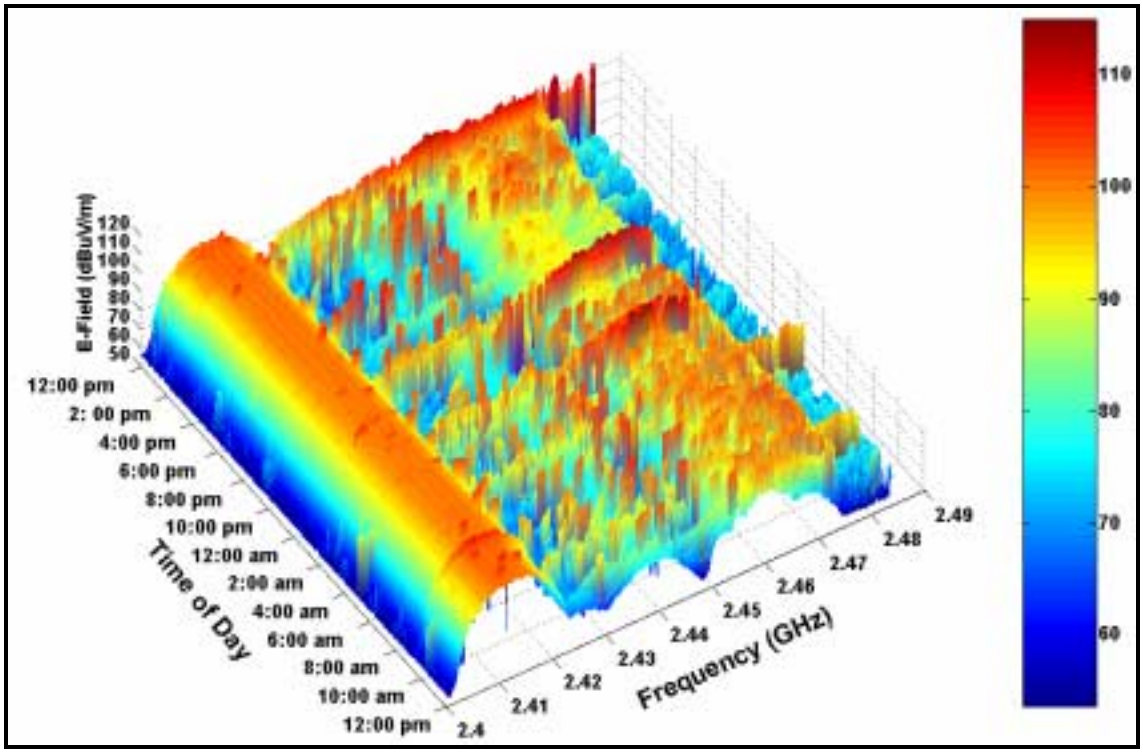

Figure 4.20 Different view of the Maximum Observed Background EMI noise in the 2.4 GHz ISM band from all 5 sites on the South Section of the 7th Floor of Carilion Memorial Hospital

Table 4.4 summarizes the maximum EMI recorded on Floor 2, 4 and 7 of the Carilion Memorial Hospital.

Table 4.4

Maximum Recorded EMI on the South Section of the 2nd and 4th Floors and East Section of the 7th Floor of Carilion Memorial Hospital

Location	Maximum Recorded EMI		Time of Day
	dBμV/m	V/m	
2nd Floor, South Section	102.33	0.1306	7:00 pm
4th Floor, South Section	108.84	0.2767	10:40 am
7th Floor, East Section	114.83	0.5516	2:20 am

4.3.4 Discussion of Results

The maximum field levels from the measurement campaign at the Carilion Memorial Hospital in Roanoke were well below the FDA recommended immunity level of 130 dBμV/m or 3 V/m. The highest field strength recorded was 114.83 dBμV/m (0.5516 V/m). The majority of the EMI activity on the 2nd was observed between the hours of 7:00 am to 3:00 pm and on the 4th floor between the hours of 7:30 am to 11:00 pm. The EMI activity on the 7th floor was prominent throughout the day. Microwave oven interference was observed on all three floors. Most of the strong interference can be attributed to the WLAN APs deployed in the hospital and the use of microwave ovens.

4.4 Conclusion

In this Chapter we have demonstrated PRISM to be an effective system for measuring and studying EMI in the ISM band. EMI measurements were performed at the Virginia-Maryland College of Veterinary Medicine at Virginia Tech and the Carilion Memorial hospital in Roanoke, Virginia.

The majority of EMI activity at the Virginia Tech veterinary hospital was observed during normal business hours. Microwave ovens accounted for a majority of the recorded interference. In the Carilion Memorial Hospital, the EMI recorded on floors 2, 4 and 7 were found to be time varying and dynamic. WLANs and Microwave ovens accounted for a majority of the recorded interference, though microwave oven activity was less prominent compared to the veterinary hospital.

The maximum interference levels observed at the veterinary hospital and the Carilion memorial hospital were 103.71 dBμV/m (0.1533 V/m) and 114.83 dBμV/m (0.5516 V/m) respectively. These interference levels are far below the recommended immunity level of 130 dBμV/m (3 V/m) for medical devices specified by the FDA.

The impact of wireless devices such as Bluetooth on the electromagnetic environment is also expected to be minimal, since the device output level is comparable to recorded levels of EMI. On the other hand, it is necessary to analyze the performance of Bluetooth in the presence of the electromagnetic environment in hospitals. Based on

the measurement campaigns performed in the two hospitals, we can consider WLANs and microwave ovens to be the worst case interferers for Bluetooth devices in hospitals. Hence studying the throughput performance of Bluetooth in the presence of microwave ovens and WLANs would help us to estimate the QoS for Bluetooth transmissions in hospital environments.

In Chapter 5 we will describe the Bluetooth throughput simulator in detail and use the simulator to predict the throughput of six ACL Bluetooth transmissions in the presence of 802.11b WLAN and microwave ovens.

Chapter 5

5 Interference Analysis for 2.4 GHz Wireless Devices in a Hospital Environment

5.1 Introduction

Currently Bluetooth and WLAN applications seem to be the most popular of wireless standards that are attracting health care providers. Since both WLAN and Bluetooth share the same spectrum and can come within close proximity to each other, there is concern on the interference and the resulting performance degradation posed by one another. Apart from the two devices there are unintentional RF radiators such as microwave ovens and cordless phones which operate in the same spectrum. Additionally, there may be other electrical devices that can cause EMI in the same spectrum.

Bluetooth and WLAN are complaint to FCC Part 15 regulations, thereby operation of these devices are subject to the following two conditions [Fcc15]:

(1) These devices may not cause harmful interference, and
(2) These devices must accept any interference received.

Therefore, Bluetooth devices should be resilient to operate in the presence of WLANs and other unintentional RF radiators.

In order to predict the performance of Bluetooth applications and estimate the QoS of Bluetooth transmissions in hospital environments, it is necessary to study the throughput performance of Bluetooth transmissions as a function of RFI. Consequently, a Bluetooth Throughput Simulator that utilizes channelized interference from PRISM was developed in MATLAB. The simulator's channels model and receiver structure adhere to those specified by the IEEE P802.15 Working Group for Wireless Personal Area

Networks™. The IEEE P802.15 Working Group focuses primarily on co-existence issues between Bluetooth and 802.11 WLAN.

The results of the measurement campaign in the two hospital environments clearly indicate microwave ovens and WLAN to be the primary source of interference in the 2.4 GHz ISM band. Therefore, through a number of experiments, we measure the interference from two microwave ovens and an 802.11b access point. The interference measured is then used in the throughput simulator to estimate the maximum average throughput of six Bluetooth ACL packet types.

The chapter is organized as follows: Section 5.2 and 5.3 provide a brief background on WLAN and Bluetooth standards required for understanding the measurements and Bluetooth throughput analysis. In Section 5.4 the throughput analysis for the six Bluetooth ACL packet types is explained in detail. The validation for the analysis is also provided. Section 5.5 describes the experimental setup for measuring interference from an 802.11b access point and two microwave ovens using PRISM. Then, the results of the simulated throughput for Bluetooth in the presence of these devices are presented. Finally a short chapter summary is presented in Section 5.6.

5.2 Wireless Local Area Network (WLAN)

A wireless LAN is a local area network (LAN) without wires. WLANs combine data connectivity with user mobility. Figure 5.1 shows a typical WLAN setup, where the network is divided into cells (BSS) and each cell is controlled by an access point (AP). The access points are connected trough a backbone wired network.

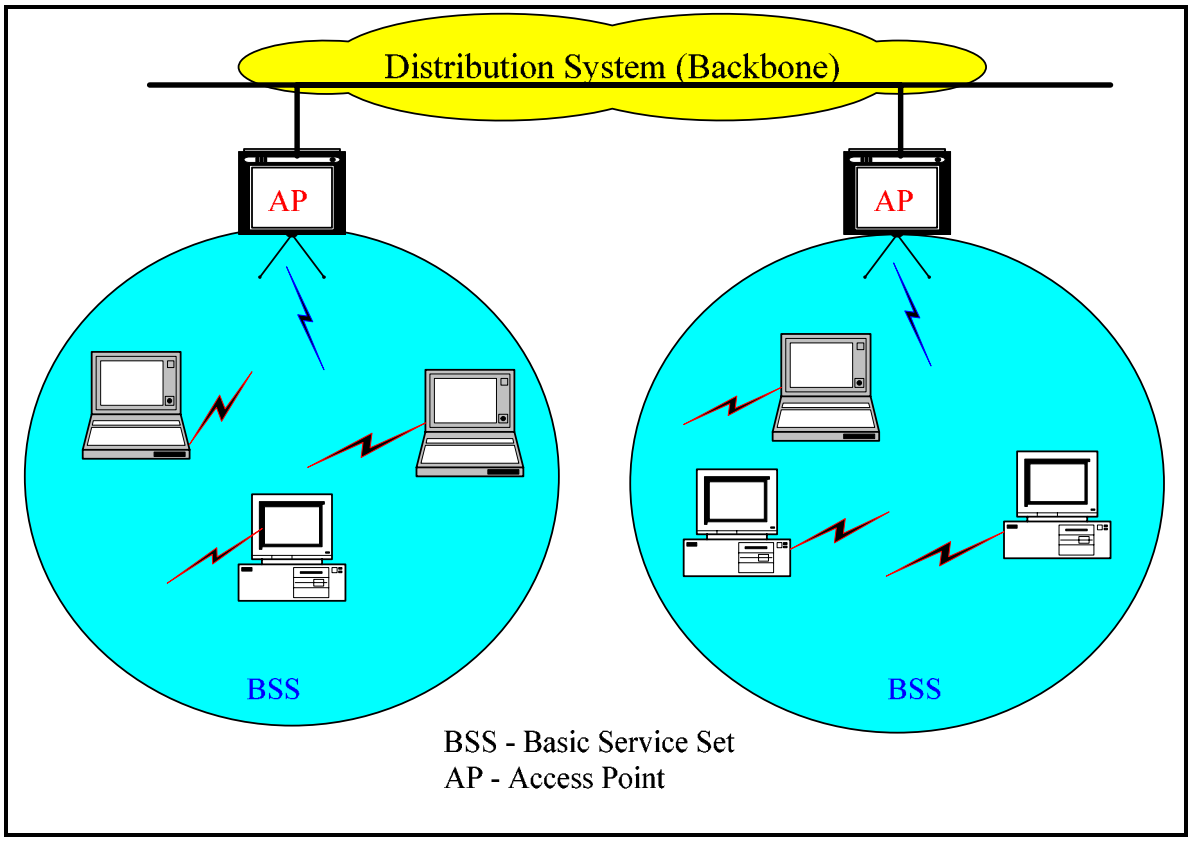

Figure 5.1 A Typical WLAN Setup

5.2.1.1 Frequency Bands and Channel Arrangement

Current commercially available WLANs operate in the ISM band and the Unlicensed National Information Infrastructure (UNII) band. The IEEE 802.11 standard was established in 1997 to define both the Media Access Layer (MAC) and Physical layer (PHY) requirements of WLAN. The 802.11 standard supports different communication techniques for transmitting a message over the air. It accommodates direct spread spectrum sequencing (DSSS), frequency hopping spread sequencing (FHSS), and infrared with pulse position modulation (PPM). These WLANs are capable of providing a maximum throughput of 2 Mbps.

In 1999, IEEE 802.11a and IEEE 802.11b were added to the existing 802.11 PHY. WLANs adhering to the 802.11 and 802.11b standard operate in the 2.4 GHz ISM band [Wla99a], [Wla99b]. The addition of 802.11b introduced higher data rates and basically extended the capabilities of 802.11. IEEE 802.11b employs DSSS exclusively, by dividing the ISM band into 14 partially-overlapping 22-MHz channels. In the United States and Canada 11 of the 14 802.11b channels are supported. The 11 802.11b channels

are spaced 5 MHz apart thereby resulting in 3 non-overlapping channels (Channels 1, 6 & 11). The channel allocations for 802.11 b are summarized in Table 5.1.

Table 5.1

WLAN Channel Allocations for 802.11b

802.11b Channels	Lower Frequency	Center Frequency	Upper Frequency
1	2.4010	2.4120	2.4230
2	2.4060	2.4170	2.4280
3	2.4110	2.4220	2.4330
4	2.4160	2.4270	2.4380
5	2.4210	2.4320	2.4430
6	2.4260	2.4370	2.4480
7	2.4310	2.4420	2.4530
8	2.4360	2.4470	2.4580
9	2.4410	2.4520	2.4630
10	2.4460	2.4570	2.4680
11	2.4510	2.4620	2.4730

The 802.11a WLAN was introduced to meet the demands for higher data rates. The 802.11a uses OFDM technology and operates in the 5.2 GHz UNII band. 802.11a allows for 8 channels whose frequencies do not overlap.

Table 5.2 summarizes the 802.11a and 802.11b WLAN standards.

Table 5.2

IEEE WLAN Standards

Standard	PHY	Frequency and Channel Specifications	Data Rates (Mbps)	
802.11b	DSSS (CCK, BPSK, QPSK)	2.4 to 2.4835 GHz (ISM band) 11 channels, 22 MHz wide between 2.412 GHz and 2.462 GHz Only channels 1, 6 & 11 do not overlap	5.5 or 11	
802.11a	OFDM (BPSK, QPSK, 16-QAM, 64-QAM)	5.15 to 5.825 GHz (UNII band) 12 channels, 20 MHz wide between 5.150-5.350 GHz and 5.725 and 5.825 GHz (No overlapping channels)	Mandatory 6,12 and 24	Optional 9,18,36 and 54

5.2.1.2 Power Requirements and Range

The 802.11b transmitters have a nominal power of 100mW (20dBm). This signal strength was chosen to accommodate coverage of the approximately 100 meter radius area and to limit battery power consumption in portable devices.

5.3 Bluetooth

Bluetooth is a de-facto open standard for short range digital radio. Bluetooth was an effort by a consortium of companies to design a royalty free technology to fulfill the vision of a low-cost, low-power radio cable replacement. This effort began in 1998 with the formation of the Special Interest Group (SIG) by Ericsson, Nokia, Toshiba, IBM and Intel. The result was an open specification for a technology that would enable short range radio link between mobile PCs, mobile phones and other portable devices.

Bluetooth is named after a 10^{th} century Viking Harald Blatand. His diplomatic reign unified the nations of Denmark and Norway, which he then ruled from 940-981. He got his name Bluetooth because he liked blueberries so much that they stained his teeth (well this one of the reasons, there are many more!). Even the trademark for the group reflects these origins. It is made up of the two runic characters "H" and "B". It also reflects the Scandinavian origins of two of the founding companies, Ericsson and Nokia.

5.3.1 Radio Specification

The Bluetooth Radio specification defines the requirements for a Bluetooth transceiver operating in the 2.4GHz ISM band. It is the lowest layer of the Bluetooth specification. This section describes the frequency bands, channel allocations, transmitter and receiver characteristics of the Bluetooth radio as provided in the Bluetooth Core 1.0 specification [Sig01].

5.3.1.1 Frequency Bands and Channel Arrangement

Bluetooth radio uses frequency-hopping spread spectrum (FHSS) technology. In United States, Europe and most other countries, the frequency band over which Bluetooth

operates is divided into 79 1-MHz wide channels between 2400 and 2483.5 MHz. In France, Spain and Japan the frequency range is reduced, and a 23 1-MHz channel system is used. Table 5.3 provides the international frequency band and channel allocation for Bluetooth.

Table 5.3
Bluetooth International Frequency Allocations

Geography	Regulator Allocation	Bluetooth Channels
USA, Europe and most other countries	2.400 – 2.4835 GHz	f = 2402 + k MHz k = 0,1,…,78
France, Spain and Japan	2.4465 - 2.4835 GHz	f = 2454 + k MHz k = 0,1,…,22

5.3.1.2 Transmitter Characteristics

Bluetooth radios are grouped into three classifications based on their maximum transmit power. The three classes of Bluetooth radios are shown in Table 5.4

Table 5.4
Bluetooth Radio Power Levels

Power Class	Maximum Output Power (Pmax)	Nominal Output Power	Minimum Power (at maximum power setting)
1	100 mW (20 dBm)	N/A	0 dBm
2	2.5 mW (4 dBm)	0 dBm	0.25 mW (-6 dBm)
3	1 mW (0 dBm)	N/A	N/A

Power control is mandatory for devices with maximum transmit power greater than 4 dBm, namely power class 1. Bluetooth devices currently have a maximum range of 10 m at low powers (0dBm) and 100 m at high powers (20 dBm).

5.3.1.3 Modulation Scheme

Bluetooth uses Gaussian frequency shift keying (GFSK) modulation with a time-bandwidth product BT = 0.5, modulation index $0.28 \leq h \leq 0.35$ and a modulation symbol rate of 1 Mb/s.

Figure 5.2 shows the transmit modulation for Bluetooth. A positive frequency deviation is used to represent a binary one and a negative frequency deviation is used to represent a binary zero. The minimum deviation can never be smaller than 115 kHz. Maximum frequency deviation is between 140 kHz and 175 kHz. In order to reduce spectral spreading that can cause ISI, Bluetooth uses a Gaussian filter with time bandwidth product BT = 0.5.

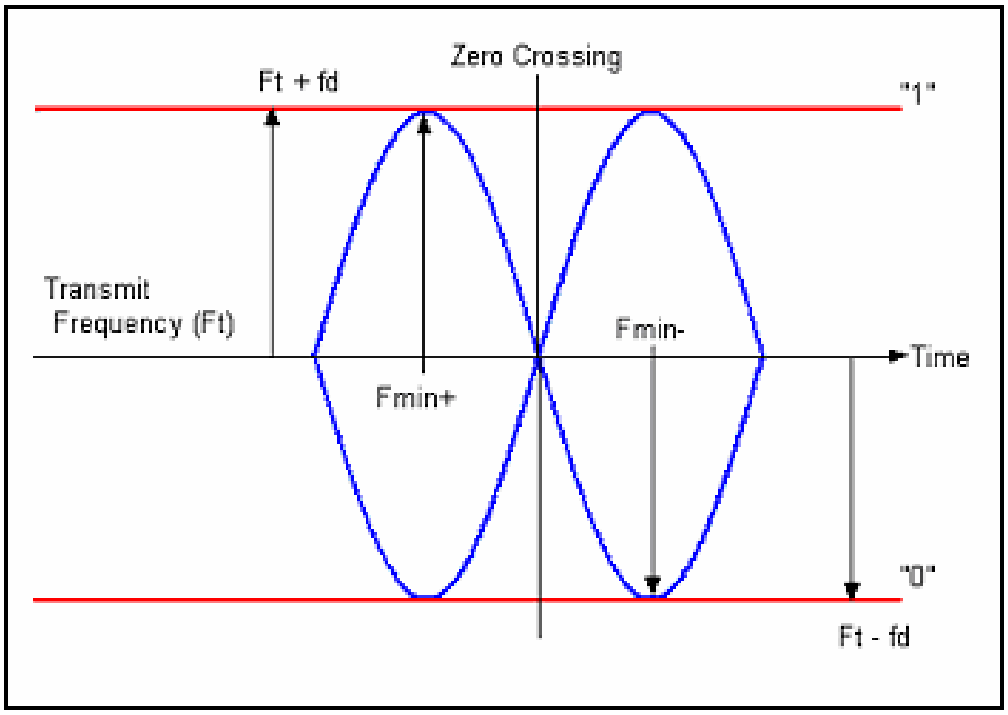

Figure 5.2 Transmit Modulation for Bluetooth

5.3.1.4 Receiver Characteristics

The Bluetooth standard requires that the Bluetooth receiver must have a sensitivity level for which the bit error rate (BER) 0.1% is met. The requirement for a Bluetooth receiver corresponding to this BER is an actual sensitivity level of –70 dBm or better.

5.3.2 Baseband

The Bluetooth system consists of a radio unit, a link control unit, and a support unit for link management and host terminal interface functions. Figure 5.3 shows the functional blocks of the Bluetooth system

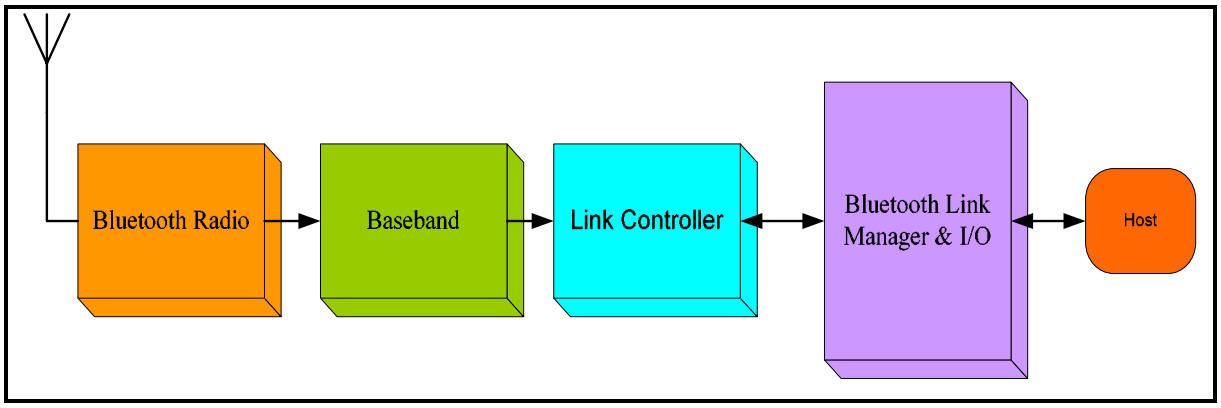

Figure 5.3 Functional Blocks in the Bluetooth System

The Physical Layer (PHY) consists of the radio and baseband units. The baseband is responsible for channel coding and decoding. It is also responsible for timing and management control of the link. The Link Controller is responsible for carrying out the baseband protocols and other low-level link routines in response to higher level commands from the Link Manager.

Full duplex transmission capability is achieved using time division duplexing (TDD), where subsequent slots are used for transmitting and receiving. Bluetooth is organized into a Master-Slave architecture, where Master devices transmit in even-indexed time slots and slave devices transmit in odd-indexed slots. Figure 5.4 shows a Bluetooth setup, known as a piconet. A piconet is formed when two or more devices share the same channel in an adhoc fashion. All devices are peer units and have identical implementations. The master in a piconet controls and synchronizes the communication of other devices in the piconet. There is only one master per piconet however, it can don the role of a slave in an adjacent piconet. A collection of piconets constitute a scatternet. A given piconet may contain up to 7 active devices and many passive devices. While the

passive devices are usually in the parked state and do not take part in communication, they still remain synchronized to the master.

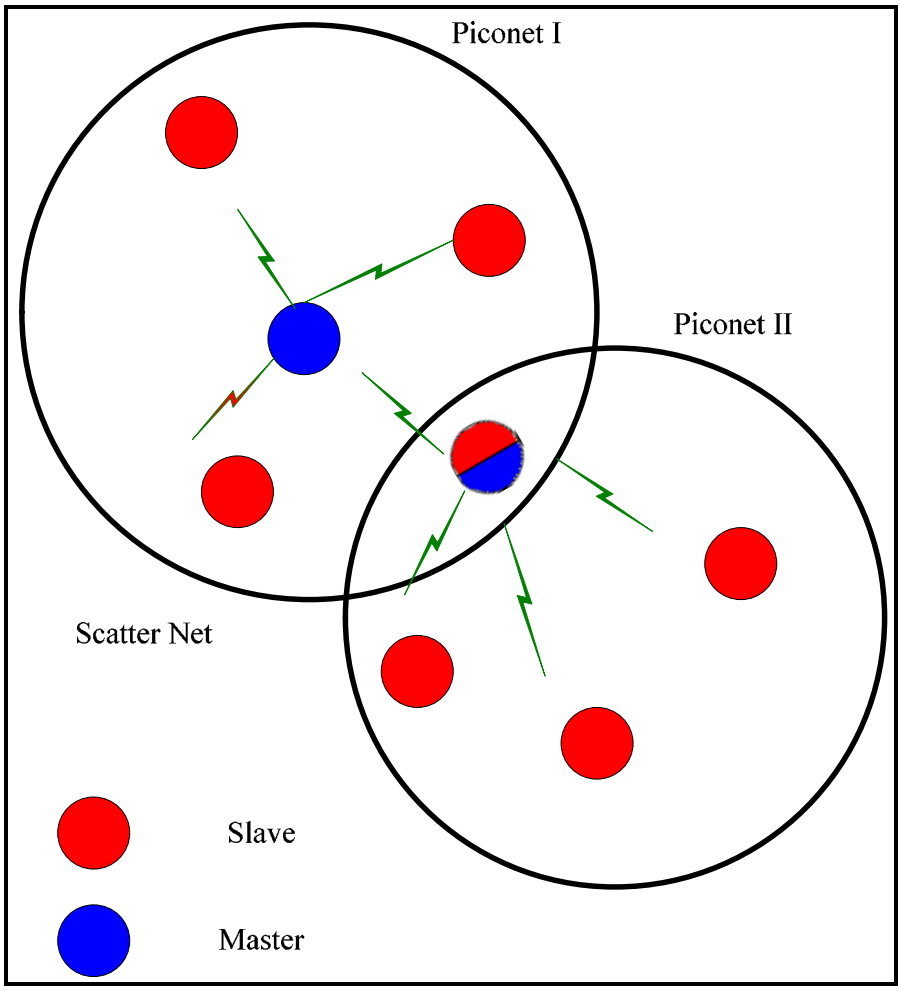

Figure 5.4 Bluetooth Setup – Piconets and Scatternets

5.3.2.1 Physical Channel

The physical channel is characterized by a pseudo-random sequence hopping through the 79 or 23 RF channels. Each piconet has a unique hopping sequence which is determined by the Bluetooth device address of the master, while the phase in the hopping sequence is determined by the master clock. The channel is divided into time slots of 625 µs and each slot corresponds to an RF hop frequency. All Bluetooth devices participating in a piconet are time and hop synchronized to the channel at a nominal hop rate of 1600 hops/s [Sig01].

5.3.2.2 Time Slots

Bluetooth uses time division duplex (TDD) scheme where master and slave alternatively transmit. TDD allows utilization of the radio spectrum by dividing time into slots. Each slot enables a user to transmit data on a given frequency channel for the entire duration of the slot. The Bluetooth channel is divided into time slots, each 625 μs in length. The slots are numbered based on the Bluetooth clock of the piconet master. The master transmits in even-numbered time slots and the slave transmits in odd-numbered time slots (Figure 5.5). Packet start is aligned with the slot start and may extend for up to five time slots. The RF hop frequency remains fixed for the duration of the packet. A single slot packet will be transmitted on the RF channel determined by the current Bluetooth clock value. For a multi-slot packet, the RF hop frequency to be used for the entire packet is obtained from the Bluetooth clock value assigned to the first slot of the packet. Figure 5.6 illustrates the hop definition on single- and multi-slot packets.

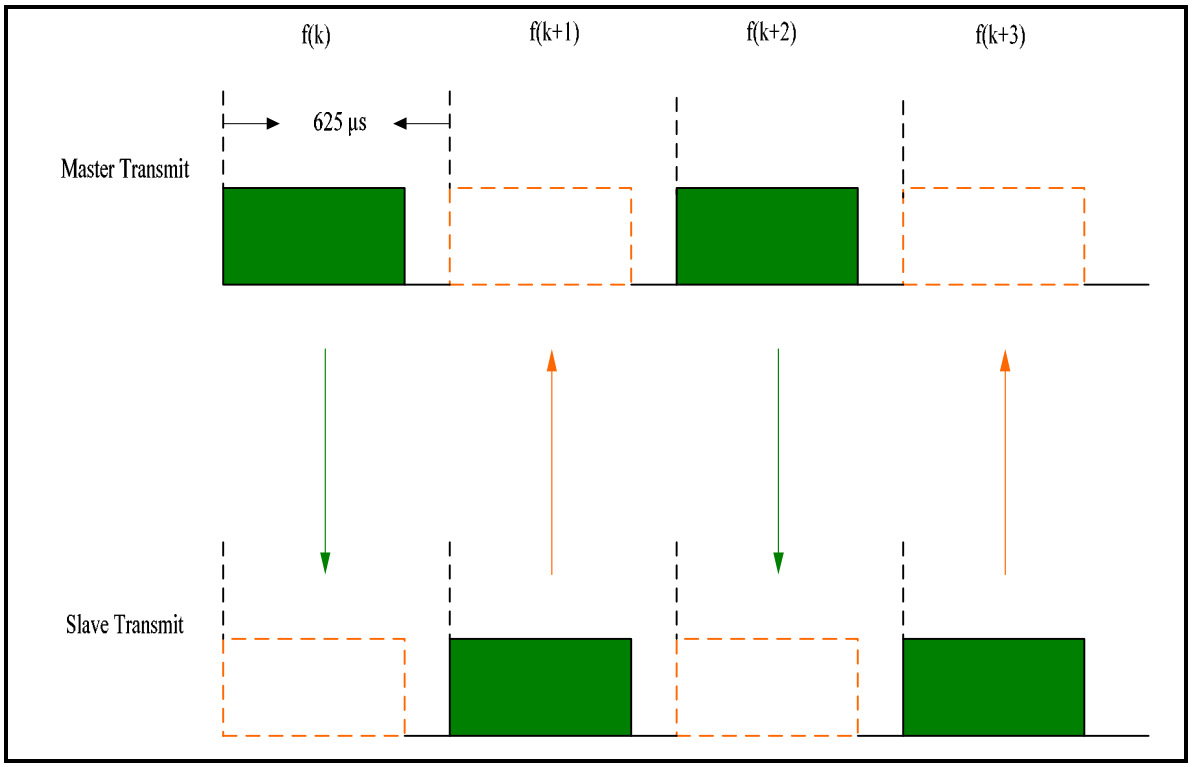

Figure 5.5 TDD and Packet Timing

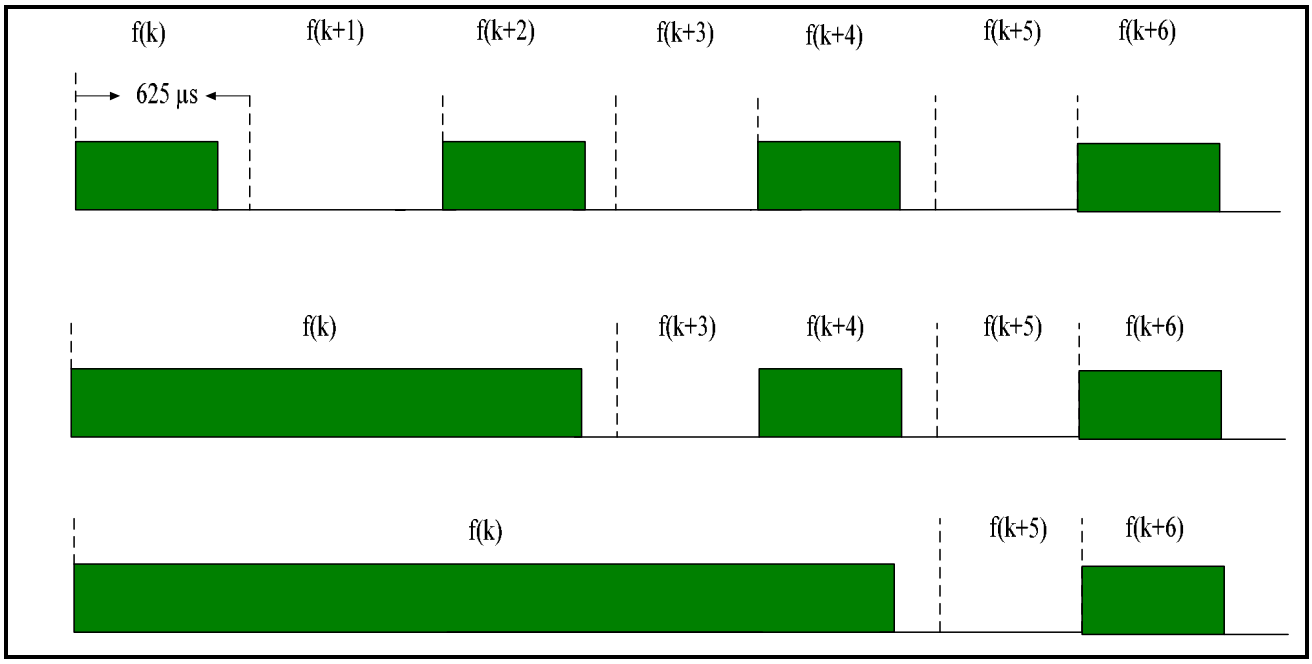

Figure 5.6 Multi-Slot Packets

5.3.2.3 Physical Links

Bluetooth devices provide data rates of 108/108 kbps (forward/ reverse) for symmetric channels and 723/57 kbps for asymmetric channels. Bluetooth uses both circuit and packet switched links, referred to as Synchronous Connection Oriented (SCO) and Asynchronous Connectionless (ACL). SCO links are primarily used for voice communication whereas ACL links are used for primarily for data and delay insensitive communication. Bluetooth supports:

(a) Up to 3 simultaneous 64 kbps SCO links

(b) Simultaneous SCO and ACL links

(c) Up to 721/57.6 kbps asymmetric or 433.9 kbps symmetric ACL link

5.3.2.4 Bluetooth Packets

Bluetooth packets are classified according to the physical links in which they are used The SCO packets are used in synchronous links which are sensitive to delay and hence used for voice applications. There is no error checking mechanism or retransmission for SCO packets. The ACL packets are used for user data and control data which are not sensitive to delay. These packets include an error checking mechanism and retransmission is possible. The Bluetooth radio standard defines 13 different ACL or

SCO packets. The ID, NULL, POLL, FHS, DM1 are packets defined for SCO and ACL links. DH1, AUX1, DM3, DH3, DM5, DH5 packets are defined for ACL links and HV1, HV2, HV3, DV packets are defined for SCO links.

The throughput simulator to be presented in Section 4 considers only the ACL data packets (DMx, DHx), which possess Cyclic Redundancy Check (CRC) and Automatic Repeat Request (ARQ). Hence we shall restrict our discussion to these packets alone. The characteristics of the six ACL packet types discussed in section 4 are presented in Table 5.5.

Table 5.5

ACL Packet Types with ARQ

Type	Payload Header (bytes)	User Payload (bytes)	FEC	Total No. of Bits (*K*)	Symmetric Max. Rate (kbps)	Asymmetric Max. Rate (kbps)		Peak Throughput (kbps)
						Forward	Reverse	
DM1	1	17	2/3 FEC	240	108.8	108.8	108.8	108.8
DM3	2	121	2/3 FEC	1500	258.1	387.2	54.4	387.2
DM5	2	224	2/3 FEC	2745	286.7	477.8	36.3	477.8
DH1	1	27	No FEC	240	172.8	172.8	172.8	172.8
DH3	2	183	No FEC	1496	390.4	585.6	86.4	585.6
DH5	2	339	No FEC	2744	433.9	723.2	57.6	723.2

An ACL data packet may occupy 1, 3, or 5 consecutive time slots, hence a packet may occupy a channel for periods longer than 625 μs. Bluetooth packets consist of a 72-bit access code for piconet identification and synchronization, a 18 bit header (54 bits gross due to triple redundancy), and a variable-length payload. The payload consists of three segments: a payload header, a payload and a 16 bit CRC for error detection. In DMx

packets, payload header, payload and 16 bit CRC are FEC coded with the (15, 10) shortened Hamming code, while the DHx packets are uncoded. The general Bluetooth packet structure is shown in Figure 5.7.

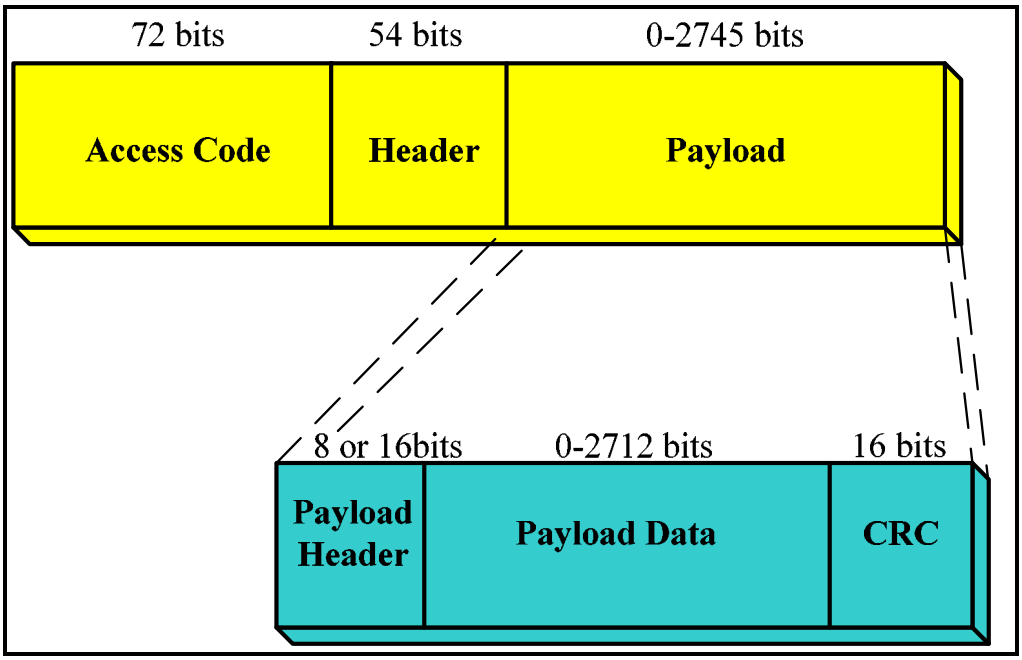

Figure 5.7 General Packet Format

5.3.2.5 Error Correction

Three error correction schemes are defined for the Bluetooth baseband protocol.

a) **1/3 rate forward error correction code (FEC)** – uses a simple repetition code that repeats every bit three times for redundancy.

b) **2/3 rate forward error correction code (FEC)** – A (15, 10) shortened hamming code is used to encode data. Each data block containing 10 information bits is encoded into a 15 bit codeword. The (15, 10) shortened Hamming code can detect all double errors and correct single errors in each code word.

c) **Automatic repeat request (ARQ)** – In the ARQ scheme packets are transmitted and retransmitted until an acknowledgement is received (or timeout is exceeded). If timeout is exceeded the transmitter proceeds with the next packet. The ARQ scheme is applicable only to the payload in the packet containing CRC.

FEC is applied to the data payload to reduce the number of retransmissions. Packet types for Bluetooth have the flexibility on the use of FEC (DMx and DHx). This is because FEC increases overhead and decreases throughput in interference free environment.

5.4 Bluetooth Throughput Analysis

In section 5.3 the six ACL packet types with ARQ were discussed. ARQ allows retransmission of lost or corrupted packets. In the slot immediately following the received packet, the destination Bluetooth radio piggy-backs an ARQ acknowledgement to inform the source Bluetooth radio of a successful acknowledgement (ACK) or unsuccessful acknowledgement (NAK) transfer of payload data with CRC. When no acknowledge is received, a NAK is assumed by default. In the event of NAK, the source radio will continue to retransmit the packet during its next slot until an ACK is received. The ARQ mechanism is illustrated in Figure 5.8 [Swee00].

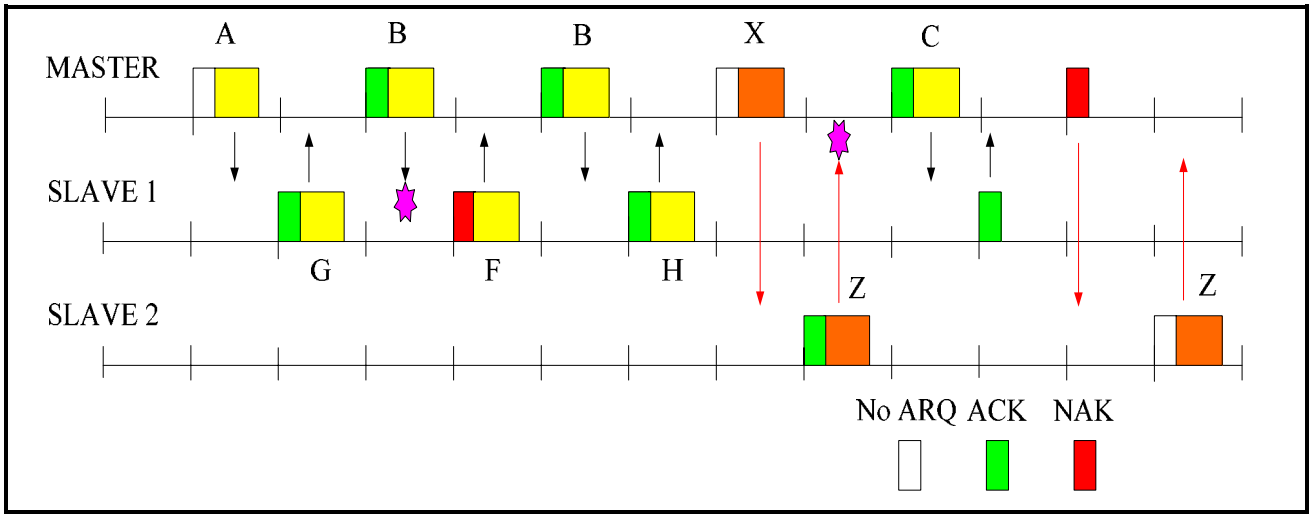

Figure 5.8 Bluetooth ARQ Mechanism

The probability of retransmission by a Bluetooth receiver is given by [Val02]:

$$P_r(\gamma) = 1 - P[\overline{A}]P[\overline{B}]P[\overline{C}]P[\overline{D}]P[\overline{E}] \tag{5.1}$$

where *A*, *B*, *C*, *D*, and *E* are the events:

A: the 72-bit synchronization of the forward channel fails.

B: the header FEC of the forward channel fails.

C: the Hamming code protecting the payload of the forward transmission fails.

D: the 72-bit synchronization of the reverse packet fails.

E: the header FEC of the reverse channel fails.

and $\gamma = \{\gamma_f, \gamma_r\}$ contains the instantaneous forward and reverse signal-to-noise ratios.

Since both the forward and return packets use a 72-bit synchronization code and a 54-bit header, the probability of the events *A* and *D* will be of a similar form, and that of event *B* and *E* will be of a similar form.

In the following analysis, it is assumed that that the CRC decoder in the payload can detect all uncorrectable errors.

If *N* is a random variable representing the total number of times a particular packet must be retransmitted and assuming that the probability density function of the SNR is constant for the duration of the frame, but varies from frame to frame, the probability mass function (pmf) of *N* is given by [2]:

$$p_N[n] = (1 - \overline{P}_r(\Gamma))(\overline{P}_r(\Gamma))^{n-1} \tag{5.2}$$

where *n* is the number of transmissions and Γ represents the average SNR and $\overline{P}_r(\Gamma)$ is the corresponding average channel error probability.

The Bluetooth standard requires a receiver sensitivity of -70dBm for a raw BER (Bit Error Rate) of 0.1% [Sig01]. Adopting the PHY model specified by the IEEE 802.15 task group and using the -70 dBm threshold, the device's allowable noise floor in an

AWGN channel was calculated to be -83.8 dBm [Rob03]. By treating the RF interference measured by PRISM as non-coherent noise, a modified SNR or SINR (Signal to Noise plus Interference ratio) for each forward $\gamma_{f(ch)}$ and reverse channel $\gamma_{r(ch)}$ can be calculated. Since the return channel is at a different frequency from the forward channel, the corresponding SINR's are different and hence result in different symbol error probabilities for the forward channel and reverse channel,

$$\varepsilon_{error\ probability} = \left\{ \varepsilon(\gamma_{f(ch)}), \varepsilon(\gamma_{r(ch)}) \right\} \tag{5.3}$$

The error probability can be different for different demodulation and decision algorithms that can be employed in the Bluetooth receiver. In our analysis we adhere to the lower bound on error probability as described by Valenti *et al.* A non-coherent detection of binary FSK with a modulation index of $h = 0.32$ is considered. This receiver implementation yields an error probability given by [Val02],

$$\varepsilon(\gamma) = e^{-\frac{\gamma}{2}} \left\{ \frac{1}{2} I_o(ab) + \sum_{k=1}^{\infty} \left(\frac{a}{b} \right)^k I_k(ab) \right\} \tag{5.4}$$

where $a = \sqrt{\frac{\gamma}{2}\left(1 - \sqrt{1 - \left(\frac{\sin(2\pi h)}{2\pi h}\right)^2}\right)}$, $b = \sqrt{\frac{\gamma}{2}\left(1 + \sqrt{1 - \left(\frac{\sin(2\pi h)}{2\pi h}\right)^2}\right)}$, I_o and I_k are the zero and kth order Bessel functions respectively.

By taking the expected value of $P_r(\gamma)$ with respect to the SINR's $\gamma_{SINR} = \left\{ \gamma_{f(ch)}, \gamma_{r(ch)} \right\}$, the average probability of retransmission $\bar{P}_r(\Gamma)$ can be calculated as,

$$\bar{P}_r(\Gamma) = E\left\{ P_r(\gamma_{SINR}) \right\} \tag{5.5}$$

It should be noted that the random variables $P\left[\bar{A}\right], P\left[\bar{B}\right]$ and $P\left[\bar{C}\right]$ are functions of the forward channel $\gamma_{f(ch)}$ whereas random variables $P\left[\bar{D}\right]$ and $P\left[\bar{E}\right]$ are functions of the reverse channel $\gamma_{r(ch)}$.

The average probability of retransmission can be expressed as,

$$\begin{aligned}\overline{P}_r(\Gamma) &= 1 - E_{\gamma_{f(ch)}}\left\{P\left[\overline{A}\right]P\left[\overline{B}\right]P\left[\overline{C}\right]\right\}E_{\gamma_{r(ch)}}\left\{P\left[\overline{D}\right]P\left[\overline{E}\right]\right\} \\ &= 1 - \frac{1}{79}\left(\sum_{\gamma_{f(ch=1)}}^{79} P\left[\overline{A}\right]P\left[\overline{B}\right]P\left[\overline{C}\right]\right)\frac{1}{79}\left(\sum_{\gamma_{r(ch=1)}}^{79} P\left[\overline{D}\right]P\left[\overline{E}\right]\right)\end{aligned} \tag{5.6}$$

where the probability of events $\overline{A}, \overline{B}, \overline{D}$ and $\overline{E}$ for all packets take the form:

$$P\left[\overline{A}\right] = \sum_{k=0}^{72-T}\binom{72}{k}(\varepsilon(\gamma_{f(ch)}))^k(1-\varepsilon(\gamma_{f(ch)}))^{72-k} \tag{5.7}$$

$$P\left[\overline{D}\right] = \sum_{k=0}^{72-T}\binom{72}{k}(\varepsilon(\gamma_{r(ch)}))^k(1-\varepsilon(\gamma_{r(ch)}))^{72-k} \tag{5.8}$$

The packets use a 72-bit synchronization code, and become synchronized if the output of the correlator in the demodulator exceeds a certain threshold *T*. $T = 65$ was chosen for the simulator; hence if 65 of the 72 bits are demodulated correctly, frame synchronization is achieved.

$$P\left[\overline{B}\right] = (3\varepsilon(\gamma_{f(ch)})(1-\varepsilon(\gamma_{f(ch)}))^2 + (1-\varepsilon(\gamma_{f(ch)}))^3)^{18} \tag{5.9}$$

$$P\left[\overline{E}\right] = (3\varepsilon(\gamma_{r(ch)})(1-\varepsilon(\gamma_{r(ch)}))^2 + (1-\varepsilon(\gamma_{r(ch)}))^3)^{18} \tag{5.10}$$

The 54-bit header formed by triple redundancy of the 18-bits in the header using a simple (3, 1) code. Hence the packet can get corrupted if there are more than one errors i.e., for 2 bit errors and 3 bit errors.

The DHx packets have no FEC, therefore the probability of event $\overline{C}$ for DHx packets is given by

$$P\left[\overline{C}\right] = (1-\varepsilon(\gamma_{f(ch)}))^K \tag{5.11}$$

where *K* is the number of bits in the packet (Table 5.5), *K* = 240 for DH1, *K* = 1496 for DH3 and *K* = 2744 for DH5.

For DMx packets the (15,10) shortened Hamming code allows correction of 1 bit for every 15 bits, therefore probability of event $\overline{C}$ can be evaluated as,

$$P\left[\overline{C}\right] = (15\varepsilon(\gamma_{f(ch)})(1-\varepsilon(\gamma_{f(ch)}))^{14} + (1-\varepsilon(\gamma_{f(ch)}))^{15})^{m} \tag{5.12}$$

where $m = \frac{K}{15}$, K is obtained from Table 5.5. Hence, m = 16 for DM1, m = 100 for DM3 and m = 183 for DM5.

Equation 5.6 allows us to estimate the average probability of retransmission of Bluetooth ACL packets taking into account the interference experienced by each individual Bluetooth channel.

For DMx and DHx packets, if D represents the total number of slots occupied in each transmission including ACK and K represents the total number of bits in the packet, then the average throughput τ_{avg} can be calculated by taking the expected value of the data rate with respect to N [Val02]

$$\tau_{avg} = E_N\left[\frac{K}{DN(625\times10^{-6})}\right] \tag{5.13}$$

The values for K and D for various ACL packet types can be obtained from Table 5.5.

Large Scale Fading Model

In order to predict the throughput of a particular Bluetooth receiver in practical environments, the effect of distance of separation from the Bluetooth transmitter and its associated path loss is integrated into the Bluetooth throughput model. As described in Chapter 2, we have used the indoor propagation path loss model for 2.4 GHz as specified by the IEEE P802.15 Working Group for Wireless Personal Area Networks™ [Kam99], [Lan01a]. This model is widely used for developing and simulating 802.11 and Bluetooth networks in order to study their coexistence. Hence, the use of the IEEE P802.15 indoor channel model shown in Table 5.6 will allow the throughput results to be used and compared on a common platform.

Table 5.6
802.15 WPAN In-building Path loss Model
$f = 2.45 GHz, \lambda = 0.1124 m$

Distance	n	Path Loss (dB)
d ≤8 m	2	$40.2 + 20\log(d)$
d > 8 m	3.3	$58.5 + 33\log(d/8)$

Validation of Throughput Simulator

In order to test the validity of the analysis the mean interference power at 3 meters (Figure 5.9, Point A) from a microwave oven was measured using PRISM according to the procedures described in Section 3.4. The mean interference power was quantified into 79 individual Bluetooth channels and the modified SNR (or SINR) for each corresponding channel was computed. Using the SINR per channel, the corresponding channel symbol error probabilities were calculated and applied to Equation 5.6 to yield the maximum average throughput.

Consider an experimental setup as shown in Figure 5.9, wherein a Bluetooth receiver is placed at Point A (Point A is fixed) and a Bluetooth transmitter is place at Point B. The simulator considered the Bluetooth receiver located at the fixed Point A in the place of PRSIM, experiencing interference as measured by PRISM

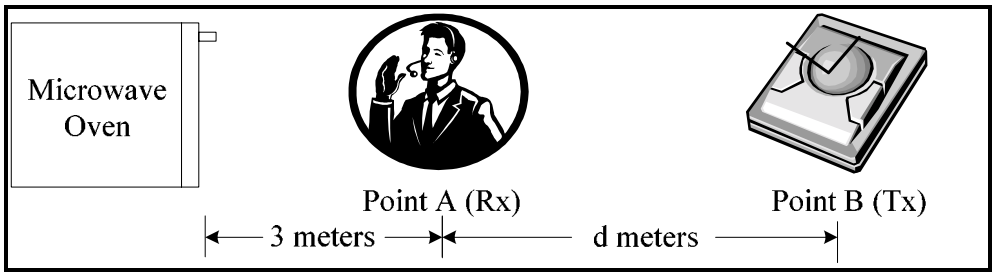

Figure 5.9 Experimental Setup consisting of Two Bluetooth Devices and a Microwave Oven

Figure 5.10 shows the average throughput for the six ACL Bluetooth packet types as a function of T-R separation *d* i.e., piconet size. It can be observed as the distance increases signal strength decreases and hence SINR decreases leading to decreasing throughput. Figure 5.11 shows an identical scenario with the microwave oven switched off. This results in a strong SINR and a higher throughput. From Figure 5.11 it can be seen that the

maximum throughput obtained for all six ACL packet types conforms to those listed in Table 5.5.

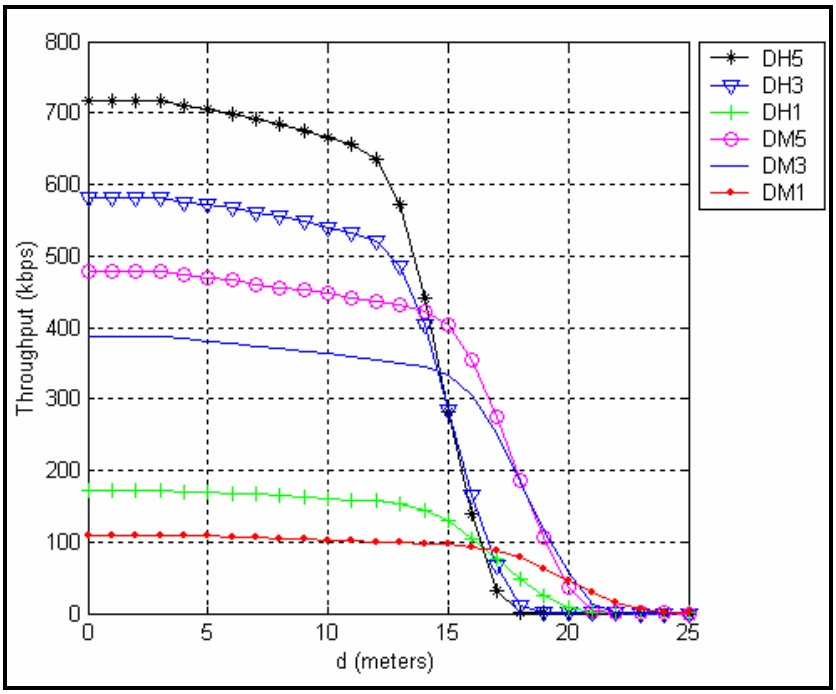

Figure 5.10 Bluetooth Average Throughput for Experimental Setup with Microwave Oven Switched ON

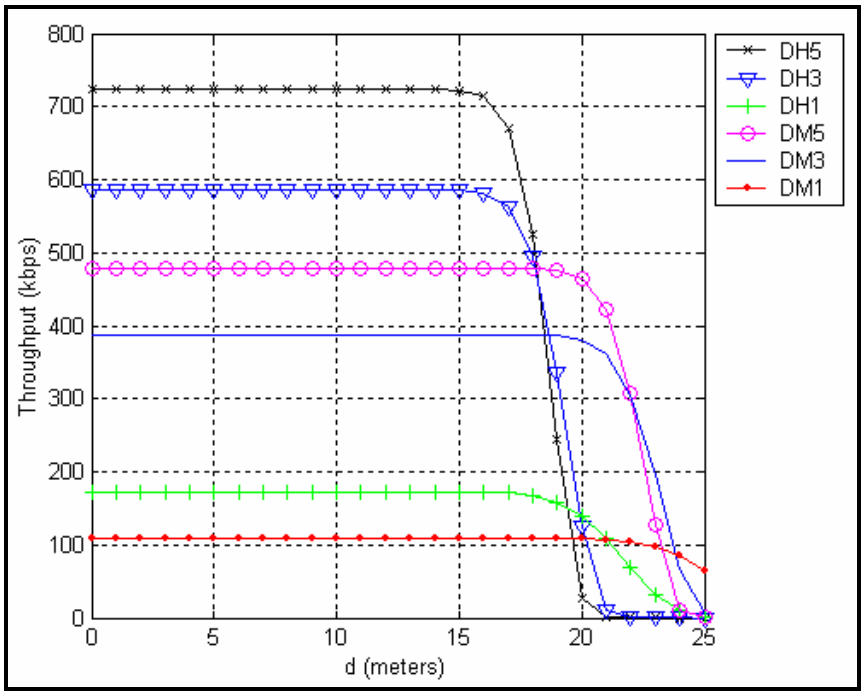

Figure 5.11 Bluetooth Average Throughput for Experimental Setup with Microwave Oven Switched OFF

5.5 Estimated Bluetooth Throughput in the Presence of Interference – Experimental Scenarios

5.5.1 Throughput Analysis Scope

The IEEE P802.15 Working Group for Wireless Personal Area Networks™ has over the years looked into a number of issues regarding co-existence of Bluetooth and 802.11 networks. Preliminary simulated results for decrease in throughput due to interference experienced by one another have been presented in [Chi02]. However, the experimental details and assumptions have not been clearly detailed. Some researches have also investigated the effect of microwave ovens on these WLANs [Lan01b] and Bluetooth devices [Mar02], but the study has been restricted to specific Bluetooth packet types (DM1 & DH1) alone.

In this section we discuss two experimental scenarios:

1. Bluetooth piconet operating in the presence of a WLAN network.
2. Bluetooth piconet operating in the presence of a microwave oven.

The experiments were performed in a LOS environment along the hallway on the 4th Floor of Durham Hall at Virginia Tech (Figure 5.12). PRISM was used to record and post process interference as a function of distance from the devices under test (WLAN/ Microwave Ovens). The post processed data was fed to the Bluetooth Throughput Simulator to yield expected maximum average throughput for the six Bluetooth ACL transmission types.

Figure 5.12Map of the 4th Floor of Durham Hall at Virginia Tech

Fifteen different receiver (PRISM) locations, in steps of 1 meter from the transmitter (WLAN/ Microwave Ovens) along the LOS were selected (Figure 5.13).

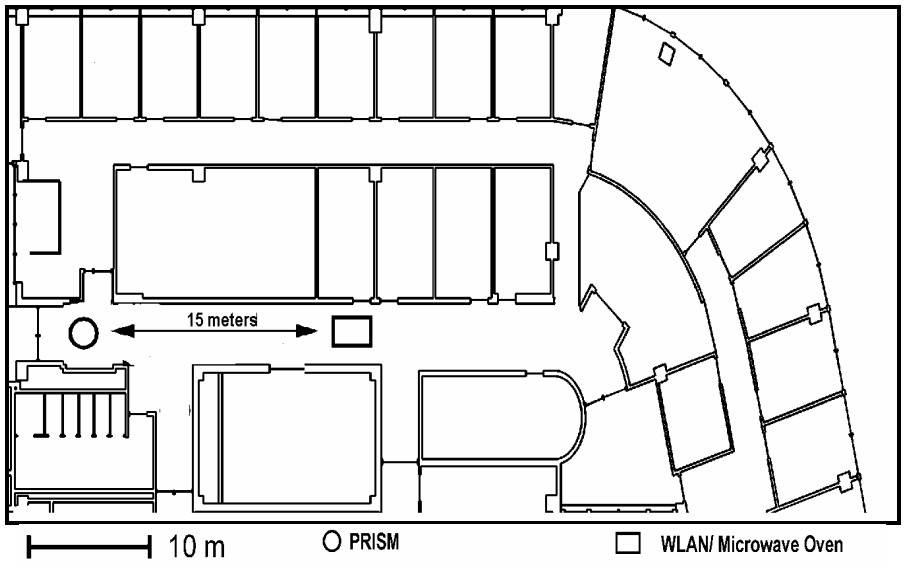

Figure 5.13 TX-RX Locations along the Hallway on the 4th Floor of Durham Hall

5.5.1.1 Bluetooth Throughput Performance in the Presence of WLAN

In the first scenario, the transmitter consisted of an 802.11b Orinoco AP 1000 WLAN access point operating on channel 6 (arbitrary choice). An IBM laptop with an 802.11b Orinoco Gold PCMCIA card was operating 0.5 meters away from the access point and

oriented perpendicularly to the LOS direction of the access point. The Orinoco access point and Orinoco wireless PCMCIA card have a nominal output power of 15 dBm. PRISM was setup to measure and record RFI over a period of 4 minutes at each location. The receiver configuration details are listed in Table 5.7.

Table 5.7
PRISM Configuration for WLAN Setup

Frequency	2.4 – 2.4835 GHz
Resolution Bandwidth	100 kHz
Video Bandwidth	100 kHz
Sweep Time	20 ms
Maximum Hold	2 Minutes
Trigger	Free

The Maximum Hold feature allows the display to hold on to the maximum observed power levels in each bin on the frequency band for the duration specified. The transmissions from an 802.11b access point are bursty and in order to observe a worst case scenario for estimating the Bluetooth throughput, the Maximum Hold duration was set to two minutes. Figure 5.14(a) shows the recorded interference from the access point at a distance of two meters. Figure 5.14 (b) shows the interference posed by the WLAN AP to the 79 individual Bluetooth channels. Bluetooth Channels 27 to 49 (i.e., of the 22 - 1MHz Channels) were affected the most. The maximum observed signal strength at 2 meters was -39.5 dBm.

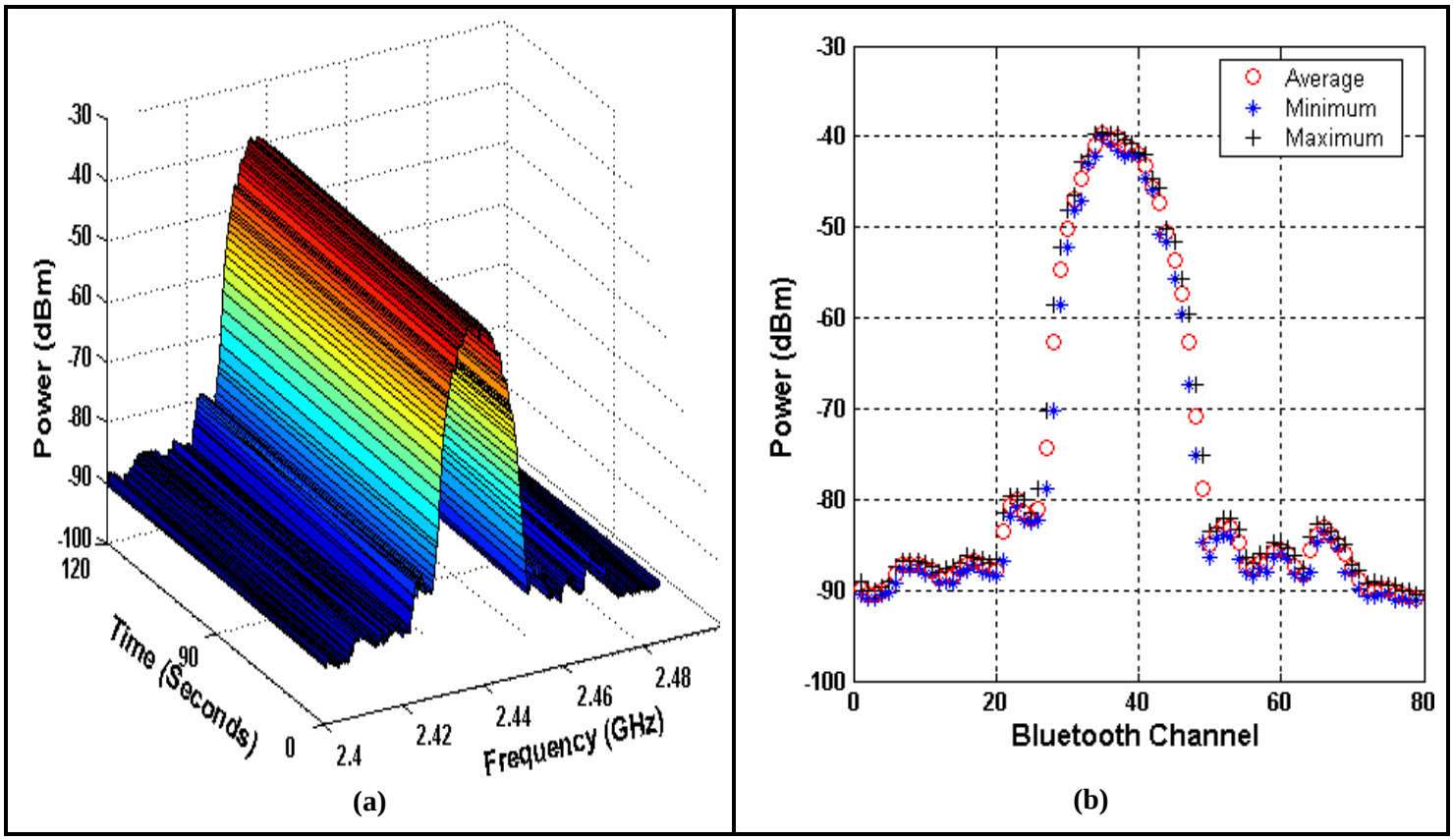

Figure 5.14 Interference Measured from the WLAN AP at a Distance of Two meters

The interference due to the WLAN measured along the hallway was fed to the throughput simulator. The simulator considered a Bluetooth receiver located along the hallway in the place of PRSIM, experiencing interference as measured by PRISM. The simulator considered a Bluetooth transmitter to be transmitting along the LOS of the Bluetooth receiver (Figure 5.15). The Bluetooth transmitter under consideration in the simulation is a Class I device (0 dBm).

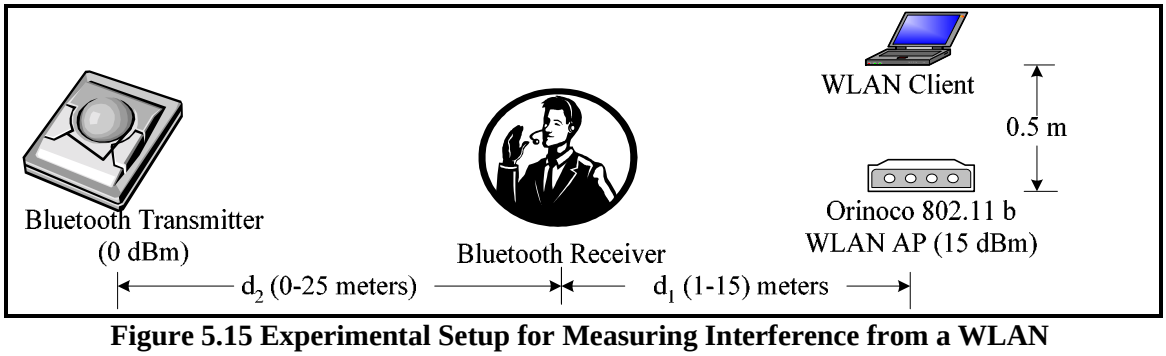

Figure 5.15 Experimental Setup for Measuring Interference from a WLAN

The throughput simulator predicted the throughput for the Bluetooth receiver at distances d_1 and d_2 away from the WLAN AP and Bluetooth transmitter respectively. Figure 5.16 shows the performance of six ACL transmissions types.

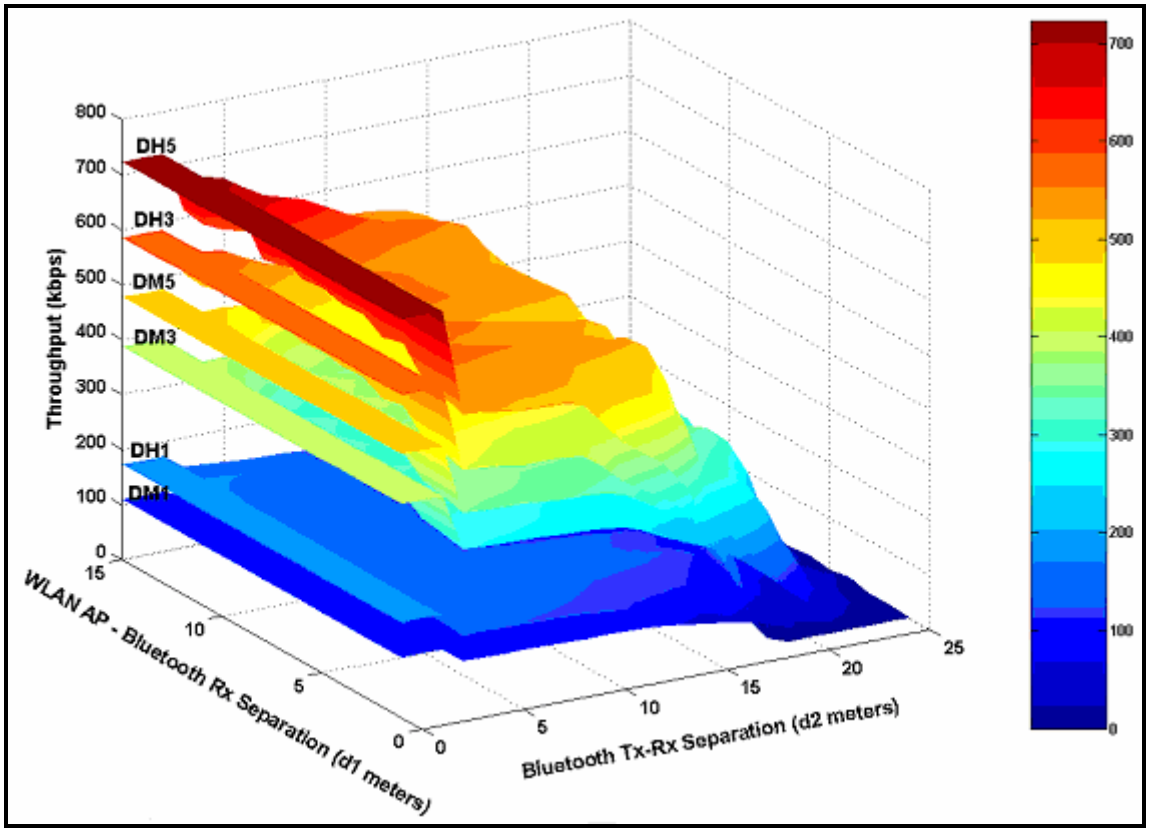

Figure 5.16 Average Throughput of Bluetooth ACL Packet Transmissions in the Presence of WLAN

Table 5.8 shows the throughput reduction for a Bluetooth piconet with Master-Slave separation of d_2 = 5, 10 meters at various distances d_1 from the WLAN AP.

Table 5.8

Average Throughput in kbps for Six Bluetooth ACL Transmission types in the Presence of WLAN

Bluetooth piconet with Master-Slave separation of d_2 = 5 meters						
d_1 (meters)	DM1	DM3	DM5	DH1	DH3	DH5
1	79	281	347	126	425	525
3	83	293	362	131	440	543
5	89	310	382	138	465	573
7	91	315	388	140	469	579
9	92	322	396	143	480	592
11	93	350	431	155	519	641
Bluetooth piconet with Master-Slave separation of d_2 = 10 meters						
d_1 (meters)	DM1	DM3	DM5	DH1	DH3	DH5
1	77	273	338	122	409	502
3	79	282	348	126	427	527
5	82	290	358	130	439	542
7	81	282	346	125	419	515
9	85	300	369	133	449	554
11	86	305	375	135	454	560

Analysis: The percentage reduction in throughput for DH packets is similar compared to the DM in the presence of WLAN. This similarity is expected because WLANs produce broadband noise and subject a group of 22 Bluetooth channels to high interference levels. The error correction schemes in DM packets are an inefficient way of recovering data errors caused by WLAN interference, whereas the DH packets for the same corresponding packet length can send more data (no error correction overhead) thereby achieving better throughput. Therefore, Bluetooth packets without error correction perform better in the presence of WLAN interference.

Bluetooth transmissions in the presence of WLAN interference achieve max throughput only when the distance between the Master and Slave in the piconet is less than 3.5 meters.

5.5.1.2 Bluetooth Throughput Performance in the Presence of Microwave Oven

In the second scenario, we replace the WLAN with a microwave oven as shown in Figure 5.17. All microwave ovens use magnetrons, which typically produce 700 to1000 watts RF power centered on 2.45 GHz.

Figure 5.17 Experimental Setup for Measuring Interference from a Microwave Oven

A microwave oven's emission has a time period of 16.67 ms. PRISM is limited by the sweep time of the spectrum analyzer as the fastest rate at which the HP 8594E is capable of sweeping across the frequency band is 20 ms. However there is a particular measurement method to overcome this draw back.

Residential microwave ovens employ half wave rectifiers or use the magnetron as the rectifier. Thereby, microwave ovens output power during only 45% (~50% = 8.33 ms) of the power line cycle and they are CW (Continuous Wave signal) in nature [Mar02]. The AC power supply line can therefore serve as a trigger for sweeping the frequency band periodically with the start of the microwave oven emission cycle. PRISM was configured to trigger by its power supply (120 V AC line), with the sweep time set to 33.33 ms (2 x 16.67), a multiple of the microwave oven's cycle [Swe02]. Hence, under single sweep setting, the analyzer would sweep the frequency span of 83.5 MHz (2.4 – 2.4835 GHz) over a period 33.33 ms. During this period there would be two ON periods and two OFF periods for the microwave oven as depicted in Figure 5.18.

Previous research on microwave oven radiation measurements show that the majority of the microwave oven's activity occur in the frequency range between 2.4 – 2.42 GHz and 2.46 – 2.48 GHz [Mar02]. In our measurement method the microwave oven is ON for these two sub-bands. Though, this measurement technique does not

capture the microwave ovens radiation over the complete frequency span (2.4 – 2.4835 GHz), it has been shown to be very accurate and the results produced were similar to those produced by a real-time spectrum analyzer [Mar02].

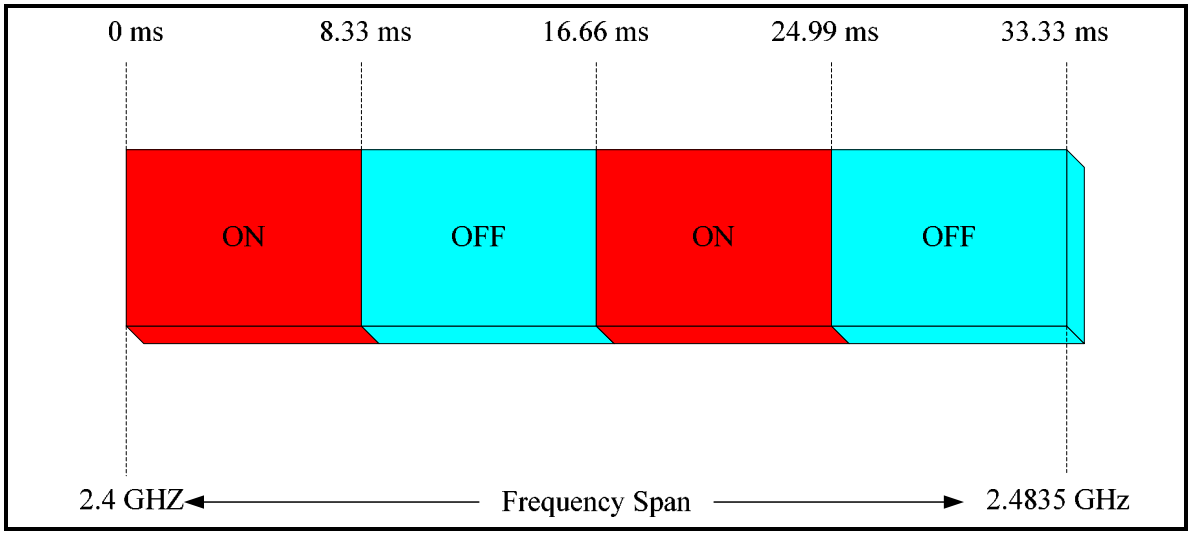

Figure 5.18 Relationship between Microwave Oven's Operation Cycle and PRISM's Frequency Span

RFI measurements for the microwave oven heating a mug of water (650 ml) were performed over a period of 2 minutes. The receiver configuration details are listed in Table 5.9. The values for the resolution and video bandwidth were based on experimental testing results by [Mar02].

Table 5.9

PRISM Configuration for Microwave Oven Setup

Frequency	2.4 – 2.4835 GHz
Resolution Bandwidth	100 kHz
Video Bandwidth	100 kHz
Sweep Time	33.33 ms, Single Sweep
Maximum Hold	OFF
Trigger	120 V, 60 Hz, 15 A single phase AC

Two independent runs of this experiment were performed using two different residential microwave ovens (Microwave oven I: GE, Model JES1131GB001, 1999; Microwave oven II: Panasonic, Model NN-7553A, 1994).

Microwave oven I: GE, Model JES1131GB001, 1999

Figure 5.19(a) shows the recorded interference from Microwave Oven I at a distance of two meters. Figure 5.19 (b) shows the interference posed by Microwave Oven I to the 79 individual Bluetooth channels. Bluetooth Channels 11-17, 33-35 and 58-68 were the most affected with a maximum interference level of -44.35 dBm on channel 36.

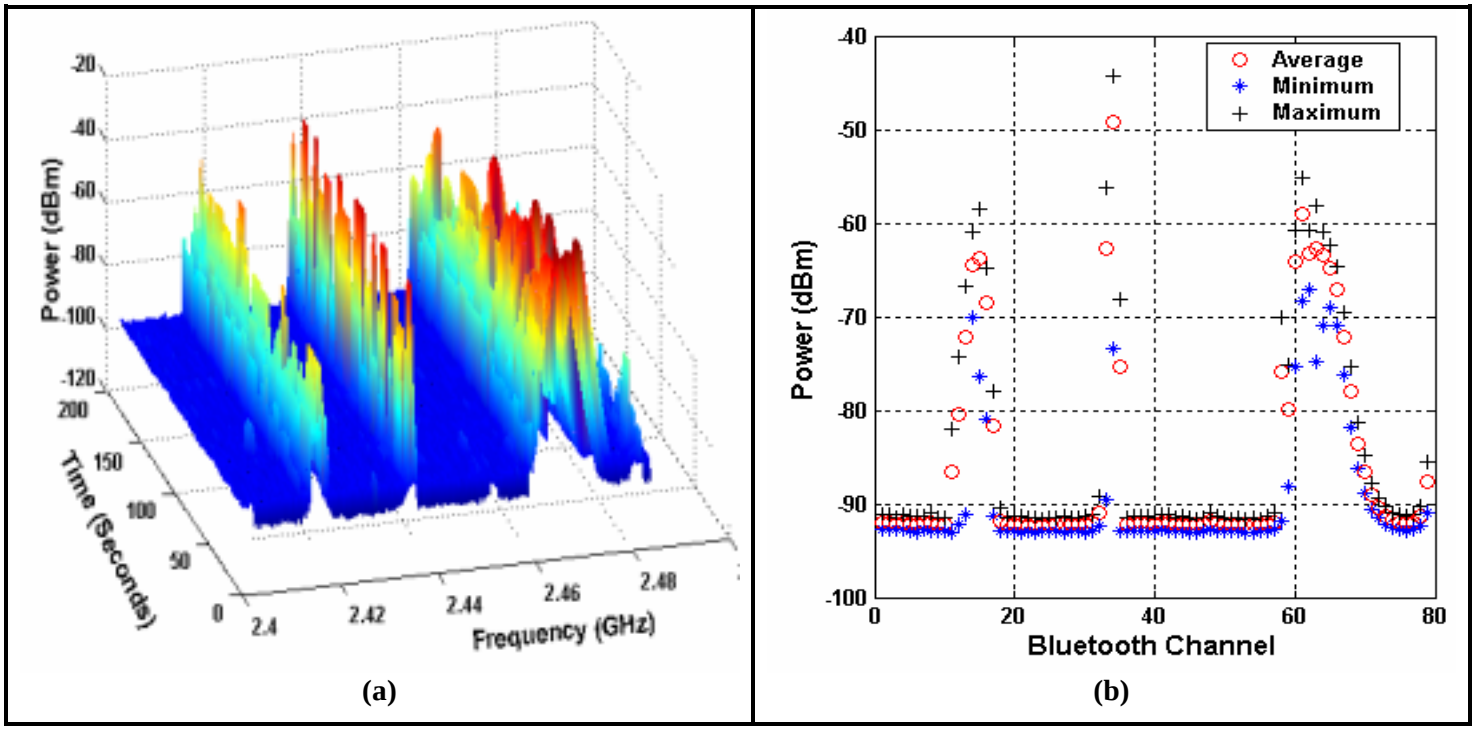

Figure 5.19 Interference Measured from Microwave Oven I at a Distance of Two meters

Figure 5.20 shows the average expected throughput for the six Bluetooth ACL packet transmissions as a function of Bluetooth Master-Slave separation.

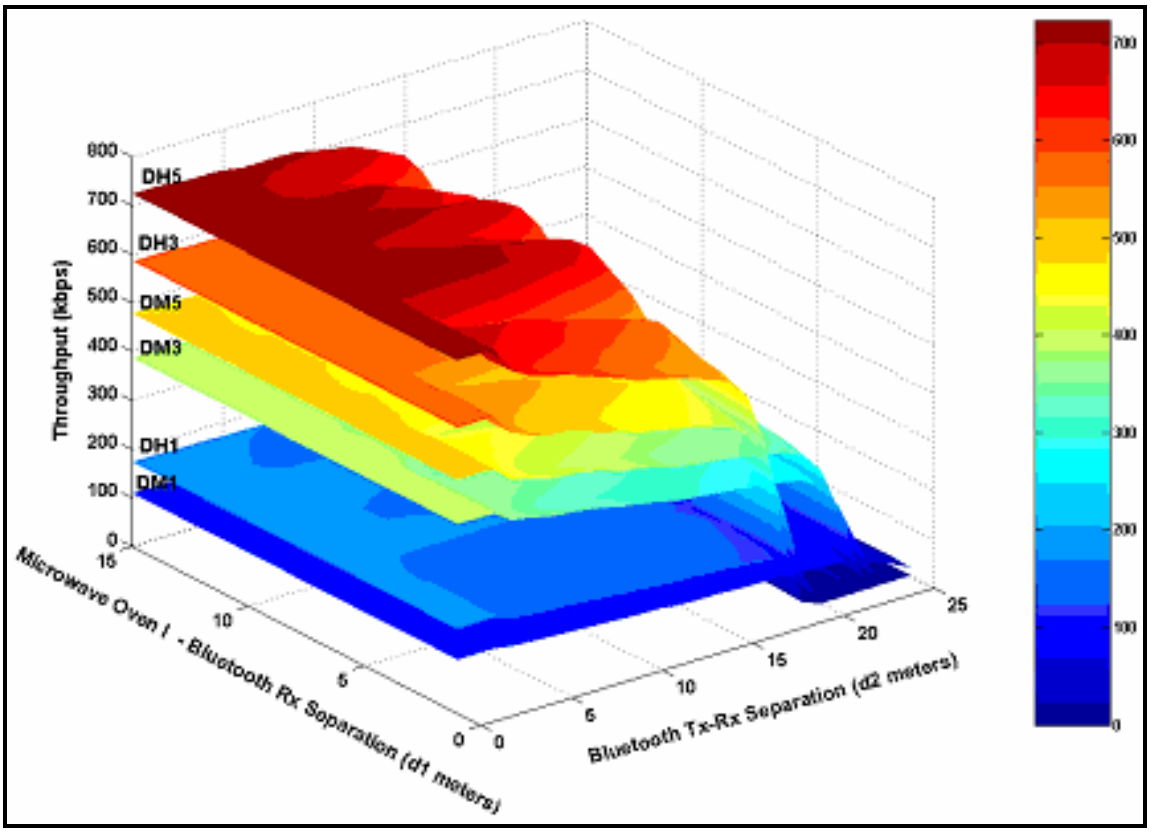

Figure 5.20 Average Throughput of Bluetooth ACL Packet Transmissions in the Presence of Microwave Oven I

Table 5.10 shows the throughput reduction for a Bluetooth piconet with Master-Slave separation of d_2 = 5, 10 meters at various distances d_1 from Microwave Oven I.

Table 5.10

Average Throughput in kbps for Six Bluetooth ACL Transmission types in the Presence of Microwave Oven I

Bluetooth piconet with Master-Slave separation of d_2 = 5 meters						
d_1 (meters)	DM1	DM3	DM5	DH1	DH3	DH5
1	100	354	436	156	524	646
3	102	361	445	160	537	662
5	105	375	456	169	555	683
7	107	382	472	171	578	714
9	108	382	471	170	577	713
11	108.8	387	478	172.8	585.6	723
Bluetooth piconet with Master-Slave separation of d_2 = 10 meters						
d_1 (meters)	DM1	DM3	DM5	DH1	DH3	DH5
1	92	321	395	142	477	586
3	94	334	412	148	498	613
5	100	362	452	160	571	703
7	107	382	472	170	576	709
9	104	369	456	164	552	679
11	107	376	463	167	564	695

Analysis: The number of Bluetooth Channels experiencing high level of interference due to Microwave Oven I is significantly fewer as compared to the WLAN. In contrast to the WLAN discussed previously, DM packets do better than DH packets because the error correcting codes of DM packets can to an extent combat the narrow band interference of the microwave oven. When the Master-Slave separation in a piconet is increased, signal strength at the receiver decreases causing reduction of SINR and the improved performance of DM packets over DH packets is more noticeable.

As the distance of separation between the piconet and microwave oven increases, the throughput increases and Bluetooth achieves maximum rates at a distance of 10 meters.

Microwave oven II: Panasonic, Model NN-7553A, 1994

Figure 5.21(a) shows the recorded interference from Microwave Oven II at a distance of two meters. Figure 5.21 (b) shows the interference posed by Microwave Oven II to the 79 individual Bluetooth channels. Bluetooth Channels 12-18, 33-35 and 61-72 were the most affected with a maximum interference level of -33 dBm on channel 67.

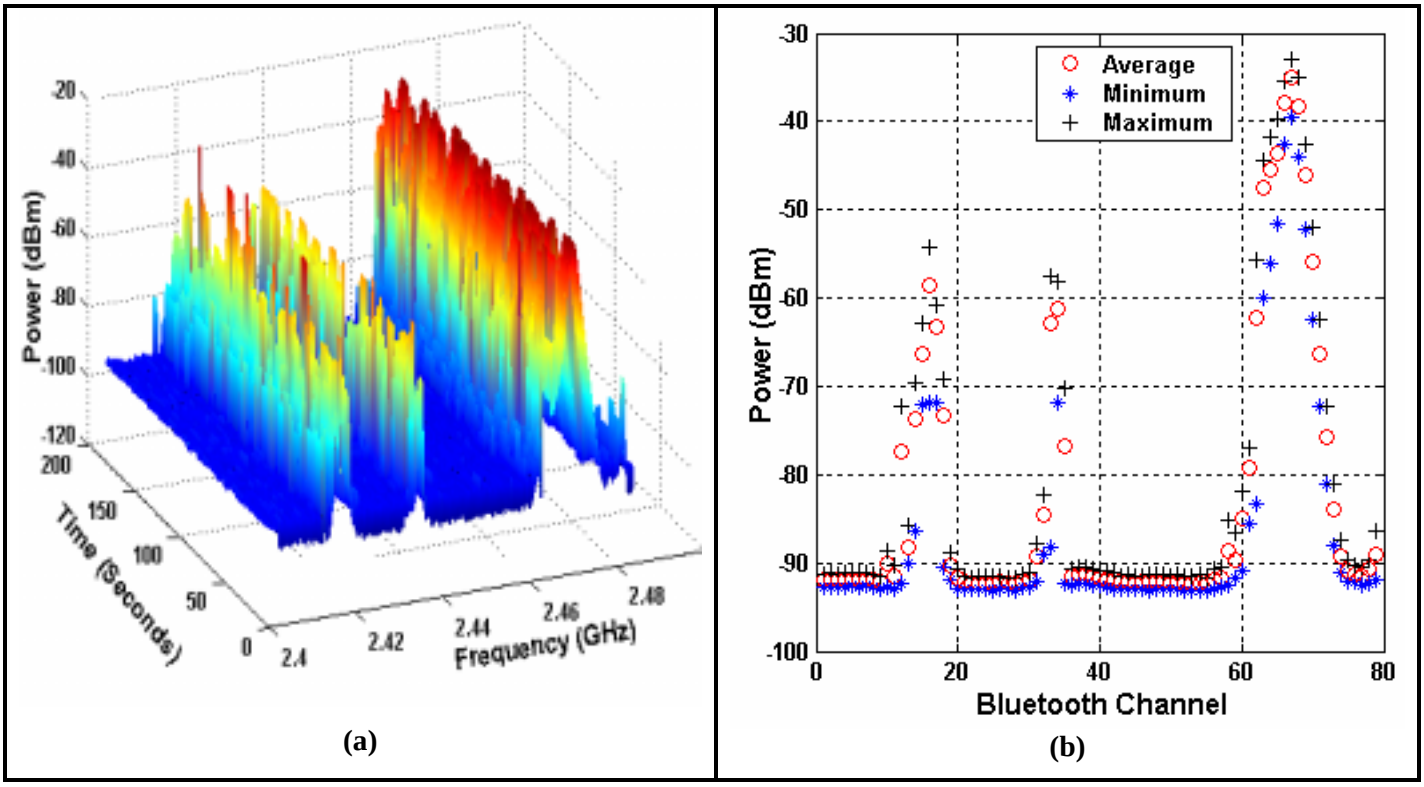

Figure 5.21 Interference Measured from Microwave Oven II at a Distance of Two meters

It can be observed that the spectral characteristics of the two microwave ovens are different. Microwave Oven II produced higher interference levels compared to Microwave Oven I. This could be attributed to the age of the Microwave Oven II, since newer microwave ovens like Microwave Oven I are expected to have better shielding. Also ageing effects and usage could alter radiation from the oven. Other researches have also shown that different microwave ovens have different spectral characteristics [Mar02].

Figure 5.22 shows the average expected throughput for the six Bluetooth ACL packet transmissions as a function of Bluetooth Master-Slave separation

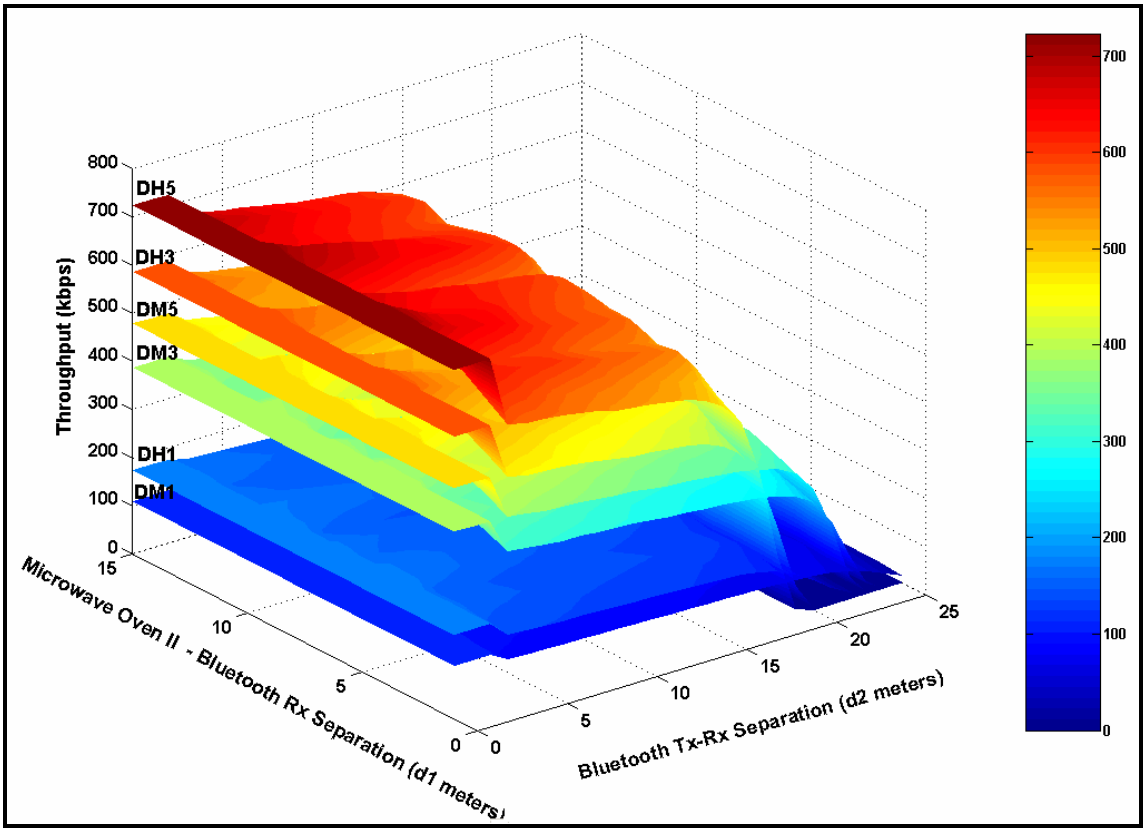

Figure 5.22 Average Throughput of Bluetooth ACL Packet Transmissions in the Presence of Microwave Oven II

Table 5.11 shows the throughput reduction for a Bluetooth piconet with Master-Slave separation of d_2 = 5, 10 meters at various distances d_1 from Microwave Oven II.

Table 5.11

Average Throughput in kbps for Six Bluetooth ACL Transmission types in the Presence of Microwave Oven II

Bluetooth piconet with Master-Slave separation of d_2 = 5 meters						
d_1 (meters)	DM1	DM3	DM5	DH1	DH3	DH5
1	87	308	380	137	459	567
3	97	342	422	152	513	633
5	98	345	424	153	514	634
7	99	352	433	156	529	653
9	105	370	455	164	548	675
11	107	379	467	168	562	692
Bluetooth piconet with Master-Slave separation of d_2 = 10 meters						
d_1 (meters)	DM1	DM3	DM5	DH1	DH3	DH5
1	83	293	362	130	437	537
3	90	321	396	143	482	595
5	91	322	398	144	484	595
7	94	334	412	149	494	612
9	95	336	414	149	501	616
11	99	349	431	155	525	648

Analysis: Throughput performance of Bluetooth in the presence of Microwave Oven II is lower than when in presence of Microwave Oven I, this is primarily because of the higher interference levels produced by Microwave Oven II.

As observed in the case of Microwave Oven I, the throughput performance of DM packets is better then the throughput performance of DH packets, simply because Microwave Ovens exposes fewer Bluetooth channels to high level of interference, for which the error correcting codes of DM packets provide some error correcting capability. Bluetooth piconets in the presence of Microwave Oven II will achieve close to maximum throughput at distances > 10 meters.

5.6 Conclusion

In this Chapter, we discussed the WLAN and Bluetooth PHY standard and provided a throughput analysis for Bluetooth transmissions as a function of channel interference. IEEE 802.15 WPAN channel models and post-processing module of PRISM was combined with the analysis and a Bluetooth throughput simulator was developed in MATLAB. PRISM along with the throughput simulator was demonstrated to be a very valuable tool for predicting maximum average throughput of Bluetooth piconet as a function of the environment.

PRISM and the Bluetooth throughput simulator were used to predict the performance of six Bluetooth ACL packet types in the presence of interferers such as WLAN and microwave ovens in a LOS environment along a hallway. It was shown that under the presence of a WLAN, DM and DH packets had a similar percentage of throughput reduction whereas in the presence of microwave ovens DH packets had a greater percentage of throughput reduction then DM packets. This difference is due to the fact that a greater number of Bluetooth channels are affected by strong interference signal from a WLAN (operating on a single channel) when compared to a microwave oven. A higher number of channels affected by interference will have a catastrophic effect on the data packets, making it difficult for the correction code used in DM packets to significantly recover data errors. The DH packets on the other hand benefit from the fact that they are able to carry a larger amount of data over the same packet length, thereby yielding a larger throughput. It was also observed that Bluetooth piconets at distances greater than 10 meters from a microwave oven experience little or no interference and can hence achieve maximum throughput.

Chapter 6

6 Conclusions

6.1 Summary of Findings

An overview of the electromagnetic environment in hospitals between 20 MHz and 2 GHz was provided. In order to study the RF spectrum in the 2.4 GHz ISM band, PRISM – a completely automated software reconfigurable EMI measurement system was designed and built. PRISM was demonstrated to be an effective system for measuring EMI over non-contiguous frequency bands between 9 kHz and 2.9 GHz. In addition, the ability to monitor EMI from a remote location via the internet is an important feature of the system. At this early point in the development of the medical-wireless market such a system can be a very valuable tool and could find a place as standard equipment for a typical health care provider.

An extensive measurement campaign at the Virginia-Maryland College of Veterinary Medicine at Virginia Tech and the Carilion Memorial Hospital in Roanoke, Virginia was undertaken to investigate the EMI in the 2.4 GHZ ISM band. We have presented here what we believe to be the first study of EMI in the 2.4 GHz ISM band in hospital environments. Results of EMI as a function of frequency and time of occurrence at various locations including radiology, MRI, Critical Care Units, ECG, Clinical pathology and surgery units was presented. The results showed that electromagnetic activity in hospitals is dynamic and time varying. Background EMI levels in both hospitals were well below the FDA recommended immunity level of 3 V/m for medical devices. WLANs and Microwave Ovens contributed to the majority of the recorded activity.

A Bluetooth throughput simulator using semi-analytic results was developed. PRISM and the Bluetooth simulator were used to predict the throughput of six Bluetooth

ACL transmission types in the presence of a WLAN and a microwave oven. The throughput results were presented as a function of piconet size and interferer distance. The throughput simulator and PRISM were shown to be an excellent tool that could be used for estimating the performance of Bluetooth applications in medical environments.

6.2 Suggested Further Research

This research has established a working prototype for recording and analyzing EMI and predicting the QoS of Bluetooth devices in hospitals. However, miniaturizing the current measurement system is necessary so that it can aid in the wider deployment and maintenance of wireless devices in hospitals. A plausible approach is to replace the current bulky spectrum analyzer with a hand-held spectrum analyzer or broadband ADC and DSP chip. This would be an ideal product for health care providers, requiring only software upgrades for analyzing and updating network planning algorithms.

Other avenues and improvisations include integration of the miniaturized product with existing deployment tools – such as CAD tools, wireless planning tools and network monitoring tools. Moreover, the product's software could be developed to accommodate building floor plans for providing a building-specific radio environment outlook. In addition algorithms could be developed for 802.11b and other wireless standard for predicting throughput using recorded data. Also, it would be interesting to develop software techniques to transport measured data through existing wired/ 802.11 infrastructure for post-processing and analysis.

A product of this nature is very much feasible and could proliferate in hospitals within the next couple of years. The measurement product will demonstrate health care provider's best effort in maintaining and ensuring patient care. It will also provide proof of the existing levels of EMI, thus reducing liability involving equipment that may be susceptible to EMI. Furthermore, a product that can monitor RF radiation can evolve to include alarms to prevent interruption of wireless services or to prevent hazardous RF emissions. Given the scope of today's wireless market, such a product may become essential.

Appendix A

A Individual EMI Snap Shots and Site Photos

A1 Individual EMI Snap Shots from CRMH

The following figures show individual snap shots of EMI recorded at all 15 measurement sites in the Carilion Memorial Hospital. The 3-D plots show E-field as a function of frequency and time of day.

Floor 2:

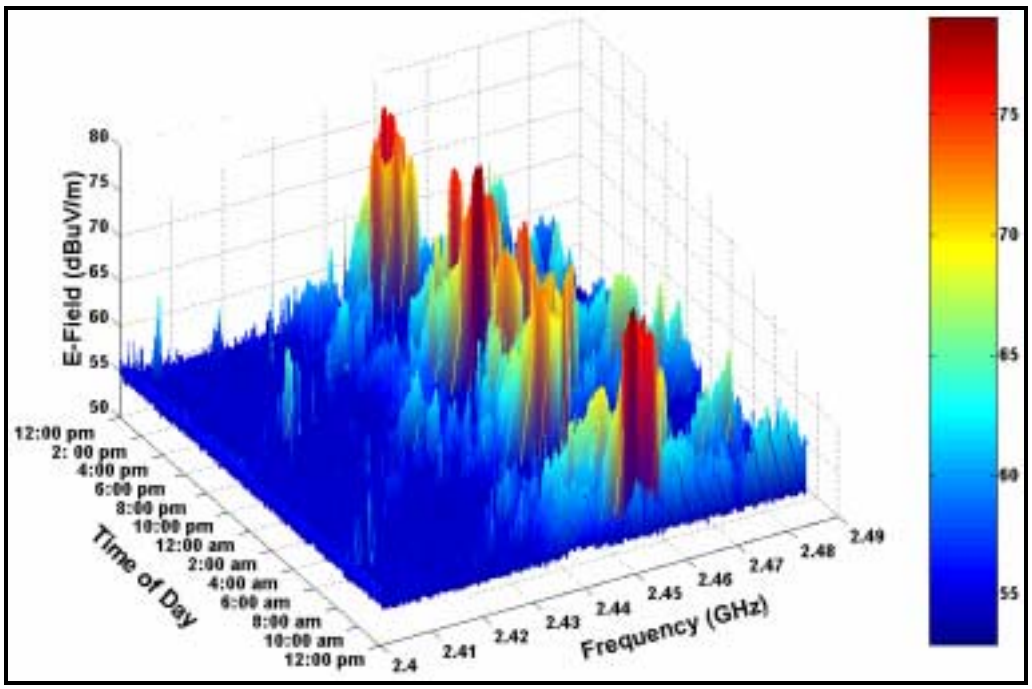

Figure A1.1: Observed Background EMI noise in the 2.4 GHz ISM band from Site 1 on the South Section of the 2nd Floor of Carilion Memorial Hospital

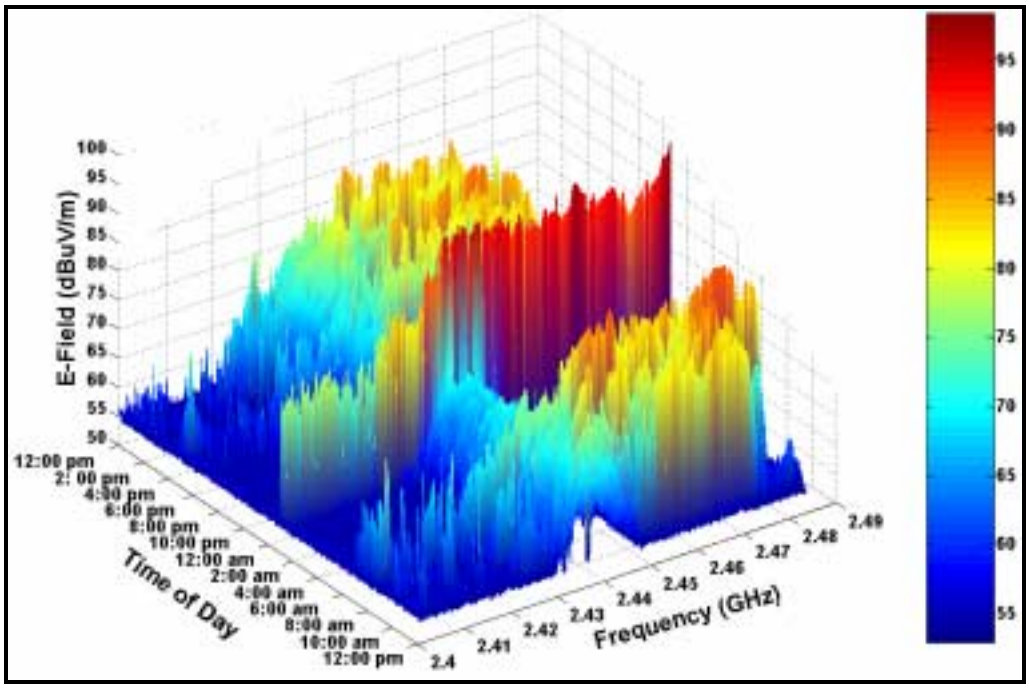

Figure A1.2: Observed Background EMI noise in the 2.4 GHz ISM band from Site 2 on the South Section of the 2nd Floor of Carilion Memorial Hospital

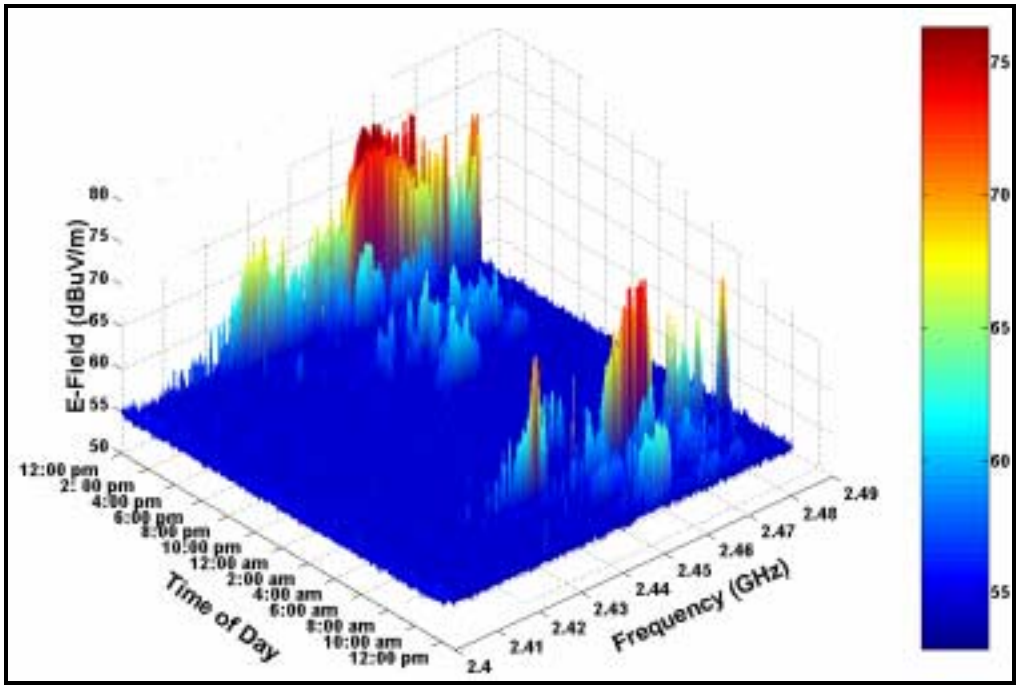

Figure A1.3: Observed Background EMI noise in the 2.4 GHz ISM band from Site 3 on the South Section of the 2nd Floor of Carilion Memorial Hospital

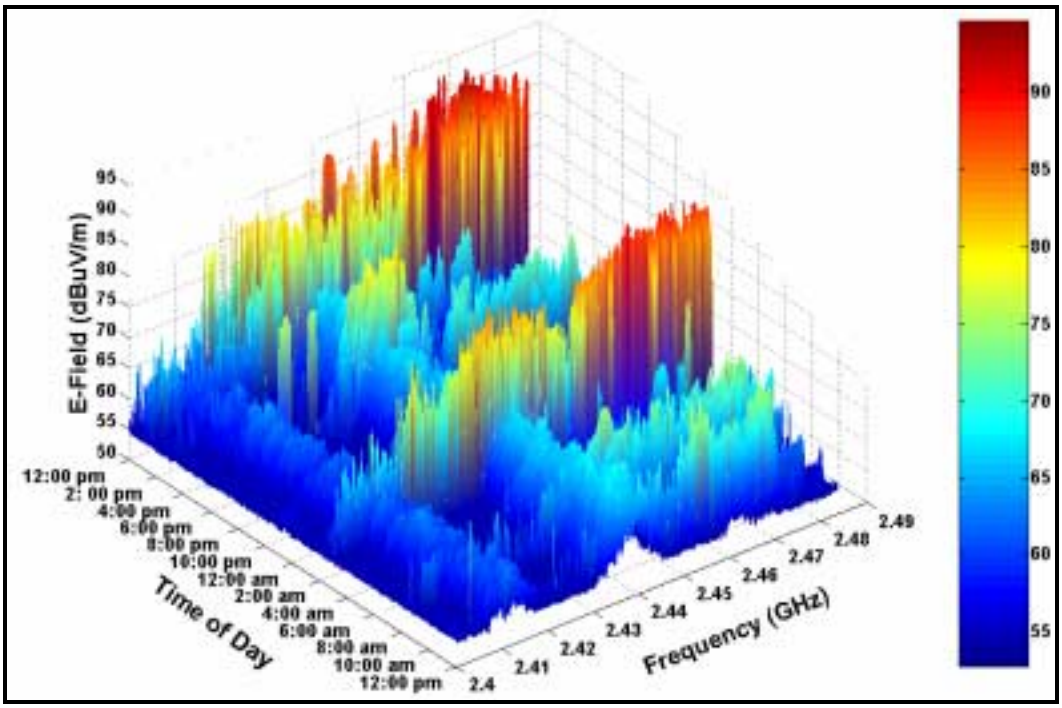

Figure A1.4: Observed Background EMI noise in the 2.4 GHz ISM band from Site 4 on the South Section of the 2nd Floor of Carilion Memorial Hospital

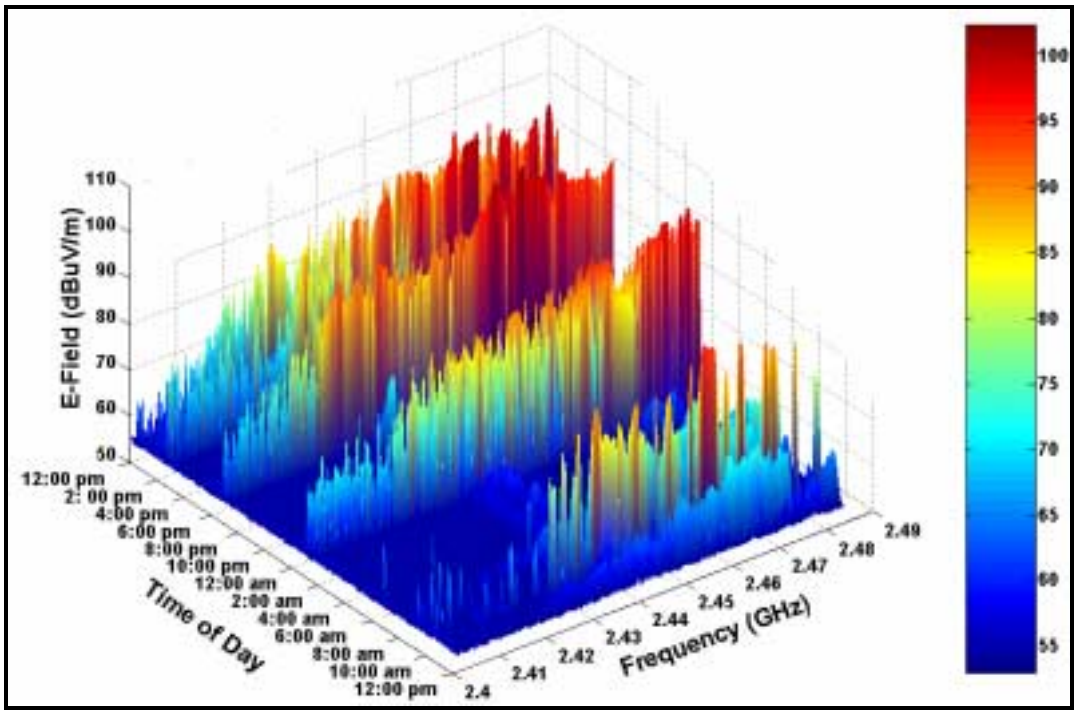

Figure A1.5: Observed Background EMI noise in the 2.4 GHz ISM band from Site 5 on the South Section of the 2nd Floor of Carilion Memorial Hospital

Floor 4:

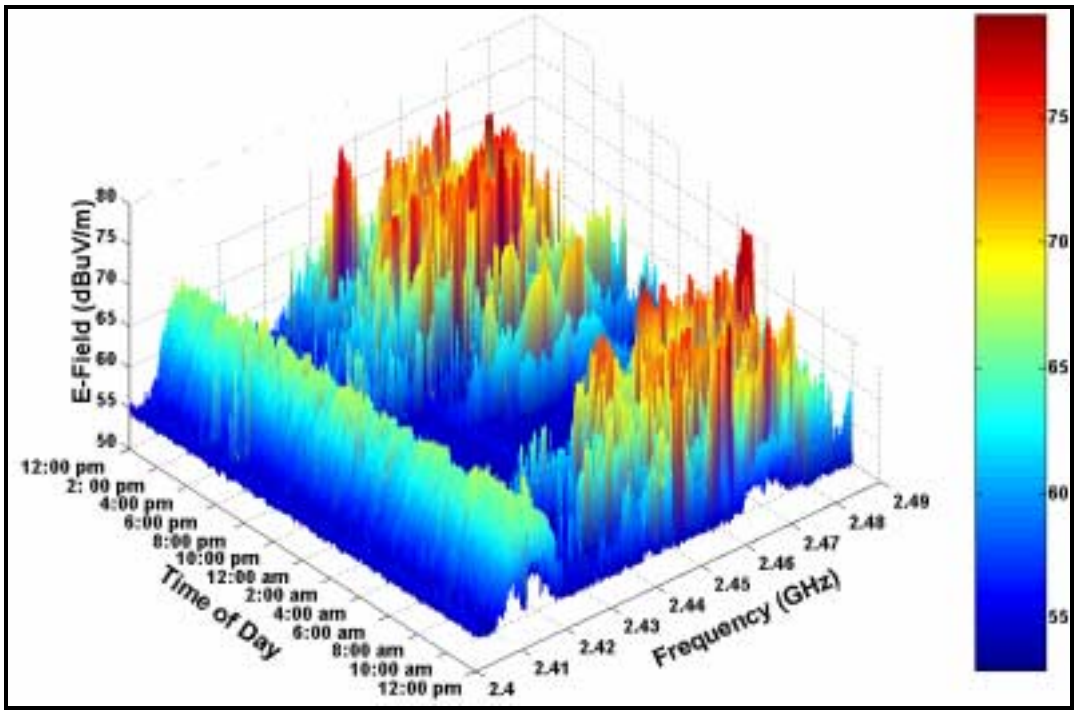

Figure A1.6: Observed Background EMI noise in the 2.4 GHz ISM band from Site 1 on the South Section of the 4th Floor of Carilion Memorial Hospital

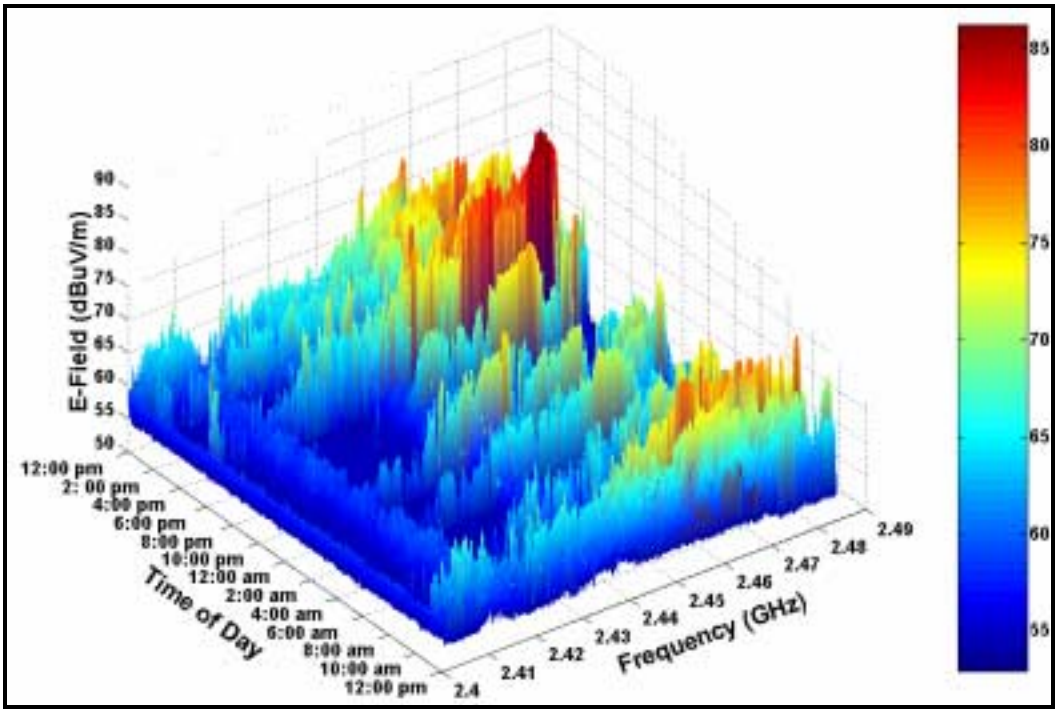

Figure A1.7: Observed Background EMI noise in the 2.4 GHz ISM band from Site 2 on the South Section of the 4th Floor of Carilion Memorial Hospital

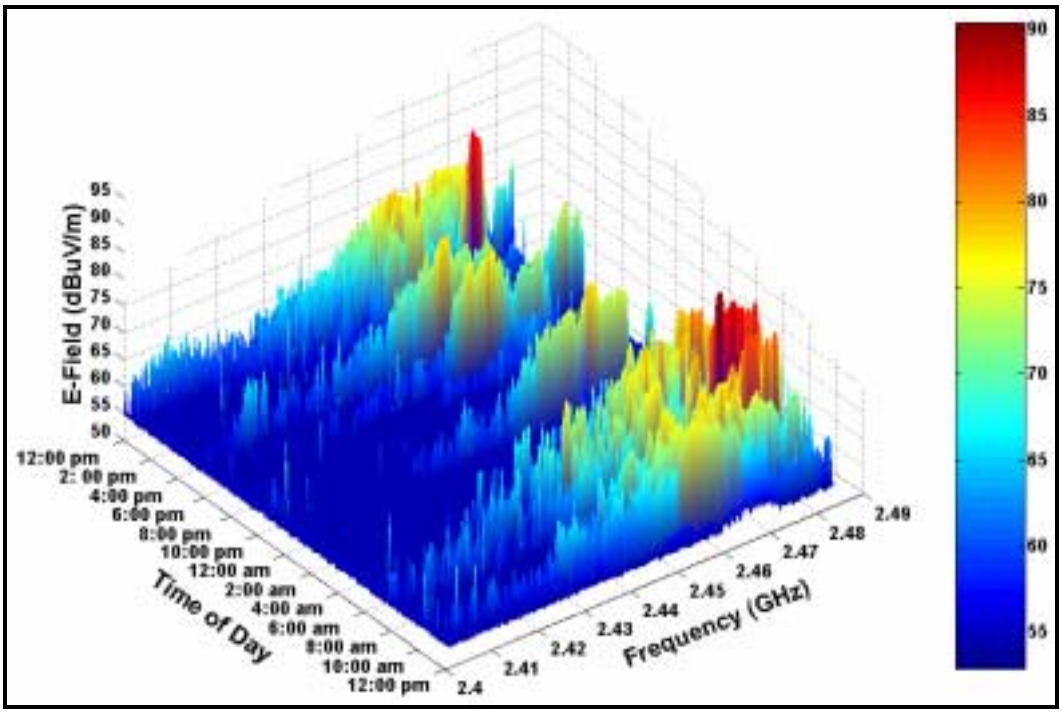

Figure A1.8: Observed Background EMI noise in the 2.4 GHz ISM band from Site 3 on the South Section of the 4th Floor of Carilion Memorial Hospital

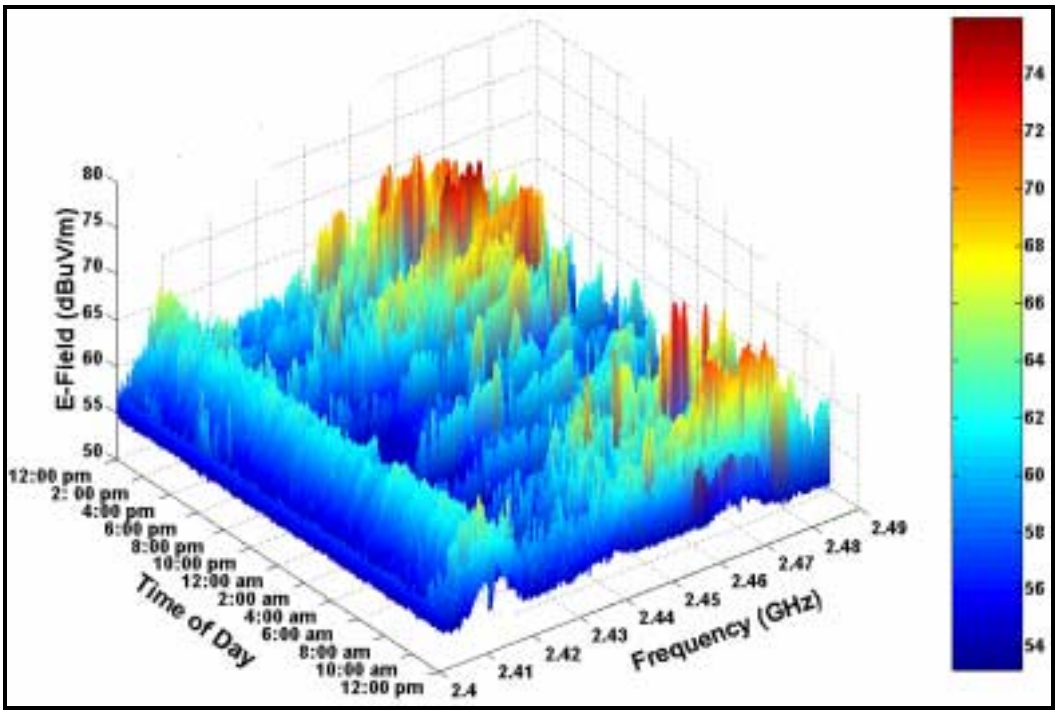

Figure A1.9: Observed Background EMI noise in the 2.4 GHz ISM band from Site 4 on the South Section of the 4th Floor of Carilion Memorial Hospital

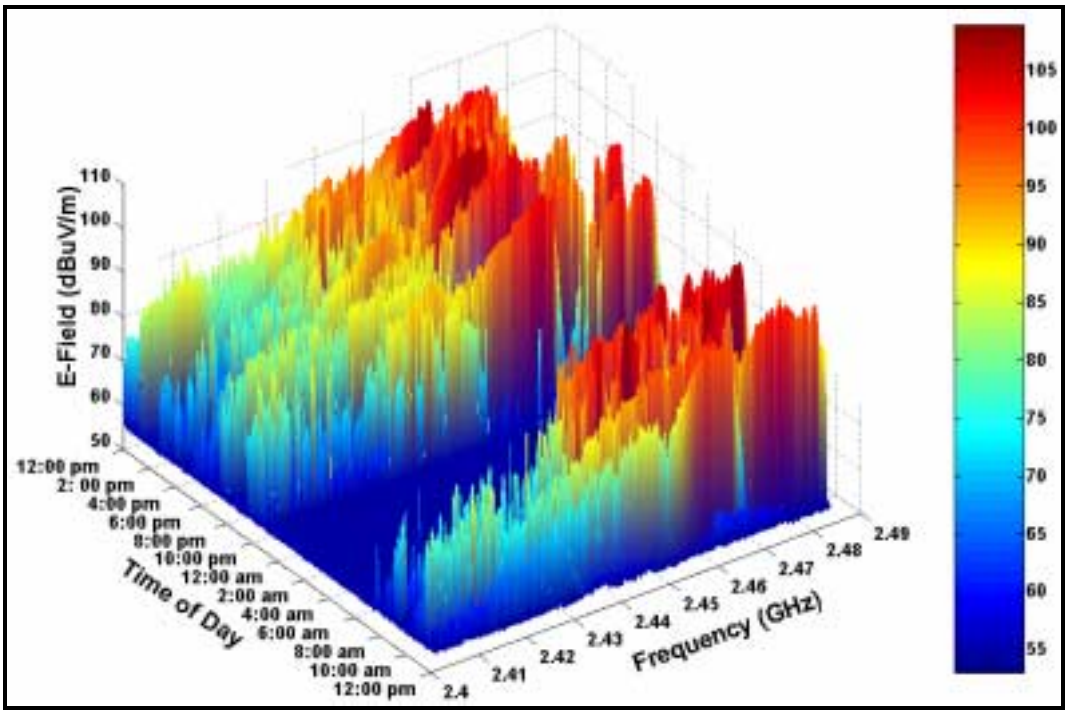

Figure A1.10: Observed Background EMI noise in the 2.4 GHz ISM band from Site 5 on the South Section of the 4th Floor of Carilion Memorial Hospital

Floor 7:

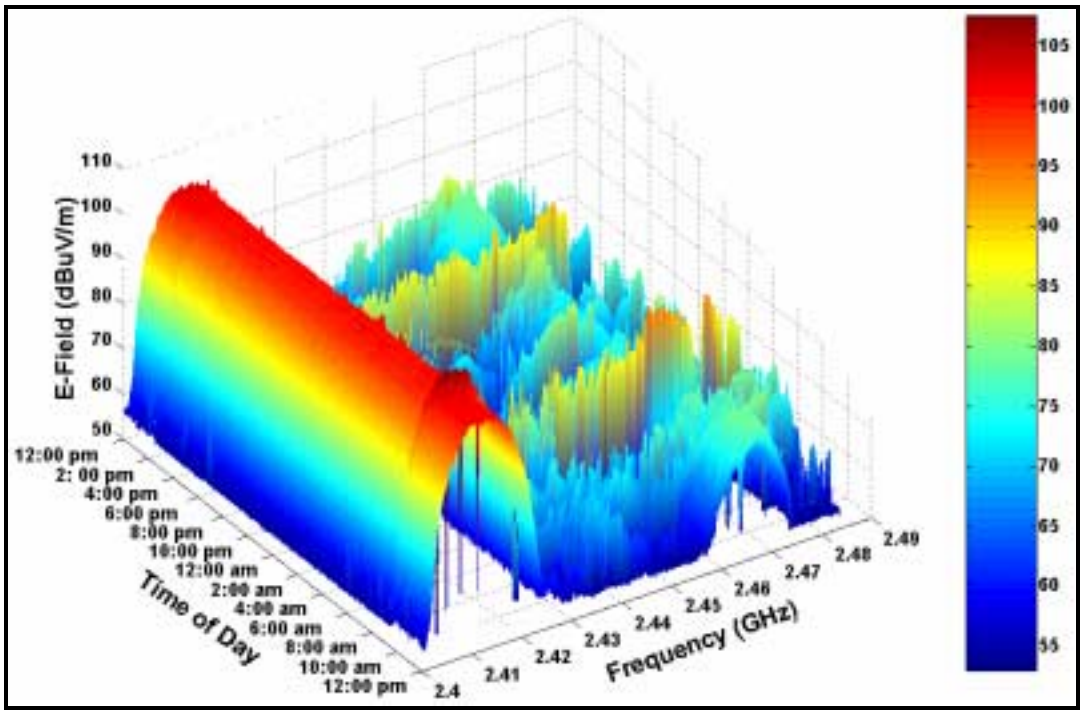

Figure A1.11: Observed Background EMI noise in the 2.4 GHz ISM band from Site 1 on the East Section of the 7th Floor of Carilion Memorial Hospital

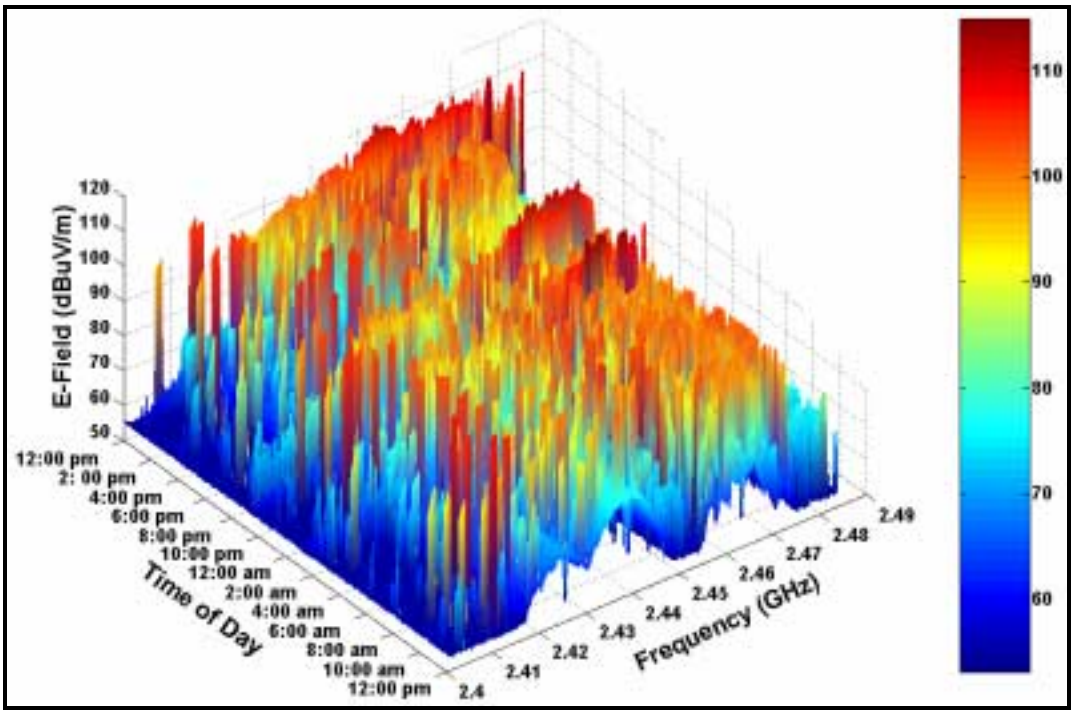

Figure A1.12: Observed Background EMI noise in the 2.4 GHz ISM band from Site 2 on the East Section of the 7th Floor of Carilion Memorial Hospital

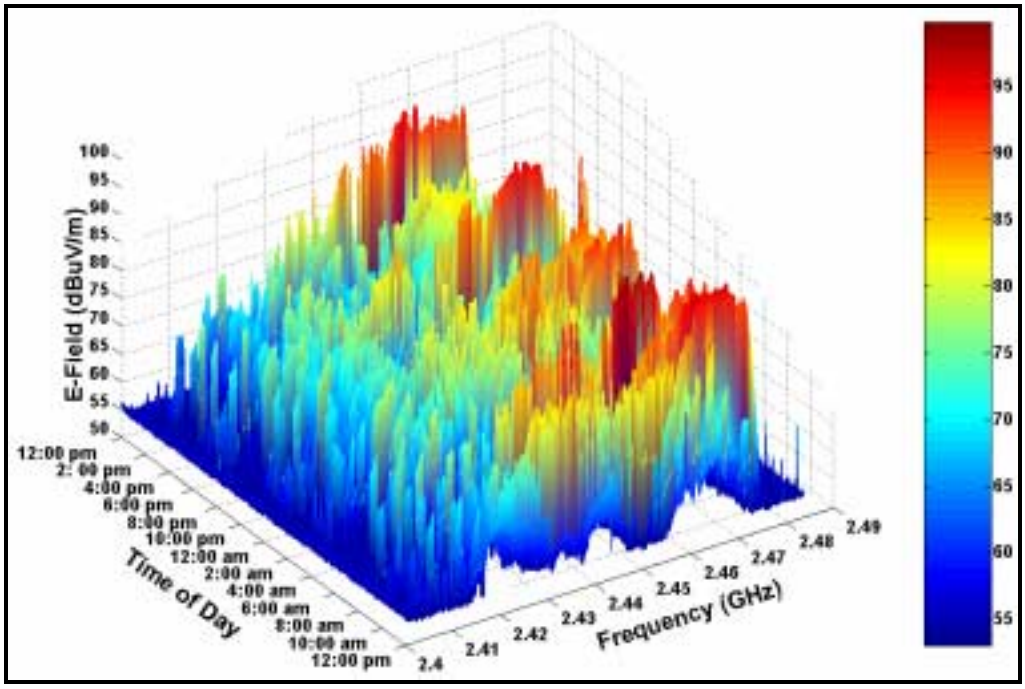

Figure A1.13: Observed Background EMI noise in the 2.4 GHz ISM band from Site 3 on the East Section of the 7th Floor of Carilion Memorial Hospital

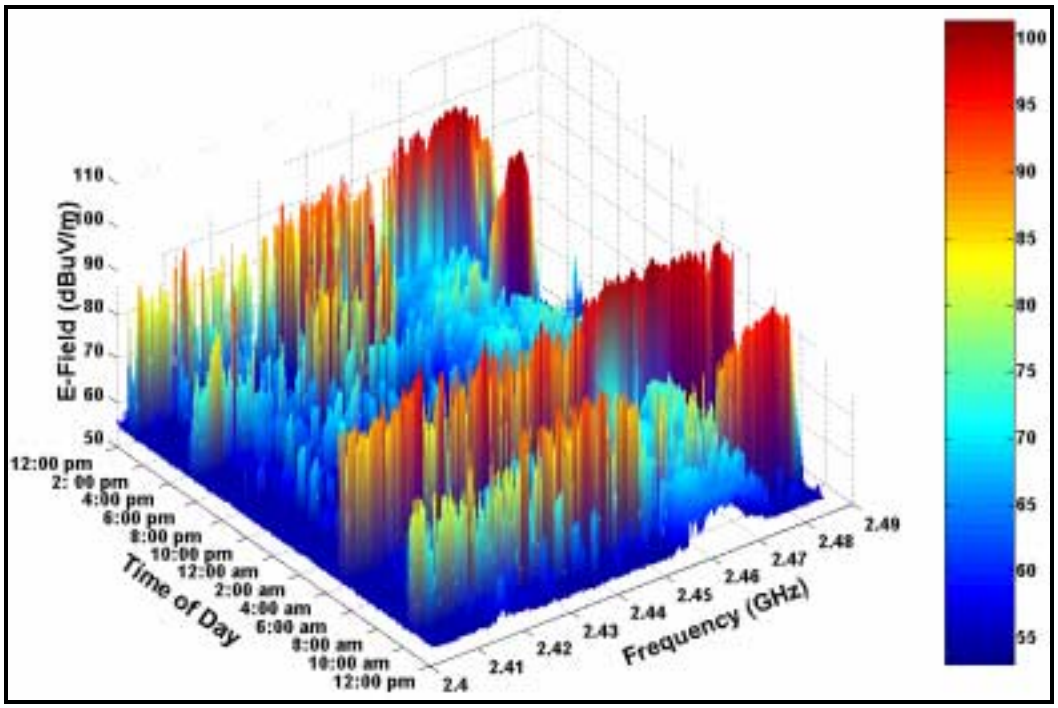

Figure A1.14: Observed Background EMI noise in the 2.4 GHz ISM band from Site 4 on the East Section of the 7th Floor of Carilion Memorial Hospital

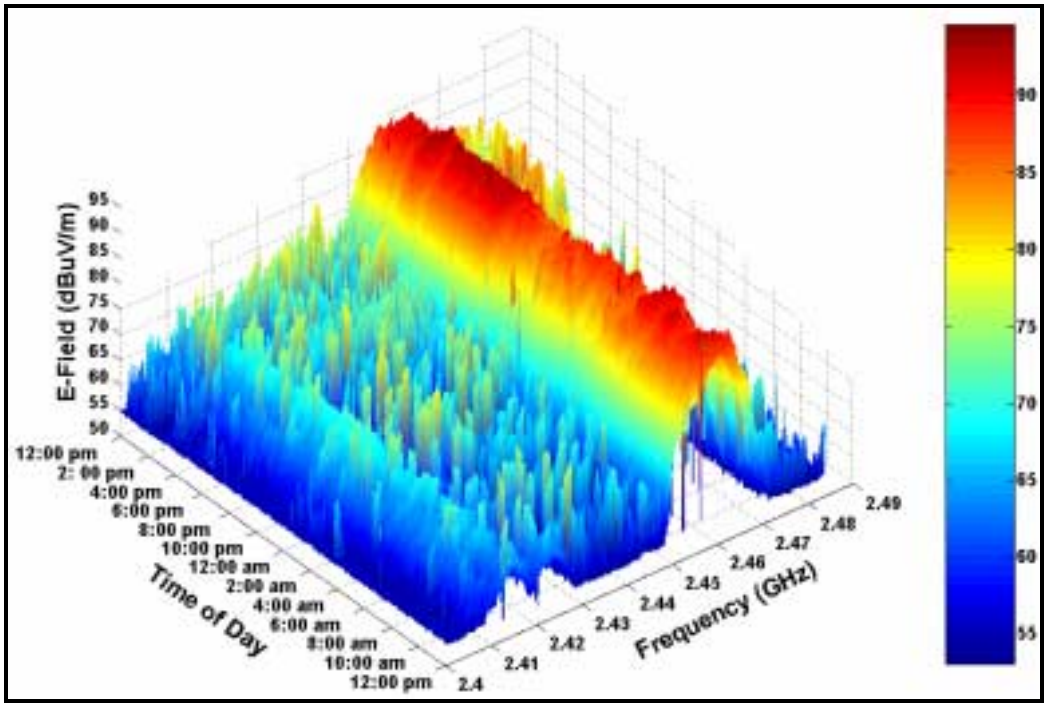

Figure A1.15: Observed Background EMI noise in the 2.4 GHz ISM band from Site 5 on the East Section of the 7th Floor of Carilion Memorial Hospital

A2 PRISM Measurement Site Photos

A2.1 Carilion Roanoke Memorial Hospital

Floor 2:

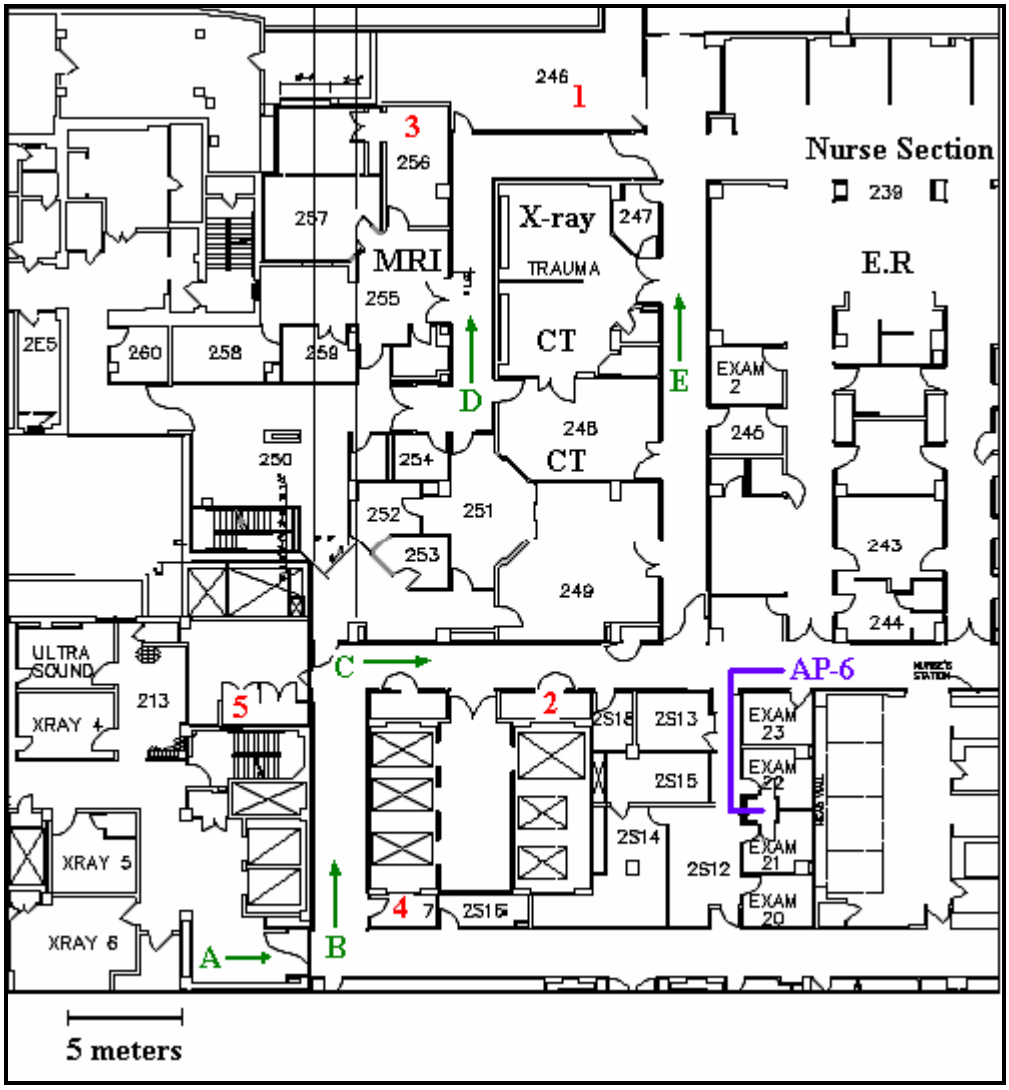

Figure A2.1.1: Measurement Sites 1-5, 2nd Floor, South Section, Carilion Memorial Hospital

Figure A2.1.2: Reference Spot A, 2nd Floor, South Section, Carilion Memorial Hospital

Figure A2.1.3: Reference Spot B, 2nd Floor, South Section, Carilion Memorial Hospital

Figure A2.1.3: Reference Spot C, 2nd Floor, South Section, Carilion Memorial Hospital

Figure A2.1.4: Reference Spot D, 2nd Floor, South Section, Carilion Memorial Hospital

Figure A2.1.5: Reference Spot E, 2nd Floor, South Section, Carilion Memorial Hospital

Floor 4:

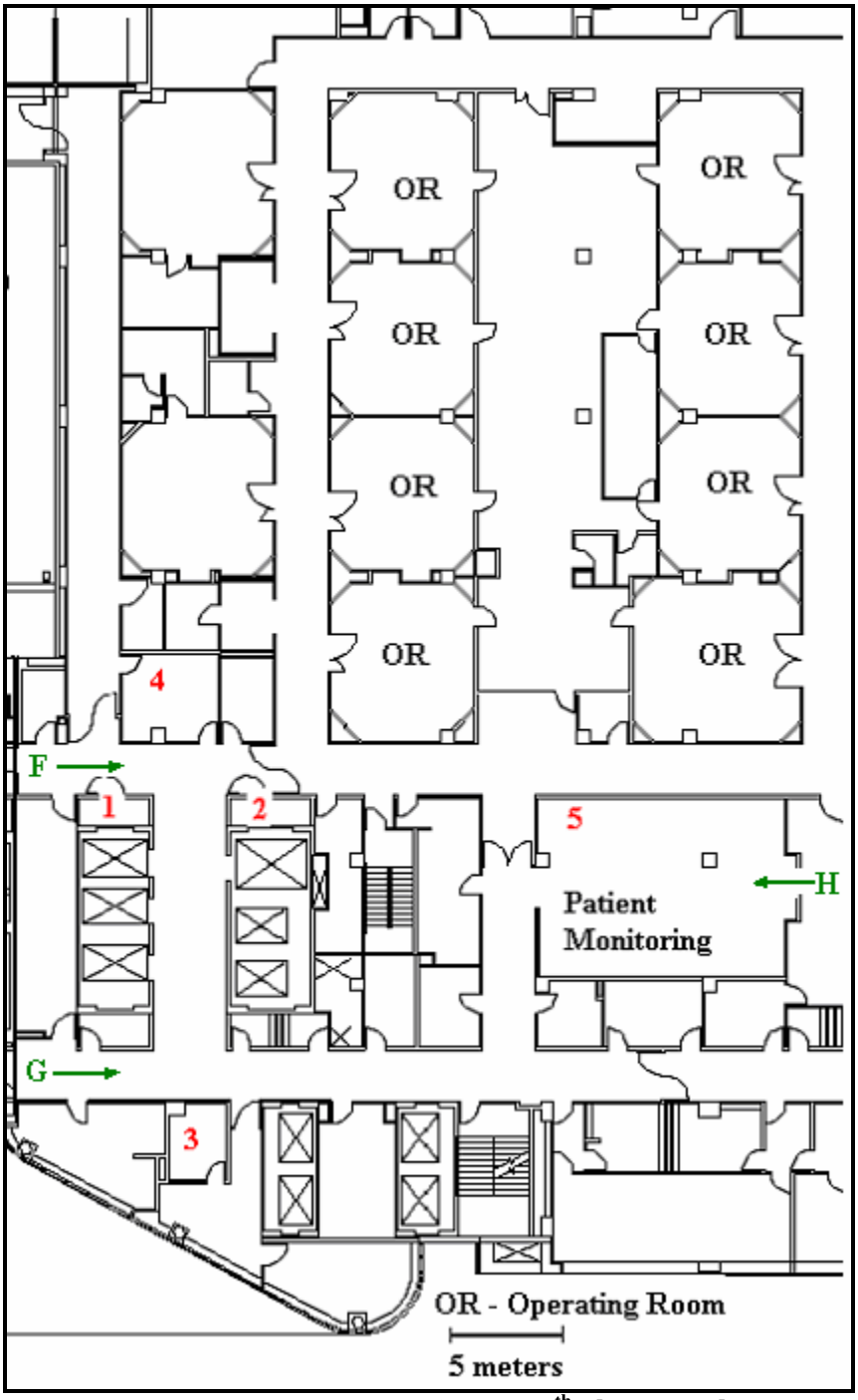

Figure A2.1.6: Figure 4.12 Measurement Sites 1-5, 4th Floor, South Section, Carilion Memorial Hospital

Figure A2.1.7: Reference Spot F, 4th Floor, South Section, Carilion Memorial Hospital

Figure A2.1.8: Reference Spot G, 4th Floor, South Section, Carilion Memorial Hospital

Figure A2.1.9: Reference Spot H, 4th Floor, South Section, Carilion Memorial Hospital

Floor 7:

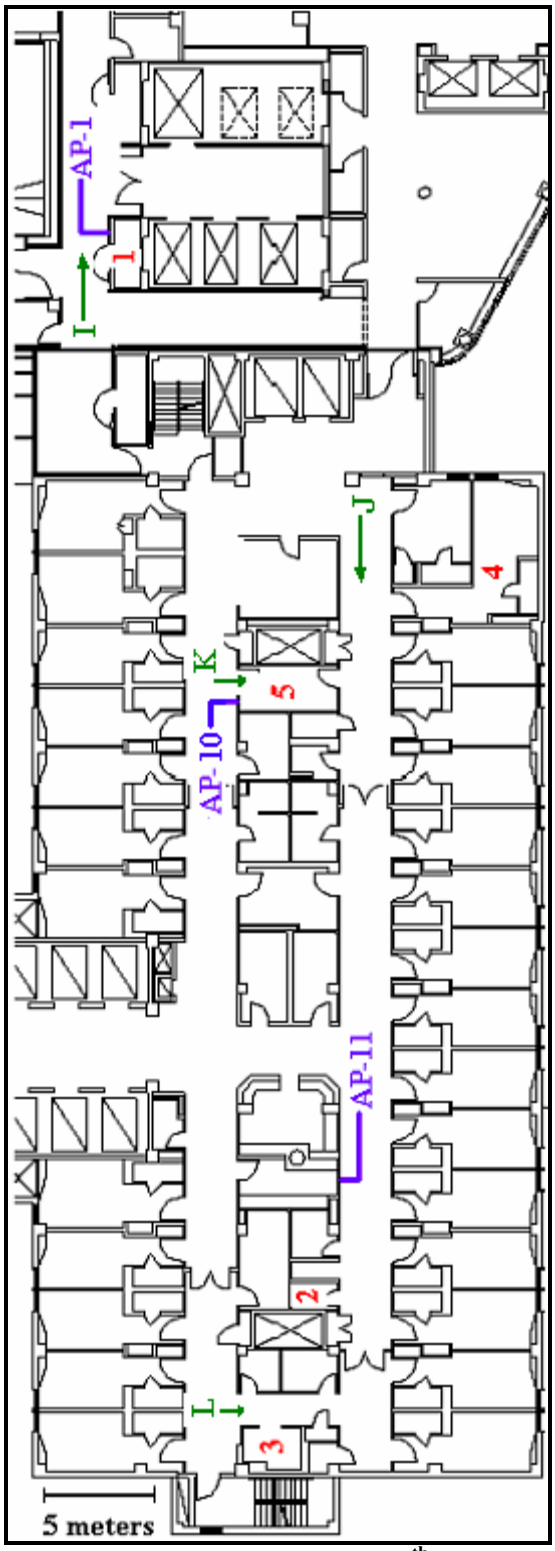

Figure A2.1.10: Figure 4.14 Measurement Sites 1-5, 7th Floor, South Section, Carilion Memorial Hospital

Figure A2.1.11: Reference Spot I, 7th Floor, South Section, Carilion Memorial Hospital

Figure A2.1.12: Reference Spot J, 7th Floor, South Section, Carilion Memorial Hospital

Figure A2.1.13: Reference Spot K, 7th Floor, South Section, Carilion Memorial Hospital

Figure A2.1.14: Reference Spot L, 7th Floor, South Section, Carilion Memorial Hospital

A2.2 Virginia Maryland College of Veterinary Medicine

Phase I, First Floor:

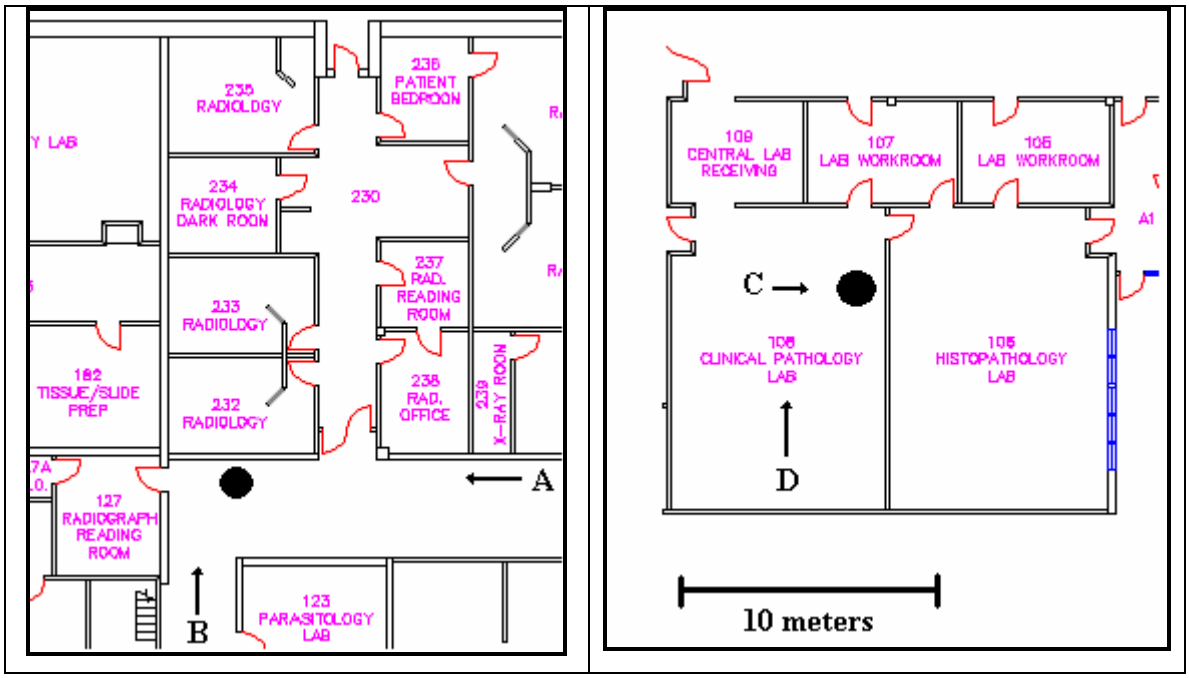

Figure A2.2.1: Measurement Locations V1 and V2, Phase I, First Floor, VMRCVM, Virginia Tech. PRISM was located outside Radiology (room 232) and inside the Clinical Pathology Lab (room 106)

Figure A2.2.2: Reference Spot A, Phase I, First Floor, VMRCVM, Virginia Tech

Figure A2.2.3: Reference Spot B, Phase I, First Floor, VMRCVM, Virginia Tech

Figure A2.2.4: Reference Spot C, Phase I, First Floor, VMRCVM, Virginia Tech

Figure A2.2.5: Reference Spot D, Phase I, First Floor, VMRCVM, Virginia Tech

Phase III, First Floor:

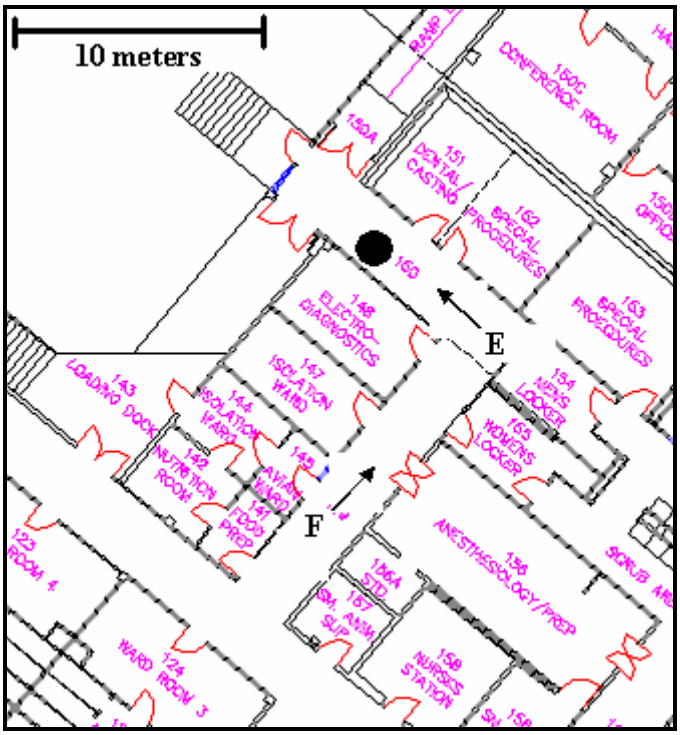

Figure A2.2.6: Measurement Location V3, Phase III, First Floor, VMRCVM, Virginia Tech. PRISM was located on the hallway in between the dental/ casting lab (room 151) and the electro-diagnostics lab (room 148)

Figure A2.2.7: Reference Spot E, Phase III, First Floor, VMRCVM, Virginia Tech

Figure A2.2.8: Reference Spot F, Phase III, First Floor, VMRCVM, Virginia Tech

A2.3 4th Floor Durham Hall, Virginia Tech

Figure A2.3.1: Hallway, 4th Floor Durham Hall, WLAN LOS Measurements

Figure A2.3.2: Hallway, 4th Floor Durham Hall, WLAN LOS Measurements

Figure A2.3.3: Hallway, 4th Floor Durham Hall, Microwave Oven I LOS Measurements

Figure A2.3.4: Hallway, 4th Floor Durham Hall, Microwave Oven II LOS Measurements

Abbreviations and Acronyms

A

AAMI Association for the Advancement of Medical Instrumentation

ACK Acknowledgement

ACL Asynchronous Connectionless

AF Antenna Factor

AM Amplitude Modulation

ANSI American National Standards Institute

AP Access Point

ARQ Automatic Repeat Request

AWGN Additive White Gaussian Noise

B

BER Bit Error Rate

C

CCU Critical Care Unit,
also Central Control Unit

CDRH Center for Devices and Radiological Health

CISPR International Special Committee on Radio Interference

CRC Cyclic Redundancy Check

CT Computed Tomography

D

DHx Data High 1/3/5

DMx Data Medium 1/3/5

DSSS Direct Spread Spectrum Sequencing

E

ECG Electrocardiogram

ECRI Emergency Care Research Institute

EMC Electromagnetic Compatibility

EME Electromagnetic Environment

EMI Electromagnetic Interference

ER Emergency Room

ESD Electro Static Discharge

ESU Electro Surgical Unit

F

FCC Federal Communications Commission, Inc.,

FDA Food and Drug Administration

FEC Forward Error Correction

FHSS Frequency Hopping Spread Sequencing

FM Frequency Modulation

FSK Frequency Shift Keying

G

GFSK Gaussian Frequency Shift Keying

GPIB General Purpose Interface Bus

GUI Graphical User interface

I

ICU Intensive Care Unit

IEC International Electrotechnical commission

ISI Inter Symbol Interference

ISM Industrial, Scientific, and Medical

ITU International Telecommunications Union

L

LNA Low Noise Amplifier

LOS Line of Sight

M

MAC Media Access Layer

MDD Medical Device Directive

MRI Magnetic Resonance Imaging

MRT Magnetic Resonance Tomography

N

NAK Unsuccessful acknowledgement

O

OBS Obstructed

OFDM Orthogonal Frequency Division Multiplexing

OR Operating Room

P

PBX Private Branch Exchange

PCS Personal Communication System

PHY Physical Layer

PPM Pulse Position Modulation

Q

QoS Quality of Service

R

RF Radio Frequency

RFI Radio Frequency Interference

S

SCO Synchronous Connection Oriented

SINR Signal to Noise plus Interference Ratio

SNR Signal to Noise Ratio

T

TDD Time Division Duplexing

U

UHF Ultra High Frequency

UNII Unlicensed National Information Infrastructure

V

VHF Very High Frequency

VISA Virtual Instrumentation Software Architecture

W

WLAN Wireless Local Area Network

WPAN Wireless Personal Area Network

References

[Aeg00] Leeson, H., Hansell, P., Burns, J., and Spasojevic, Z., "Demand for the use of the ISM band – Final Report," Spectrum Management Advisory Group, Aegis Spectrum Engineering, 2000.

[All98] Allen. R. C., "IC susceptibility from ESD-induced EMI. EE evaluation Engineering, pp. 116-121.

[And96] Anderson, R., "The European Medical Device EMC Specifications," *IEEE 1996 International Symposium on Electromagnetic Compatibility*, August 1996, pp.31-33.

[App] "Nursing Shortage - A Crisis in US Hospitals" vol 4, number 23, www.applesforhealth.com.

[Arn95] Arnofsky, S., Doshi, P., Foster, K.R., Hanover, D., Mercado, R., Schleck, D., and Soltys, M., "Radiofrequency Field Surveys in Hospitals," *IEEE Annual Northeast Bioengineering Conference*, May 1995, pp. 129 -131.

[Ban95] Bandopadhyay, S., and Varkey, J. K., "EMI Susceptibility Characteristics of Electromedical Equipment in a Typical Hospital Environment with Particular Reference to Electrocardiography," *IEEE International Conference on Electromagnetic Interference and Compatibility*, 1995, pp. 266-272.

[Bas94] Bassen, H., Ruggera, P., Casamento, J., and Witters, D., "Sources of Radiofrequency Interference for Medical Devices in the Non Clinical Environment," *IEEE 16th Annual International Conference on Engineering in Medicine and Biology*, 1994, vol.2, pp. 896 -897.

[Boi91] Boisvert, P., Segal, B., Pavlasek, T., Retfalvi, S., Sebe, A., and Caron, P., "Preliminary Survey of the Electromagnetic Interference in Hospitals," *IEEE International Symposium on Electromagnetic Compatibility*, August 1991, pp. 214 -219.

[Boi97a] Boivin, W.S., Boyd, S.M., Coletta, J.N., Harris, C.D., and Neunaber, L.M., "Measurement of Electromagnetic Field Strengths in Urban and Suburban Hospital Operating Rooms," *IEEE 19th Annual International Conference on Engineering in Medicine and Biology*, November 1997, vol.6, pp. 2539 -2542.

[Boi97b] Boivin, W.S., Boyd, S.M., Coletta, J. A., and Neunaber, L. M., "Measurement of Radio Frequency Electromagnetic Fields in and around Ambulances," *Biomedical Instrumentation and Technology*, April 1997, pp. 145-154.

[Car95] Carillo, R., Garay, O., Balzano, Q., and Pickels, M., "Electromagnetic Near Field Interference with Implantable Medical Devices," *IEEE International Symposium on Electromagnetic Compatibility*, August 1995, pp. 1-3.

[Chi02] Chinn, G., "Mobile PC RF Coexistence Design Techniques," Intel Developers Forum, September, 2002.

[Cor02] de M. Cordeiro, C., and Agrawal., D. P., " Mitigating the Effects of Intermittent Interference on Bluetooth Ad hoc Networks," *IEEE 13th International Symposium on Personal , Indoor and Mobile Radio Communications*, 2002, Vol. 1, pp. 496 -500.

[Cou97] Couch II, L. W., "*Digital and Analog Communication Systems*," 5th Edition, Prentice Hall, New Jersey, 1999.

[Dav97] Davis, D., Skulic, B., Segal, B., Vlach, P., and Pavlasek, T., "Hospital Emergency Room Electromagnetic Environment," *IEEE 19th Annual International Conference on Engineering in Medicine and Biology*," November 1997, vol.6, pp. 2543 -2546.

[Dav98] Davis, D., Skulic, B., Segal, B., Vlach, P., and Pavlasek, T., "Variation of Emergency-Room Electromagnetic-Interference Potential," *IEEE International Symposium on Antennas and Propagation*, June 1998, vol.4, pp. 1996-1999.

[Dav99] Davis, D., Segal, B., Cinquino, A., Hoege, K., Mastrocola, R., and Pavlasek, T., "Electromagnetic Compatibility in Hospital Corridors,"

IEEE International Symposium on Electromagnetic Compatibility, 1999, vol.1, pp. 268 -272.

[Don94] Witters, D.M. and Ruggera, P.S., "Electromagnetic Compatibility (EMC) of Powered Wheelchairs and Scooters," *IEEE 16th Annual International Conference on Engineering in Medicine and Biology*," November 1994, vol.2, pp. 894 -895.

[Fcc15] FCC Regulations Part 15, 2001. http://www.fcc.gov/oet/info/rules/

[Fra71] Frank, V.A. and Lodner, R.T., "The Hospital Electromagnetic Interference Environment," *Journal of the Association for the Advancement of Medical Instrumentation*, Vol. 5, No. 4, August 1971, pp. 246-254.

[Gra98] Grant, H., and Schlegel, R. E., "In Vitro Study of the Interaction of Wireless Phones with Cardiac Pacemakers, Phase II: Planar separation Effects of Air," EMC report 1998-2, Norman, OK: University of Oklahoma Center for the Study of Wireless Electromagnetic Compatibility.

[Hof75] Hoff, R. J., "EMC Measurements in Hospitals," *EMI Symposium*, 1975.

[Hoo97] Hoolihan, D. D., "Medical Device Electromagnetic Interference – ANSI issues. *IEEE Professional Program Proceedings*: Electronic Industries Forum of New England, pp.123-130.

[Hoo98] Hoolihan, D. D., "Protecting Devices from Radio-Frequency Transmitters," Medical Device and Diagnostic Industry, pp. 58-60.

[Hpa95] Hewlett Packard, "HP 8590 E-Series Spectrum Analyzers and HP 8591C Cable TV Analyzer- Calibration Guide," June 1995.

[Hpp95] Hewlett Packard, "HP 8590 E-Series and L-Series Spectrum Analyzers and HP 8591C Cable TV Analyzer- Programmer's Guide ," June 1995.

[Hpi02] Hewlett Packard, "Wi-Fi™ and Bluetooth™ - Interference Issues," White paper, 2002.

[IEC01] Regulatory Compliance Analysis EMC Standard, IEC (EN)60601-1-2 (2001 Edition).

[IEC02] www.iec.ch, International Electrotechnical Commission.

[ITU94] ITU-R P-Series Recommendations, P.525. Calculation of Free-Space Attenuation.

[ITU01] ITU-R P.1238-2, Propagation Data and Prediction Methods for the Planning of Indoor Radio Communication Systems and Radio Local Area Networks in the Frequency Range 900 MHz to 100 GHz.

[Jam] James Mclean, Robert Sutton and Rob Hoffman, "Interpreting Antenna Performance Parameters for EMC Applications – part 3," TDK RF Solutions Inc.

[Jan96] Janssen, G.J.M., Stigter, P.A., and Prasad, R., "Wideband Indoor Channel Measurements and BER Analysis of Frequency Selective Multipath Channels at 2.4, 4.75, and 11.5 GHz," *IEEE Transactions on Communications*, October 1996, Vol. 44, pp. 1272 -1288.

[Kam99] Kamerman, A., "Coexistence between Bluetooth and IEEE 802.11 CCK Solutions to Avoid Mutual Interference," Lucent Technologies, Bell Laboratories, January 1999.

[Kim95] Kimmel, W. C., and Gerke, D. D., "Electromagnetic Interference in the Hospital Environment," Medical Device and Diagnostic Industry, 1995, pp. 88-92.

[Kni95] Knickerbocker, C. G., and Barbell, A. S., "Medical Device Malfunction Caused by Electromagnetic Interference: The ECRI perspective," *IEEE Engineering in Medicine and Biology*, pp. 24-28.

[Kri02a] Krishnamoorthy, S., Anderson, C. R., Srikanteswara, S., Robert, P. M., and Reed, J. H., "Background Interference Measurements at 2.45 GHz in a Hospital Environment," *Virginia Tech and University of Wake Forest Bio-Medical Symposium*, 2002, pp. 26-28.

[Kri02b] Krishnamoorthy, S., Robert, M., Srikanteswara, S., Valenti, M.C., Anderson, C.R., Reed, J.H., "Channel Frame Error Rate for Bluetooth in the Presence of Microwave Ovens," *IEEE Vehicular Technology Conference*, Fall 2002, Vol.2, pp. 927 -931.

[Kri02c] Krishnamoorthy, S., "PRISM – Measurement System for the ISM band," submitted to MPRG newsletter '*The Propagator*', 2003.

[Kri02d] Krishnamoorthy, S., "Programming the Bluetooth Protocol Stack," Preliminary report and software, May 2002.

[Kur98] Kuriger, G. W., Grant, H., and Schlegel, R. E., "In Vitro Study of the Interaction of Wireless Phones with Implantable Cardioverter Defibrillators. EMC report 1998-1, Norman, OK: University of Oklahoma Center for the Study of Wireless Electromagnetic Compatibility.

[Lan01a] Lansford, J., and Stephens, A. P., TG2 Mobilian Draft Text - 01300r1P802-15_TG2, IEEE P802.15 Working Group for Wireless Personal Area Networks (WPANs), 2001.

[Lan01b] Lansford, J., "Adaptive Hopping," *Bluetooth Developers Conference*, December, 2001.

[Lxe02] EMS Technologies, "802.11a Wireless Network Issues in Warehouses & Distribution Centers (vs 802.11b)," White Paper December 2002.

[Mar02] D'souza, M. F., "Residential Microwave Oven Interference on Bluetooth Data Performance," Masters Thesis, Virginia Polytechnic Institute and State University, 2002.

[Mat02] Mathworks, www.mathworks.com

[Min01] Low Noise Amplifiers, 0.1 to 2700 MHz, Model index ZQL-2700MLNW, 2001.

[Nai02] National Instruments, www.ni.com

[Pha00] Phaiboon, S., and Somkuarnpanit, S., "Modeling and Analysis the Effect of Radio-Frequency Fields in Hospitals to the Medical Equipment," *IEEE TENCON 2000*, vol.1, pp.92-95.

[Rap99] Rappaport, T. S., "*Wireless Communications – Principles and Practice*," Prentice Hall, New Jersey, 1999.

[Rav96] Ravindran, A., Schlegel, R. E., and Grant, H., "Evaluation of the Interaction between Wireless Phones and Hearing Aids, Phase I: Results of the clinical trials. EMC report 1996-2, Norman, OK: University of Oklahoma Center for the Study of Wireless Electromagnetic Compatibility.

[Ree02] Reed, J. H., "*Software Radio – A Modern Approach to Radio Engineering*," Prentice Hall, New Jersey, 2002.

[Rob97] Robinson, M. P., Flintoft, I., and Marvin, A. C., "Interference to Medical Equipment from Mobile Phones," *Journal of Medical Engineering and Technology*, 1997, pp. 141-146.

[Rob03] Robert, P. M., "Reduction in Coexistent WLAN Interference Through Statistical Traffic Management," PhD Dissertation, Virginia Polytechnic Institute and State University, 2003.

[Rug75] Ruggera, P.S., "Radio Frequency E-Field Measurements within a Hospital Environment," *IEEE EMI Symposium*, 1975.

[Sch96] Schlegel, R. E., Raman, S., Grant, H., and Ravindran, A. R., "In Vitro Study of the Interaction of Wireless Phones with Cardiac Pacemakers," EMC report 1996-3, Norman, OK: University of Oklahoma Center for the Study of Wireless Electromagnetic Compatibility.

[Sch02] Schafer, T. M., Maurer, J., and Wiesbeck, W., "Measurement and Simulation of Radio Wave Propagation in Hospitals," *IEEE Vehicular Technology Conference*, Fall 2002, Vol.2, pp. 792 -796.

[Seg95] Segal, B., and Pavlasek, T., "'Silent' Malfunction of a Critical-Care Device caused by Electromagnetic Interference," *Biomedical Instrumentation and Technology*, pp. 350-354.

[Seg96] Segal B., "Source and Victims: The potential Magnitude of the Electromagnetic Interference Problem," Electromagnetic Compatibility for Medical Devices: Issues and Solution, FDA and AAMI, 1996, pp. 24-29.

[Sig01] Bluetooth SIG, "*Specification of the Bluetooth System*," Core Version 1.1, 2001.

[Sil93] Silberberg, J. L., "Performance Degradation of Electronic Medical Devices due to Electromagnetic Interference," Compliance Engineering, 1993, pp. 25-39.

[Sil95] Silberberg, J. L., "What can/should we learn from reports of Medical Device Electromagnetic Interference?" *IEEE Engineering in Medicine and Biology*, 1995, pp. 10-19.

[Sko85] Skomal, E. N., and Smith, A. N., "Measuring the Radio Frequency Environment," Van Nostrand Reinhold, 1985, pp. 187-189.

[Sko98] Skopec, M., "Hearing Aid Electromagnetic Interference from Digital Wireless Telephones," *IEEE Transactions on Rehabilitation Engineering*, June 1998, Vol.6, pp. 235 -239.

[Smi82] Smith, A. A., Jr., "Standard-site Method for Determining Antenna Factors," *IEEE Transactions on Electromagnetic Compatibility*," August 1982, Vol.24, pp. 316-322.

[Stu81] Stutzman, W. L., and Thiele, G. A., "*Antenna Theory and Design*," John Wiley & Sons, 1981.

[Swe00] Sweeney, D., and Robert, P. M., "Bluetooth Tutorial", Virginia Polytechnic Institute and State University, June 2000.

[Swe01] Personal Communication, Dr. Dennis Sweeney, Virginia Polytechnic Institute and State University, March 2001.

[Tan94] Tan, K-S and Hinberg, I., "Radiofrequency Susceptibility Tests on Medical Equipment," *IEEE 16th Annual International Conference on Engineering in Medicine and Biology*," November 1994, vol.2, pp. 998-999.

[Tan95a] Tan, K-S., and Hinberg, I., "Investigation of Electromagnetic Interference with Medical Devices in Canadian Hospitals," *Workshop on Electromagnetics, Health Care and Health: IEEE Engineering in Medicine and Biology*," 1995, pp. 20-23.

[Tan95b] Tan, K-S., and Hinberg, I., "Walkie-Talkies and Cellular Telephones: The Hazards of Electromagnetic Interference in Hospitals," Leadership in Health Services, 1995, vol.3, pp. 11-15.

[Tan97] Tan, K-S., and Hinberg, I., "In Vitro Testing of Implanted Cardiac Pacemakers for Radio Frequency Interference from Wireless Communication Devices," Workshop on Electromagnetic Compatibility in Health Care and Cardiac Pacemakers, Canadian Wireless Telecommunication Association.

[Tan01] Tan, K-S., Hinberg, I., and Wadhwani, J., "Electromagnetic Interference in Medical Devices: Health Canada's Past and Current Perspectives and Activities," *IEEE International Symposium on Electromagnetic Compatibility*, 2001, vol.2, pp. 1283 -1288.

[Tol75] Toler, J.C., "Electromagnetic Interference Levels in Hospitals," *IEEE EMI symposium*, 1975.

[Tra01] TransEra Corporation, "GPIB Tutorial,"
http://www.transera.com/htbasic/tutgpib.html#Bus%20History

[Val02] Valenti, M. C., Robert, P. M., and Reed, J. H., "On the Throughput of Bluetooth Data Transmissions," *IEEE Wireless Communications and Networking Conference*, 2002, Vol.1, pp. 119 -123.

[Vla95a] Vlach, P., Segal, B., and Pavlasek, T.," The Measured and Predicted Electromagnetic Environment at Urban Hospitals," *IEEE International Symposium on Electromagnetic Compatibility*, August 1995, pp. 4 -7.

[Vla95b] Vlach, P., Liu-Hinz, C., Segal, B., Skulic, B., and Pavlasek, T.," The Electromagnetic Environment due to Portable Sources in a Typical Hospital Room," *IEEE 17th Annual Engineering in Medicine and Biology Society Conference*, September 1995, vol.1, pp. 683 -684.

[Wla99a] Wireless LAN Medium Access Control (MAC) and Physical Layer (PHY) Specifications, ANSI/IEEE Std 802.11, 1999 Edition.

[Wla99b] Wireless LAN Medium Access Control (MAC) and Physical Layer (PHY) Specifications, ANSI/IEEE Std 802.11 b, 1999 Edition.

[Wpaa] IEEE Working Group for WPAN, http://grouper.ieee.org/groups/802/15/

[Wpab] IEEE 802.15-00/294r1 Steve Shellhammer, Overview of ITU-R P.1238-1 "Propagation Data and Prediction Methods for Planning of Indoor Radiocommunication Systems and Radio LAN in the Frequency Band 900 MHz to 100 GHz".

[Wpa01] Heile, R. F., and Shellhammer, S., IEEE 802.15-01/265r0, IEEE P802.15 Working Group for Wireless Personal Area Networks™.

[You97] Young, C., Ahmed Saoudy, S., and Budwill, S., "EMI Levels at a 'Patient Care Location' in a Hospital," *IEEE Canadian Conference on Electrical and Computer Engineering*, May 1997, vol. 2, pp. 625 -628.

Vita

Seshagiri Krishnamoorthy was born on December 20, 1977 in the cosmopolitan city of Dubai, U.AE. He returned to Madras, India in 1992 to complete his high school education. In the fall of 2000 he graduated with distinction and secured a University rank from the University of Madras, India in Electronics and Communication Engineering.

In the fall of 2000, Sesh began work towards a Master of Science degree in Electrical Engineering with the Mobile and Portable Radio Research Group at the Virginia Polytechnic Institute and State University. His research included algorithm development for 3rd generation wireless systems, position location and range estimation using Bluetooth, RF test and measurement equipment design and implementation. He has authored two conference papers. During the summer and fall of 2002, he interned with the Digital Design and Signal Processing Group at Allen Telecom's Mikom US R&D division in Lynchburg, Virginia. At Allen Telecom, he was involved with the development and implementation of interference cancellation techniques and wireless channel modeling for UMTS, GSM and TETRA repeaters.

Upon completion of the requirements for the Master of Science degree in Electrical Engineering, he will return to work for Allen Telecom.